DISSERTATION

Activation of Carbon-Element and Silicon-Chlorine Bonds by a Pt(II) Complex with a Hemilabile Ligand

ausgeführt zum Zwecke der Erlangung des akademischen Grades eines Doktors der Naturwissenschaften unter der Leitung von

o.Univ.Prof. Dipl.-Ing. Dr.rer.nat. Ulrich SCHUBERT
E 165 – Institut für Materialchemie

eingereicht an der Technischen Universität Wien
Fakultät für technische Chemie
von

Mag.rer.nat. Christian Martschitsch
9601533
Anton-Baumgartner-Straße 44
1230 Wien

Wien am 29. April 2010

Ein großer Entdecker hat, als man ihn einmal befragte, wie er es anstelle, dass ihm so viel Neues eingefallen sei, darauf geantwortet: indem ich unablässig daran dachte. Und in der Tat, man darf wohl sagen, dass sich die unerwarteten Einfälle durch nichts anderes einstellen, als dass man sie erwartet.

Robert Musil, *Der Mann ohne Eigenschaften*

Danksagung

Ich danke Prof. Ulrich Schubert für die Möglichkeit, meine Doktorarbeit am Institut für Materialchemie zu erstellen, für seine Ratschläge, wie man das kreative Chaos dutzender Experimente in einen verständlichen wissenschaftlichen Text verwandelt und dafür, dass er mir freie Hand ließ, Grundlagenforschung ohne Einschränkung durch vorgegebene Ziele zu betreiben. Ich bin zwar dabei manchmal falsch abgebogen, aber Umwege erhöhen die Ortskenntnis – das gilt erst recht im Labyrinth der Wissenschaft.

Mein Dank geht des Weiteren an Prof. Markus Galanski vom Institut für Anorganische Chemie der Universität Wien für die Übernahme der Tätigkeit des Zweitprüfers und -begutachters sowie für die Benützung des 500MHz-NMRs an seinem Institut, diese Messungen waren ein wichtiger Baustein zur Fertigstellung meiner Arbeit.

Danke an alle, die während dieser Arbeit Messungen für mich durchgeführt haben, namentlich Michael Puchberger für dutzende 2D-NMR-Messungen, Maika und Stefan B. für XRD-Messungen und Walter Dazinger vom Institut für Angewandte Synthesechemie für die Charakterisierung meiner Verbindungen mittels CI-MS.

Ein großes Dankeschön geht an meine (ehemaligen) Institutskollegen Akira, Angie, Bernhard, Christina, Christoph L., Christoph R., Claudia F., Claudia. V., Denisa, Denise, Dieter, Dini, Doris B., Doris E., Fatmir, Grace, Guido, Harald, Helmut, Jim, Jakob, Maïa, Maika, Marina, Marco, Melitta, Michael, Mirka, Moshin, Nicola, Patrycia, Philipp, Ralf, René, Robert L., Robert P., Rupert, Sorin, Stefan B., Stephan. K, Stephan R. und Van An (ich hoffe, ich habe niemanden vergessen, so lange wie ich dabei war...)

Ebenso bedanken möchte ich mich bei meinen Kollegen und Vorgesetzten bei der Firma Gabriel-Chemie in Gumpoldskirchen, insbesondere bei Veronika Rihs und Helmut König, die mir als „Frischg'fangten" direkt von der Uni eine Chance gegeben und mich beim Fertigstellen dieser Arbeit unterstützt haben.

Großer Dank für Aufmunterung, Schmähführen und Hilfe bei kleinen und großen Problemen geht an meine Freunde August, Christian, Daniel, Robert und ganz besonders an meinen seit über 20 Jahren besten Freund, Trauzeugen und Caminogefährten David, der es immer wieder geschafft hat, aufkommenden Weltpessimismus in ein tatkräftiges „jetzt erst recht" zu verwandeln.

Meinen Eltern Helene und Andreas danke ich für alles, was sie in den letzten 32 Jahren für mich getan haben, für alles, das ich sofort verstand, alles, das ich erst jetzt begreife und all das, was ich erst verstehen werde, wenn ich selbst einmal Kinder haben sollte.

Ich widme diese Arbeit meiner Frau Claudia, deren unerschütterliche, durch all meine Launen, Tiefs und das oft die ganze Wohnung umfassende kreative Chaos nicht beeinträchtigte Liebe für mich den Unterschied zwischen existieren und leben ausmacht. Ich möchte ihr für ihre oft überstrapazierte Geduld mit mir danken und für die Aufmunterung weiterzumachen, sei es per von Zeit zu Zeit notwendigen Tritt in die „rear section"

KURZFASSUNG

Oxidative Additionen stellen einen wichtigen Reaktionsschritt in der Synthesechemie dar und werden in vielen bedeutenden industriellen Anwendungen, wie z.B. dem *Monsanto*-Prozess genutzt. Daher ist, abgesehen vom rein wissenschaftlichen Interesse an den Charakteristika dieser Reaktionen, die Kenntnis der diese Reaktionen beeinflussenden Bedingungen von großer Bedeutung für die Entwicklung neuer Synthesewege.

In diesem Zusammenhang spielen Komplexverbindungen mit hemilabilen Liganden (Liganden mit zwei unterschiedlichen Donoratomen) eine wichtige Rolle: Das schwächere der beiden Donorzentren kann dekoordinieren, wodurch eine Koordinationsstelle frei wird, die nun für die Addition eines neuen Liganden oder für Umlagerungen in der Koordinationssphäre genutzt werden kann. Dadurch können neue Moleküle gebildet und aus dem Komplex eliminiert werden. Die hemilabilen Liganden können maßgeschneidert für die jeweils gewünschten Reaktionen hergestellt werden.

Das Ziel dieser Arbeit war die Untersuchung der Reaktivität des über einen hemilabilen Liganden verfügenden Pt(II)-Komplexes $[(\kappa^2\text{-}P,N)\text{-}Ph_2PCH_2CH_2NMe_2]PtMe_2$ mit unterschiedlichen halogenierten Kohlenwasserstoffverbindungen und chlorierten Siliziumverbindungen. Es wurden Reaktionen mit verschiedenen halogenierten Verbindungen durchgeführt. Die Reaktionsverläufe und die Produkte der Reaktionen wurden mittels NMR-Spektroskopie, Massenspektroskopie und Röntgenbeugung untersucht.

Bei den halogenierten Kohlenwasserstoffverbindungen stellte sich heraus, dass der Reaktionstyp von der Art des Kohlenstoffes, welcher der zu addierenden halogenierten Gruppe benachbart ist, abhängt. Für halogenierte Kohlenwasserstoffverbindungen ohne CH_2-Gruppen in dieser benachbarten Position wurde basierend auf den spektroskopischen Daten ein neuer Reaktionsweg postuliert. Des Weiteren wurden mehrere neue Komplexverbindungen synthetisiert und charakterisiert.

Bei den chlorierten Siliziumverbindungen konnte festgestellt werden, dass der Reaktionsweg vor allem von der Anzahl an Chloratomen am Silizium abhängt.

ABSTRACT

Oxidative addition reactions are a very important step in synthetic chemistry and are used in various industrial catalysis pathways, such as the *Monsanto* process. Therefore, apart from pure scientific interest in the properties of these reactions the understanding of the conditions that influence oxidative additions is of tremendous interest for the development of new synthetic pathways.

In this context, complexes with hemilabile ligands (ligands with two different donor atoms) play an important role: The weaker donor atom can decoordinate and thus open a vacant coordination site for addition of a new ligand or for rearrangements in the coordination sphere that could support formation and elimination of new compounds. These ligands can be tailored to support different reactions of importance in synthetic chemistry.

The aim of this thesis was to investigate the reactivity of the Pt(II) complex $[(\kappa^2\text{-}P,N)\text{-}Ph_2PCH_2CH_2NMe_2]PtMe_2$, a compound with a hemilabile P,N ligand, towards halogenated hydrocarbons and silyl chlorides. Reactions were performed with several halogenated starting compounds. The progress as well as the products of these reactions were monitored by NMR spectroscopy, mass spectrometry and X-ray diffraction.

It turned out that halogenated hydrocarbons react through different pathways by oxidative addition, depending on the type of carbon neighboring the halogenated group to be added. For halogenated hydrocarbons without CH_2 groups in this neighbouring position a new reaction mechanism was postulated, based upon spectroscopic data. Furthermore, different new coordination compounds were synthesized and characterized.

It was demonstrated for silyl chlorides that the reaction pathway depends on the number of chlorines bound to the silicon.

Contents

1. Introduction

1.1 Platinum

1.1.1 History

With only about 10^{-6} w.% in the Earth's crust[1], platinum is one of the rarest metals. Its earliest known use as jewellery metal was by South American natives, while the Spanish *conquistadores* initially despised it as *platina* (lit. "little silver"). The first European reference to this metal can be found in the writings of the Italian scholar *Julius Caesar Scaliger*[2], as a description of a not meltable metal from South America. Scientific study of platinum started in the 18th century with the work of the English scientists *Sir Charles Wood*, *William Brownrigg* and *Sir William Watson*[3]. The following centuries saw the development of different techniques to purify the metal usually not found in a pure form but as sulfide, selenide and telluride or in iron, chromium and nickel ores together with the other platinum metals[4] (Ru, Rh, Pd, Os, and Ir, so called because of their chemical and physical properties being similar to Pt).

1.1.2. Properties, Extraction and Technical Applications

Platinum is a malleable grey-white metal with a melting point of 1772°C and crystallizes in face centred cubic form. Its electronic configuration is [Xe] $4f^{14}5d^{9}6s^{1}$. It is soluble in *aqua regia*, and due to its tendency to form complexes it is easily attacked by alkaline metal hydroxides, cyanides or sulfides. It stores considerable amounts of hydrogen at high temperatures in a very reactive form which makes it a very useful catalyst for hydrogenation reactions.

Around 230 tons of platinum are currently produced per year[5], it is purified mainly by treatment of platinum-containing mixtures in *aqua regia* and selective precipitation as $(NH_4)_2[PtCl_6]$ or extraction with tributylphosphate[4].
Its main technical application is as a catalyst for industrial applications (e.g. for the Ostwald process or the oxidation of methanol), in fuel cells and catalytic converters for combustion engines. It is also used for thermocouples, medical implants, laboratory equipment and heat-

stable elements in rocket thrusters.

1.2 Platinum Complexes

1.2.1 Structures

While monovalent and trivalent platinum rather tends to form metal clusters, zerovalent, divalent and tetravalent platinum form different types of mononuclear, diamagnetic complexes (Fig. 1):

•Pt(0) complexes are mostly tetrahedral.

•Pt(II) complexes generally exhibit square planar geometry and are usually very stable in air.

•Pt(IV) complexes are diamagnetic, octahedral low-spin compounds.

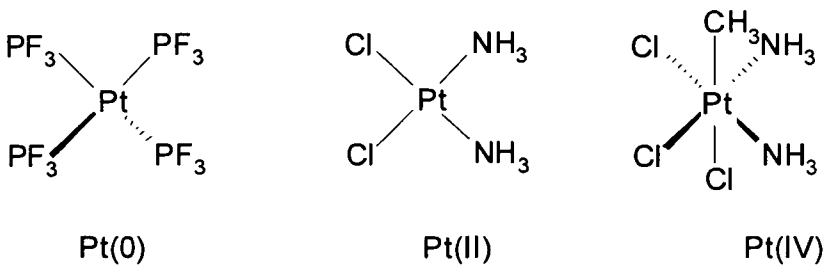

Fig. 1: Examples for platinum complexes in different oxidation states

1.2.2 Reactions with Electrophiles and Nucleophiles

Transition metal compounds can undergo various reactions with electrophilic and nucleophilic reagents[6]. With electrophiles such as the trityl cation (Ph_3C^+), abstractions of inorganic anions or alkyl groups can take place. Electrophilic compounds can add to an unsaturated group of a ligand, and electrophilic substitution reactions take place readily with electron-rich ligands as in ferrocene derivatives.

Nucleophilic attack on ligands is favoured in complexes, where the central cation is electron deficient (this can be due to its charge or to electron-withdrawing ligands). Examples for this reaction type are additions to double bonds in the coordination sphere, formation of Fischer-

carbene complexes from metal carbonyls or nucleophilic attack on such carbene ligands[7;8].

Much more common for platinum complexes are nucleophilic substitution reactions on square planar or octahedral complexes. The substitution process in general can occur either in a dissociative way or by association and activation of the complex. An important factor for the reaction rate is the dissociation energy of the leaving group, as well as the question whether association or dissociation of one ligand results in a decrease of the ligand field stabilisation energy.

Nucleophilic substitution reactions on square planar Pt(II) complexes mostly take place by association of the nucleophilic group which leads to formation of a five-coordinate trigonal-bipyramidal intermediate[9]. From the point of view of stereochemistry the configuration is retained. The reaction rate is not only influenced by the metal centre and the entering group (it increases with increasing softness of the nucleophilic group), but also by the *trans* effect: Due to orbital geometry the charge increase or decrease on the metal centre brought about by a ligand influences the rate of substitution of a ligand in *trans* position[10]. This can facilitate the substitution of this ligand and may also favour or disfavour substitution in that very position over substitution of an identical ligand in *cis* position. In platinum chemistry it is widely used for stereoselective syntheses (Fig. 2). Apart from this kinetic effect there is also a structural *trans* effect (often called *trans* influence) that influences the thermodynamic properties of a complex in the ground state[11] and the ligand in the opposite position. These properties include the bond length of the *trans* ligand to the metal, the vibration frequencies and the chemical shifts and coupling constants in NMR spectroscopy. The *trans* effect and influence can be observed in square planar and octahedral complexes, with a higher magnitude in planar compounds.

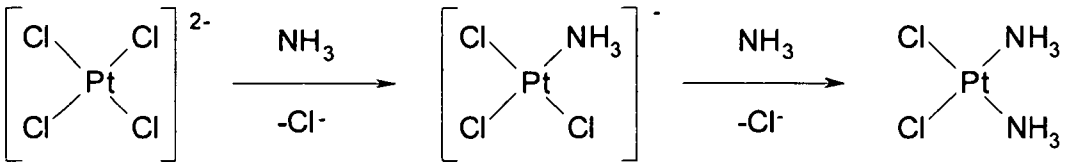

synthesis of the *cis* form

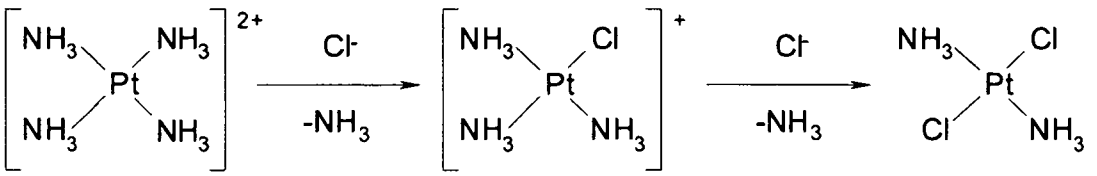

synthesis of the *trans* form

Fig. 2: The use of the *trans* effect for the synthesis of the anti-cancer drug *cisplatin* (top)

On octahedral Pt(IV) complexes the reaction rate of nucleophilic substitiutions is more difficult to estimate than for square planar complexes, it is done by means of valence bond and crystal field theory. As for square planar complexes, the configuration of the complex is retained.

1.2.3 Rearrangement Reactions [9]

Thermal or photochemical activation very often causes complexes to isomerize. These reactions can proceed either by pseudorotation (intramolecular change of ligand positions) or by associative / dissociative mechanisms. The latter reactions can be an exchange of the donor atom of a ligand (e.g. transformation of a nitrito complex into a nitro complex, Fig 3) or a consecutive stereochemical exchange of two ligands A and B by means of two substitutions, where in the first substitution A is exchanged by B and in the second step B is substituted by A.

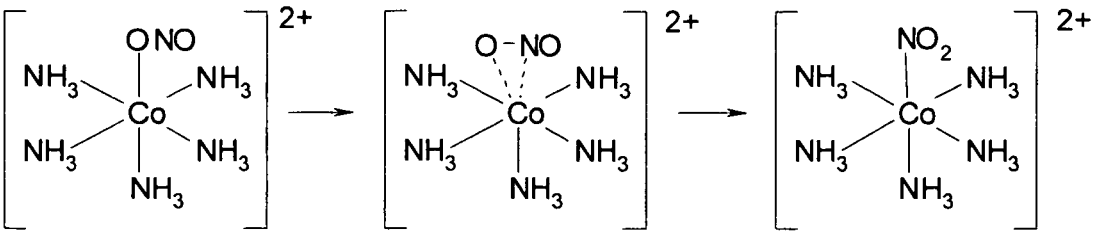

Fig. 3: Donor atom exchange by ligand rearrangement

1.2.4 Electron Transfer Reactions[12]

These reactions can be divided into two sub-groups: outer-sphere electron transfer and inner-sphere electron transfer reactions.

In outer-sphere reactions, electrons are are transferred between two complexes without changes in the coordination spheres or formation of intermediates. These transfers can take place between complexes with the same central metal as well as between complexes with different central cations. Electron transfers can also be performed photochemically if the lifetime of photo-exited states is long enough. Another possibility of photochemically induced electron transfer between two complexes is by irradiation of a charge-transfer complex. If a very fast follow-up reaction occurs after the electron transfer, the back transfer is inhibited.

Inner-sphere electron transfers proceed via bond formation between the central metals of two complexes. Usually the reaction rate of these processes is much higher than that of outer-sphere electron transfers.

1.2.5 Insertions and Extrusions of Unsaturated Molecules[13]

This reaction class consists of insertion of unsaturated groups into metal-ligand bonds. There are different subgroups:

CO Migratory Insertion:

A methyl ligand migrates and binds to a CO ligand in *cis* position[14]. For 18-electron complexes this reaction can only take place with reasonable efficiency if a potential ligand is present in the solution to fill the vacant coordination site emptied by the migrating ligand, so that no energetically unfavourable 16-electron complex is formed. To distinguish it from insertion of a molecule from the solution into the M-CH_3 bond, the process is called *migratory* insertion (Fig. 4).

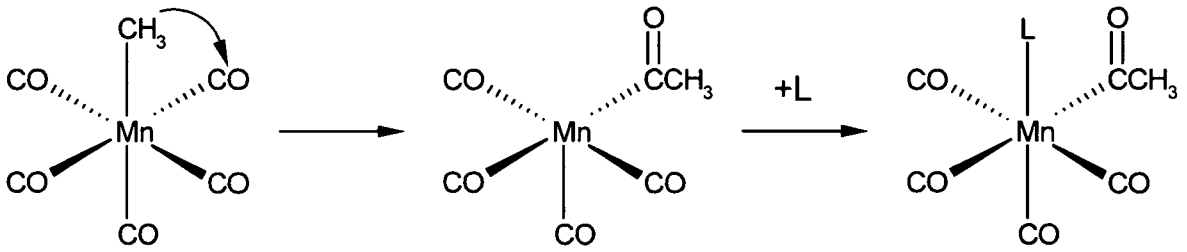

Fig. 4: Migratory insertion at $(CO)_5CH_3Mn$

Methylene Insertion:

Since the electronic structure of CH_2 ligands is somehow analogous to that of carbonyl ligands, they can also be inserted into metal-ligand bonds. Because of the low stability of carbene ligands, only few of these reactions are known.

A very interesting example of this reaction type is the formation of phosphonium ylide complexes[15,16] (Fig. 5).

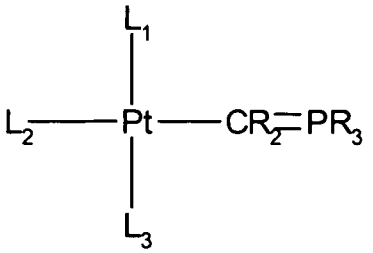

Fig. 5: General formula of a
Pt(II) P ylide complex

These compounds are usually formed by adding phosphonium ylides to complexes, nevertheless many publications show a second reaction pathway via halogen displacement by phosphorous ligands[17,18] in this reaction type the methylene group is inserted into the M-P bond (Fig 6).

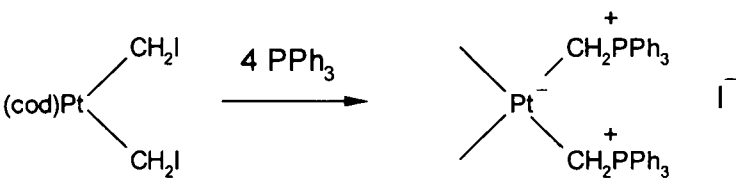

Fig 6: Formation of an ylide complex from a CH_2X ligand[17]

Insertion of Unsaturated Compounds:

Unsaturated organic molecules are very easily inserted into metal-ligand bonds. Since the reaction starts with coordination of the molecule to the metal, a vacant coordination site at the metal is necessary for this reaction to take place. Thus only complexes with at maximum 16 valence electrons can undergo this reaction. The reverse process of this reaction is called β–elimination, where a proton in β position to the metal is transferred to the metal centre, which leads to elimination of the unsaturated compound (Fig. 7).

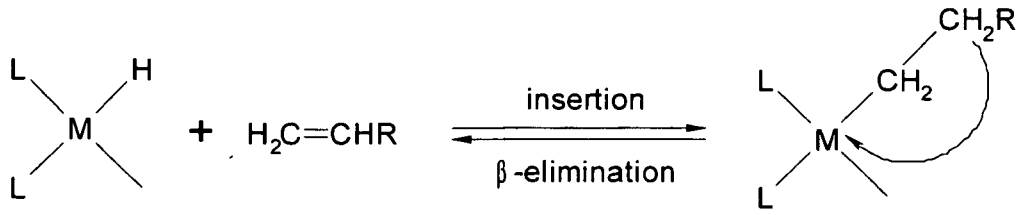

Fig. 7: Alkene insertion and β-elimination

γ-Elimination:

When no β-CH groups are present, a coordinated alkyl group can be eliminated by a metathesis reaction including a CH group in γ position (Fig. 8).

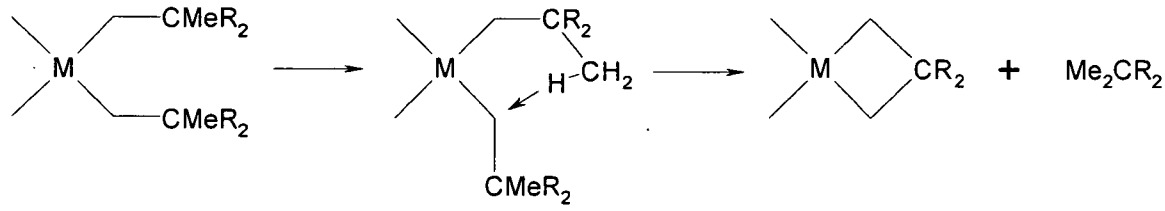

Fig. 8: γ-elimination

1.2.6 Oxidative Coupling and Reductive Decoupling

In this reversible process, two olefinic compounds form a five-membered cyclic compound with the metal cation of the complex, whose oxidation number is increased by two units.

1.2.7 Oxidative Addition and Reductive Elimination[6]

1.2.7.1 Basic Principles

Oxidative addition is defined as the insertion of a metal into a A-B bond by which the oxidation number of the metal is increased by two units. Basically there are four reaction pathways, depending on the type of complex and the A-B bond:

Concerted Addition:

This mechanism mainly takes place between 16-electron complexes such as square-planar Pt(II) complexes and substrates with low or no polarity. A three centred intermediate is formed first by interaction of an occupied σ orbital of XY with the metal (Fig. 9), followed by electron transfer from a *d* orbital of the complex to the substrate's σ* orbital.

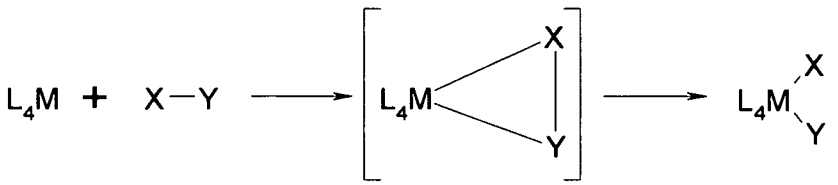

Fig. 9: Concerted addition

The A-B bond is thus broken and an octahedral 18-electron complex with A and B as new ligands usually in *cis* position to each other is formed.

This addition mechanism is a very important reaction step in catalysis, for example in hydrogenation reactions. The classical model reaction is the addition of H_2 to *trans*-$Ir(PPh_3)_2(CO)Cl$ (*Vaska's* complex, Fig. 10)

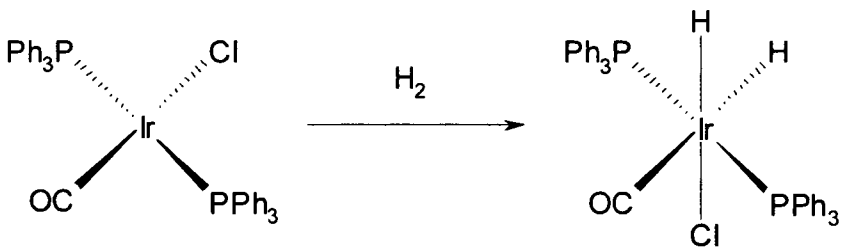

Fig 10: Addition of H_2 to *Vaska's* complex

An important topic in catalysis, activation and functionalisation of C-H bonds, is also a possible application of oxidative addition, although C-H bond are not activated as easily by transition metal complexes (first discovered by Green and Knowles[19], Fig. 11) as H-H or Si-H bonds.

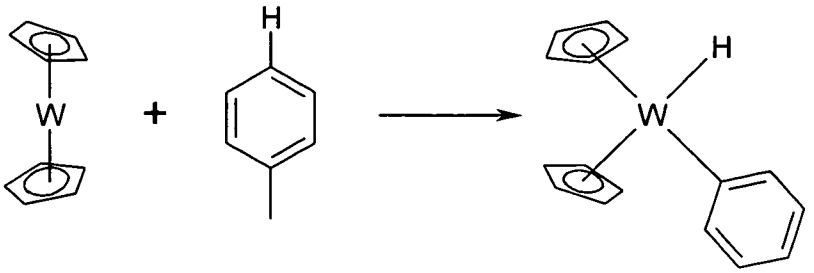

Fig. 11: Oxidative addition of toluene to $(\pi\text{-}C_5H_5)_2W$

Substitution:

Kinetics and stereochemistry of this pathway are very similar to organic substitution reactions. It proceeds by coordination of an anion to the metal centre, nucleophilic attack of the resulting anionic complex to the substrate, similar to a S_N2 reaction in organic chemistry, with subsequent coordination of the leaving group to the complex (Fig. 12).

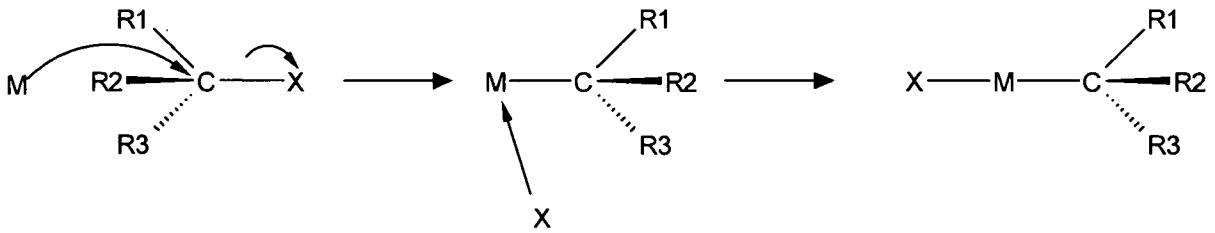

Fig. 12: Oxidative addition through a S_N2-like process

For 18-electron complexes (e.g. NiL_4 complexes) coordination of the leaving group cannot take place. In this case complete addition is only possible if another ligand dissociates from the five-coordinated intermediate.

Halogenated hydrocarbons very often react by this mechanism. The reactivity of the compounds depends on the same properties as in organic S_N2 reactions. Thus, the reactivity is the highest for methyl halogenides and the lowest for halogenated tertiary hydrocarbons[20].
An important example for the S_N2-like pathway in industrial synthesis is the *Monsanto* process (Fig. 13) that is used for the synthesis of acetic acid. This process is initiated by addition of MeI

to a rhodium complex.

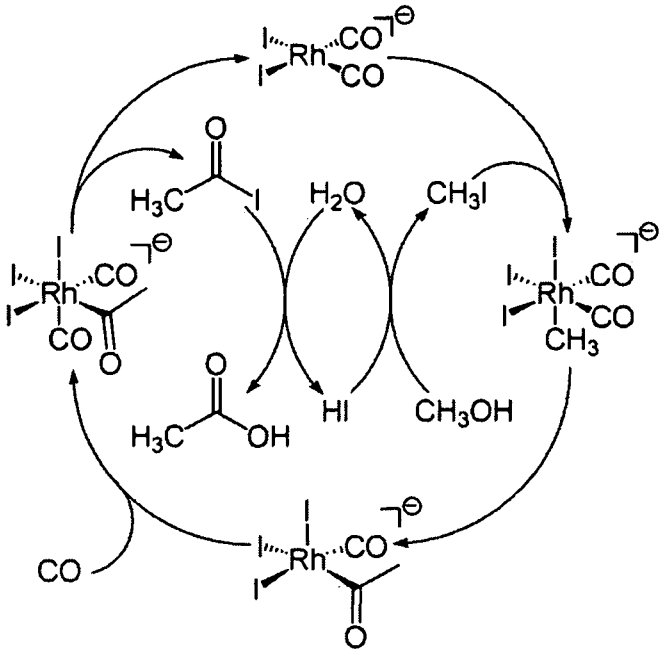

Fig. 13: Reaction scheme of the *Monsanto* process

Ionic Mechanism[21]:

In polar solvents, completely dissociated electrophilic compounds (i.e. hydrogen halides) can oxidatively add to complexes in a stepwise process. After dissociation of a ligand usually first the proton is added to the metal and then another ligand is exchanged by the halide ion. Contrary to substitution reactions these addition reactions are not stereoselective.

Radical Mechanism:

The radical mechanism takes place between transition metal complexes and polar substrates, mainly halogenated hydrocarbons. This reaction type is divided into two subtypes, nonchain reactions and free radical chain reactions.

The first type proceeds through coordination of the polar compound and subsequent electron transfer from the metal, resulting in the formation of a solvent caged radical pair. This pair can then collapse to yield the addition product[20].

The chain reactions consists of abstraction of a halide from the halogenated reaction partner, the dehalogenated molecule, now a radical, can attack another complex which can then complete its coordination sphere by abstracting a halide from another molecule, etc[22].
Radicals can also add to complexes[21]. In some cases, even chain reactions are possible.

With halogenated hydrocarbons as substrates the reactivity of a compound is high when the radical formed in the process is stable. Thus the order of reactivity with regard to the organic moieties is $C_{tert.} > C_{sec.} > C_{prim.} > Me$[20], what renders is possible to distinguish it from substitution reactions.

1.2.7.2 Reductive Elimination

The inverse process of an oxidative addition is called reductive elimination. The main route of reductive elimination is through formation of a transition state in which the two ligands to be eliminated interact with each other (Fig. 14). The formal oxidation state of the metal is concomitantly lowered. The following properties influence this reaction type[23]:

- The ligands that are to be eliminated must be in *cis* position. If they are in trans position, no transition state can be formed[24]
- The formation of the elimination product must be thermodynamically favourable
- The more unstable the higher oxidation state of the metal is, the more susceptible the complex is to reductive elimination[25]
- Other ligands can reduce the rate of reductive elimination by inhibiting the ligands to be eliminated from reaching a *cis* arrangement[26]

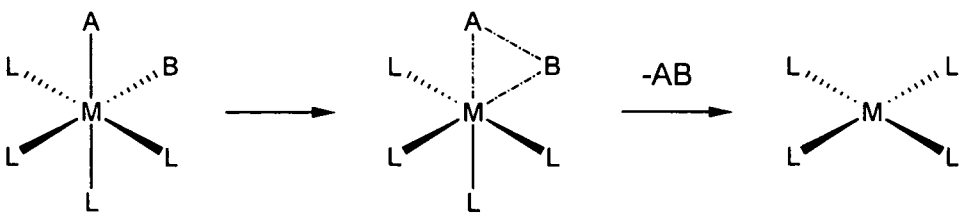

Fig. 14: Mechanism of reductive elimination

1.2.7.3 Oxidative Addition of Carbon-Halogen Bonds

Oxidative addition of C-X bonds in halogenated hydrocarbons is a very common organometallic reaction pathway. Basically there are three factors that are important for understanding of this mechanism: Kinetic and thermodynamic considerations, stereochemistry of the reaction and influence of the complex and substrate compositon.

- Kinetics and Thermodynamics

In halogenated hydrocarbons of course not only carbon-halogen bonds are present but in most cases also carbon-hydrogen bonds, that are also susceptible to oxidative addition. Nevertheless C-X addition takes place very easily,what can be explained by means of kinetics and thermodynamics: Calculations show a higher activation free-energy barrier for C-H oxidative addition compared to C-Cl activation (e.g. a difference of 7 kcal/mol in Ir complexes)[27]. Furthermore, C-X activation (except X = F) is thermodynamically favourable by 10-20 kcal/mol for C-Cl bonds, 20-30 kcal/mol for C-Br bonds and 40-50 kcal/mol for C-I bonds considering the difference of bond enthalpies of these bonds compared to C-H equivalents[28]. It has also been shown that the complexes formed by C-X activation are generally thermodynamically more stable than the hydride complexes formed by C-H activation[27,29].

- Stereochemistry

Halogenated hydrocarbons are added to metal complexes mainly by either substitution or radical mechanisms[20]. It can be expected that the radical pathway yields a mixture of isomers while in products formed by the S_N2 like mechanism R and X can be found in *trans* position to each other after addition of the R-X bond. But in reality isomerisation of the complexes takes place, it is influenced by different properties of the addition product[30]:

- Ligands with strong *trans* influence do not support the coordination of another strongly *trans* directing ligands in the opposite position
- Chlorine and nitrogen donors show a comparable *trans* influence of a magnitude that favours the coordination of alkyl groups in the opposite position, while a *trans* Cl-M-N arrangement is rather unfavourable
- Steric hindrance by other ligands

Considering these influences different geometries can be expected, depending on the ligands

- Influence of the Complex and Substrate Composition

The substrate with the bond to be activated mainly influences the reaction rate for thermodynamic and steric reasons. Generally, the bond dissociation energy of the C-Cl bond is about 10 kcal/mol higher than that of the C-Br bond and about 30 kcal/mol higher than that of the C-I bond[28], so activation of C-I bonds can be expected to be much faster than of C-Cl bonds.

The structure of the starting complex itself can influence the reaction. If the metal centre is strongly nucleophilic because of strong donor ligands, the complex is susceptible to activation reactions by nucleophilic substitution reactions[31]. Therefore addition of methyl halides is much more favourable than of halides with primary, secondary or tertiary organic moieties.

1.2.7.4 Oxidative Addition of C-C bonds

The addition of C-C single bonds to metal complexes is a very rare reaction. If C-H bonds are present in a molecule, they are more susceptible to addition than the C-C bonds for three main reasons: First the C-C bonds are normally surrounded by several C-H bonds, what renders them much less accessible by a metal[32]. Second, there is a higher kinetic barrier for C-C activation, since sp^3-sp^3 bonds show a higher degree of directionality than the sp^3-s bond between carbon and hydrogen. A CR_3 group must change its orientation to form a C-M bond from a C-C bond and vice versa. This accounts for a higher intrinsic barrier for C-C addition[33], since two alkyl groups have to rotate into an optimal position for formation of the three-centred transition state[34] (Fig. 9). Third, M-H bonds are stronger than M-C bonds[35], what makes their formation thermodynamically more favourable.

Nevertheless, C-C bond activation has been reported in certain cases, from which the most important are[34]:

- C-C bonds in strained systems

The first known C-C activation was the addition of cyclopropane to a platinum complex[36] (Fig. 15). Several other examples have been studied also with other transition metals like rhodium[37,38] and nickel[39].

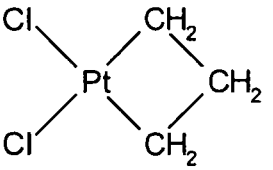

Fig. 15: Complex formed by addition of cyclopropane to platinum[36]

The driving force for this type of reaction is apparently strain relief by formation of the transition state and the coordination product. In many cases the addition reaction takes place only upon prior coordination of the organic molecule to the complex[34].

- Bonds between alkyl carbon and acyl carbon

Another type of C-C addition takes place with bonds, where one carbon is part of an acyl group. This reaction pathway is supported by the fact, that the C-CO bond is weaker than a standard C-C bond. In some reactions donor groups at the organic starting compound coordinate to the metal and are able to direct the orbitals of the metal towards the direction of the C-M bond, as observed in rhodium complexes[40] .(Fig. 16)

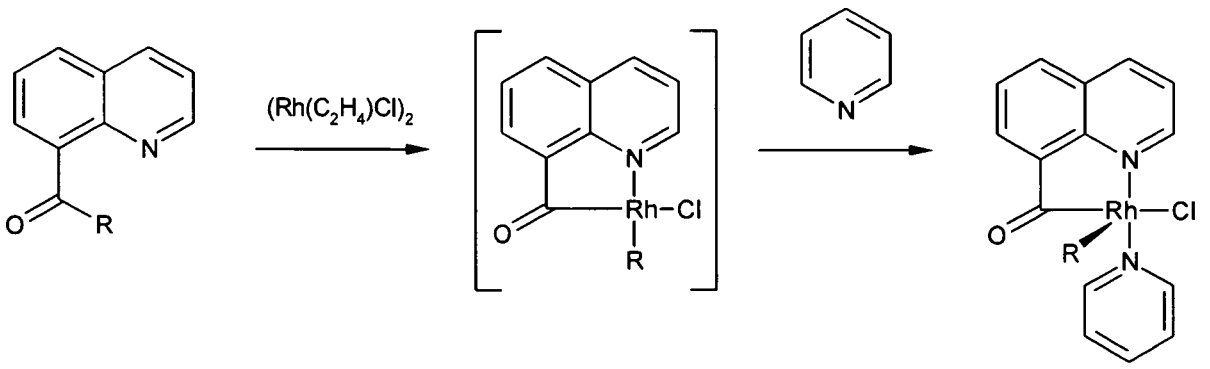

Fig. 16: Addition of a C_{acyl}-$C_{aliph.}$ bond to a rhodium complex[40]

Other examples of this mechanism have been reported for ruthenium complexes[41,42] (Fig. 17).

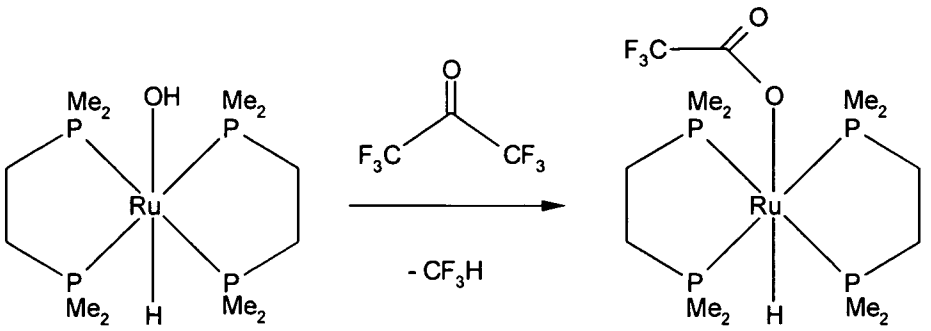

Fig. 17: Addition of a C_{acyl}-$C_{aliph.}$ bond to a ruthenium complex[41]

- Aromatization as a driving force

C-C bond addition has turned out to be thermodynamically advantageous, when an aromatic system is formed in one of the ligands[43,44] (Fig. 18). Apart from the thermodynamic advantage by aromatization, many metals, e.g. ruthenium, show a high affinity for aromatic ligands. This favours the reaction even more from a thermodynamic point of view[45].

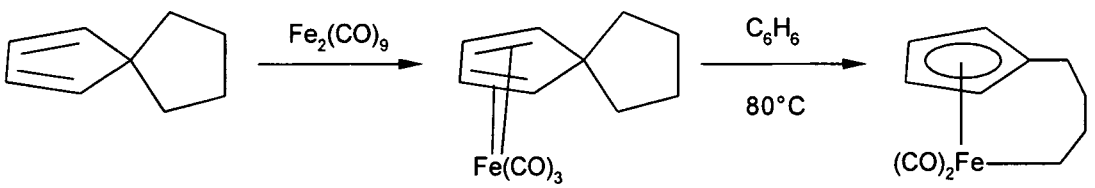

Fig. 18: C-C addition driven by aromatization[43]

- C-C bonds and complexes with P,C,P or P,C,N ligands

Important research on C-C bond activation was performed on mesitylene-based ligands with two phosphinomethyl groups[34] ("pincer ligands", Fig. 19).

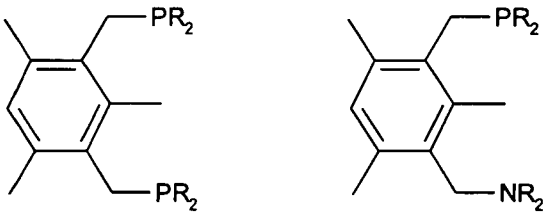

Fig. 19: P,C,P ligand (left), P,C,N ligand (right)[34]

Upon coordination of these ligands to transition metal complexes of rhodium, iridium and platinum, the C-C bond between the aryl and the methyl group between the donors was activated in many cases, resulting in elimination of a small molecule and very often coordination of a methyl ligand (Fig. 20[46], Fig. 21[47]).

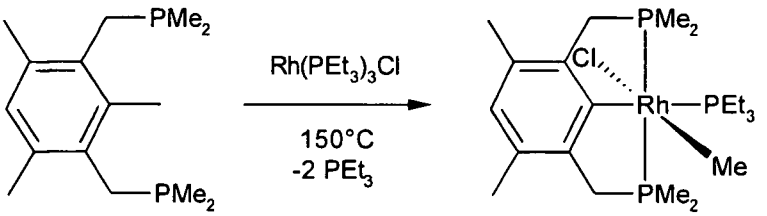

Fig. 20: Reaction of a rhodium complex with a P,C,P ligand[46]

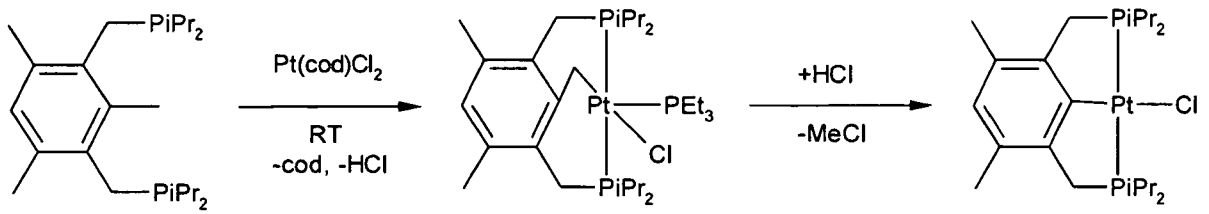

Fig. 21: Reaction of a platinum complex with a P,C,P ligand[47]

The main driving force behind this type of addition reactions is very often a thermodynamic advantage: In many cases the bond energy of metal-carbon bonds is equal or higher than the metal-hydrogen bond energy, especially when an aryl is coordinated to the metal by C-C addition[48]. This renders that pathway favourable despite the higher dissociation energy of the C_{aryl}-$C_{aliph.}$ bond compared to that of a C-H bond (103.5 kcal/mol vs. 83.7 kcal/mol[49]). It was

possible to increase the reactivity of the metal towards the C-C bond even more by replacing one phosphinomethyl group of the ligand by an aminomethyl group. Compared to the reaction with a similar P,C,P ligand not even an intermediate of a C-H activation product could be observed[50] (Fig. 22).

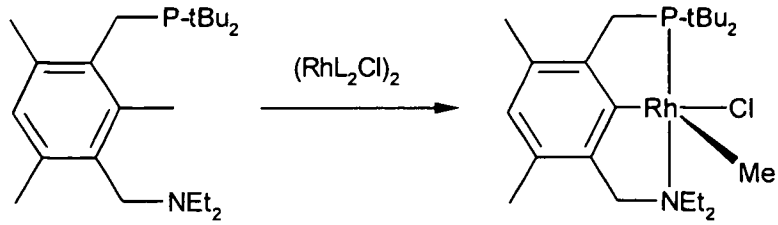

Fig. 22: Reaction of a rhodium complex with a P,C,N ligand[50]

1.2.7.5 Oxidative Addition of Si-Cl bonds

Oxidative addition of Si-Cl bonds is much more favourable than C-Cl activation from a thermodynamic point of view. While the bond dissociation energies of the Si-Cl bond and the C-Cl bond only differ by about 30 kcal/mol (113 kcal/mol for $(CH_3)_3Si$-Cl[51] vs. 83 kcal/mol for $(CH_3)_3C$-Cl[28]), the difference between the bond dissociation energies of the M-C and the M-Si bond is much higher (e.g. 233 kcal/mol for Pt-Si vs. 135 kcal/mol for Pt-C[52]), therefore the addition of Si-Cl can be expected to be much faster than the addition of C-Cl bonds.
Also Si-H bonds are susceptible to oxidative addition. If there are not only Si-Cl bonds but also Si-H bonds in a molecule, the situation is different than with chlorinated hydrocarbons. The bond dissociation energies of Si-H bonds are 10-20 kcal/mol lower than the ones of Si-Cl bonds[51], so Si-H activation is preferred.

1.2.8 NMR Spectroscopy in Platinum Complexes

1.2.8.1 General Considerations

The most important analytical method in this work was NMR spectroscopy, which was used to

gain information about the composition and structure of the reaction products as well as the conversion rates by comparison of the integration values in ^{1}H NMR spectra. The spectroscopic properties used in the structural determination were:

- The influence of the oxidation state of the platinum on the chemical shifts of the donors
- The dependency of the chemical shift of a donor on the nature of the ligand in *trans* position
- The coupling constants

1.2.8.2 ^{31}P NMR Spectroscopy

1D ^{31}P NMR spectroscopy was mainly used for fast identification of known reaction products and the oxidation state of their central metal. Since in all investigated systems only one phosphorus donor was present per complex, only one signal with platinum satellites was visible for each compound, what made it easy to monitor the progress of a reaction.

The first feature for structural determination of a complex was the oxidation state of the metal. Generally the chemical shift of ^{31}P is about 25-40ppm higher in Pt(II) complexes than in Pt(IV) compounds[53,54], this divided the complexes in this work in two groups: Square planar complexes with a ^{31}P chemical shift between 26 and 38ppm and octahedral species between 0 and 14ppm. With regard to structure determination, ^{31}P NMR gave useful information about the ligand in *trans* position. First, the stronger the *trans* influence of the ligand in that position is (high-field ligands), the stronger the chemical shift is moved downfield[53,55]. Second, the coupling constants are influenced by the σ-donor ability of the ligand in *trans* position. Strong σ-donors produce smaller $^{1}J_{Pt\text{-}P}$ couplings by elongation of the opposite Pt-P bond[53,56] (Fig. 23).

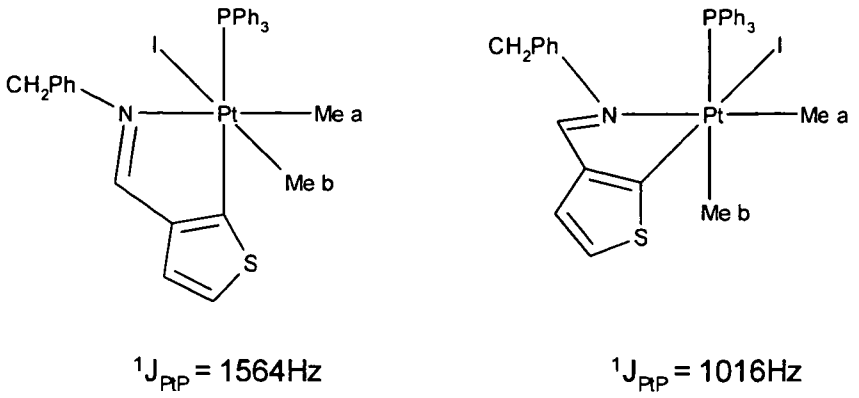

$^1J_{PtP}$ = 1564Hz $^1J_{PtP}$ = 1016Hz

Fig. 23: Dependency of $^1J_{PtP}$ coupling constants on the ligand in *trans* position[54]

In contrast, 2D ^{31}P NMR was used for determination of the type of ligands of newly formed complexes. Here correlation of ^{1}H and ^{31}P NMR spectra was the method of choice.

1.2.8.3 ^{195}Pt NMR Spectroscopy

^{195}Pt NMR measurements were performed in 2D mode for determination of the ligands bound to newly formed compounds. As usually in NMR spectroscopy the electronegativity of the neighbouring groups (in that case the ligands) also has an influence on the chemical shift: The higher it is, the more the signal is shifted downfield[57]. Therefore the shift values of different complexes can be used to determine the coordination sphere.

1.2.8.4 Methyl Ligands

The NMR signals of the methyl ligands gave useful information about the structure of the complexes. In this work platinum complexes with a *P,N*-chelated ligand were investigated. In square planar complexes with a P,N ligand the chemical shift of the methyl protons in *trans* position to the phosphorus can be found more upfield than in *trans* position to the nitrogen[58].
In octahedral compounds, the methyl group can also be situated axial to P-Pt-N. Typical examples for the chemical shifts and coupling constants of the methyl protons in *trans* position to P and N in octahedral platinum complexes were found in literature[54]:

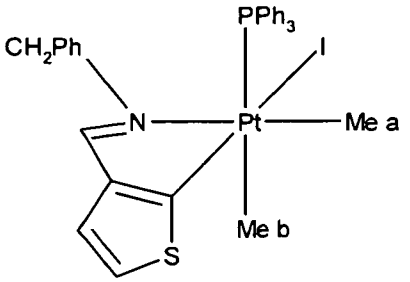

Fig. 24: Reference complex 1

Table 1: ^{1}H chemical shifts of reference complex 1

Methyl group	δ (ppm)	$^{3}J_{PH}$	$^{2}J_{PtH}$
a	1.69	7 Hz	68 Hz
b	1.15	8 Hz	60 Hz

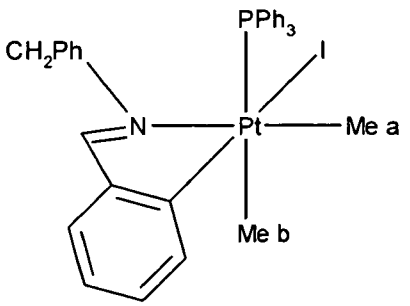

Fig. 25: Reference complex 2

Table 2: ^{1}H chemical shifts of reference complex 2

Methyl group	δ (ppm)	$^{3}J_{PH}$	$^{2}J_{PtH}$
a	1.56	7 Hz	70 Hz
b	1.12	8 Hz	62 Hz

Also in that paper data for a methyl group out of the P-Pt-N plane was found:

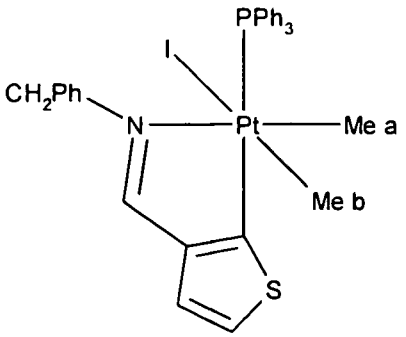

Fig. 26: Reference complex 3

Table 3: ^{1}H chemical shifts of reference complex 3

Methyl group	δ (ppm)	$^{3}J_{PH}$	$^{2}J_{PtH}$
a	1.50	7 Hz	68 Hz
b	0.35	7 Hz	67 Hz

Methyl groups in *trans* position to N or P ligands obviously show chemical shifts higher than 1ppm in the ^{1}H NMR spectrum, where the shift of the methyl protons opposite to the nitrogen has a higher value. The signals of methyl groups out of the P-Pt-N plane in *trans* position to a halogen are found more upfield. Considering the coupling constant $^{2}J_{PtH}$,the values for the methyl groups in *trans* position to nitrogen and iodine were found to be around 70Hz, while the values for the *trans* phosphine methyl group are around 60Hz. Data that match these tendency were also found in other publications[56,59].

With this data it was possible to determine the structure of the complex [(κ^2-*P*,*N*)-$Ph_2PCH_2CH_2NMe_2$]$PtMe_3Cl$ (**B1**, see chapter 1.2.11.2), an intermediate that is found very often in the current and previous work[60]. These data can be used for the structure determination of other complexes with P,N ligands.

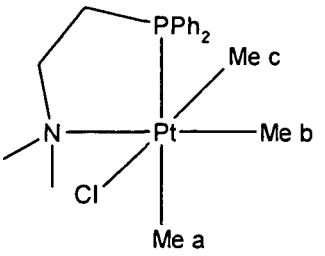

Fig. 27: Complex **B1**

Table 4: ^{1}H chemical shifts of complex **B1**

Methyl group	δ (ppm)	$^{3}J_{PH}$	$^{2}J_{PtH}$
a	1.61	8.1 Hz	57 Hz
b	2.03	7.0 Hz	73 Hz
c	0.61	7.7 Hz	71 Hz

1.2.9 Technical Applications

The most important technical application of transition metal complexes is in catalysis, where they are widely used. Their high selectivity is due to five major reasons[61]:

- Coordination of reagents leads to a very short spacial distance between them.
- Coordination can facilitate nucleophilic attack
- Chiral complexes provide asymmetric induction for enantioselective syntheses
- The easy modification of their properties by changing the coordination sphere of the central cation enables very specific reactions with the substrate

Basically there are two types of catalytic systems: Either the catalyst is fixed to a surface[62] or a phase boundary (heterogeneous catalysis) or it is dissolved in the reaction medium (homogeneous catalysis).

Catalytic cycles consist of coupled reaction steps. In the case of homogeneous catalysis with transition metal complexes, the individual steps of the cycle are identical to the most important reaction classes described above:

- Reactions with Lewis acids
- Association / dissociation of a Lewis base ligand
- Oxidative addition / reductive elimination
- Migratory insertion / extrusion
- Oxidative coupling / reductive decoupling

Since the catalytically active species are in the majority of cases formed during the catalytic cycle, the transition metal complex used for the reaction should correctly be called a catalyst precursor.

The properties of a catalytic system depend on the metal, the ligands and the solvent[63]. While the choice of the metal is rather based on empirical data, the ligands can be chosen by electronic and geometrical considerations. The basicity of the ligand strongly influences the electron density on the metal. The tip angle of the cone made up by the metal and the substituents on the ligand (ligand cone angle) affects the accessibility of the metal centre and the bite angle between the two donors of a chelating ligand strongly influences the rate of coordination and reductive elimination of ligands. The solvent is chosen by its chemical and thermal stability in the catalytic process as well by its polarity and by its reactivity.

1.2.10 Medical Applications

In 1961 the physicist *Barnett Rosenberg* started his research at the Biophysics Department at Michigan State University. Being fascinated by the optical similarity of magnetic field lines and the mitotic figures that can be seen in eukaryotic cells during the process of division he was curious to see, whether alternating electrical fields somehow influence the growth of cells[64]. He fitted a culture with platinum electrodes to generate the alternating field. The first test was not performed on eukaryotes, but on *Escherichia coli* bacteria. When turning on the field, the bacteria stopped fissioning but still continued to grow, resulting in multi-bacterial filaments about 300 times longer than the normal bacteria, but after turning off they resumed their ordinary growth behaviour. By investigation of the chemical processes in the solution they discovered,

that three different platinum compounds were present in the culture solution, namely $(NH_4)_2[PtCl_6]$, $[Pt^{IV}(NH_3)_2Cl_4]$ and $[Pt^{II}(NH_3)_2Cl_2]$. By applying these compounds separately to *E. coli* cultures they discovered, that the latter compound in its *cis* configuration was the one responsible for the unusual growth of the bacteria.

Eventually this compound, already discovered in 1845 by Michel Peyrone[65], became interesting for cancer therapy since it seemingly inhibited cell growth without being very toxic, since the bacteria were not killed and returned to their normal behaviour after application. In these tests the compound exhibited strong activity against various tumors and was applied as anti-cancer drug under the name *cisplatin* from 1978 on.

The mechanism of action of this compound consists of a series of nucleophilic ligand substitutions in the patient's body. After being applied it retains its original composition due to the high chlorine concentration in the blood. It is eventually bound to proteins, namely *apotransferrin* and *albumin*, where it is presumably attached to disulfide bridges and thiol groups[66] by nucleophilic ligand substitution. In that form, and also by simple diffusion, it is transferred into the cytoplasm of the tumor cells. There the chlorine concentration is much lower than in the blood, and therefore the chlorine ligands are replaced by water molecules. The diaqua species then reacts with the nitrogen of guanine in the DNA and forms mainly intrastrand crosslinks between two purine bases (which explains the low activity of the *trans*-form, that seemingly does not have the right geometric properties to support this double ligand substitution). The structure of the DNA is modified through this coordination in a way that renders replication no longer possible and the targeted cell then conducts its self-termination, called *apoptosis*.

In the past years two other Pt(II) complexes with anti-tumor activity were put on the market, called *carboplatin* and *oxaliplatin*, other compounds are under research.

1.2.11 Platinum Complexes with Hemilabile Ligands

1.2.11.1 Properties

Hemilabile ligands are chelating ligands with at least two different donor centres. Due to the different bonding strength of these donors to the metal, temporal decoordination of one donor is possible, while the other remains bonded. The emerging vacant coordination site on the metal is now available for different reactions such as ligand additions or abstractions. Since the de-coordinated donor stays close to the metal centre, the partial de-coordination of the chelating ligand is an easily reversible process. Recoordination can occur after elimination of a molecule from the coordination sphere, its transformation in a more weakly coordinated ligand than the dissociated donor or migratory insertion reactions (Fig. 28). This renders complexes with hemilabile ligands very useful for catalysis as well as the study of biochemical reactions that contain metalloenzymes with proteins as ligands[67].

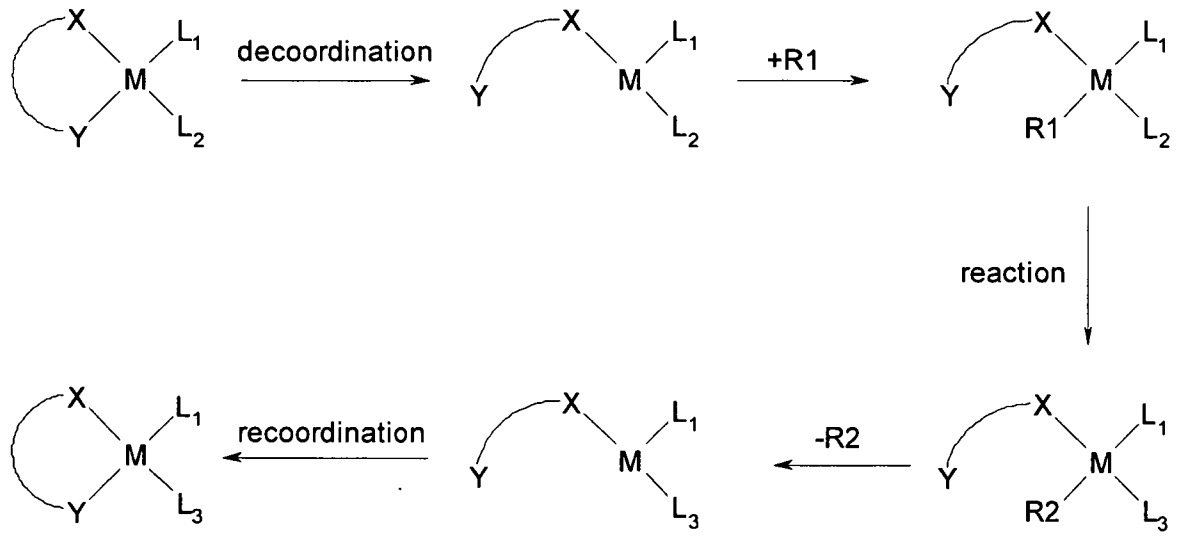

Fig. 28: A reaction enabled by a hemilabile of a ligand

The three most important groups of hemilabile ligands are carbon based, nitrogen based and phosphorus-based hemilabile ligands, named after the group with a lower tendency for de-coordination.

1.2.11.2 Reactions of *P,N*-chelated Platinum Complexes

P,N chelated ligands are very interesting in platinum chemistry due to the high stability of the P-Pt bond, the stabilizing effect of nitrogen donors for Pt(IV) compounds, the considerable π-acceptor ability of the phosphorous and the strong *trans* effect of the phosphorous in square planar Pt(II) compounds.

Several new platinum complexes with *P,N* ligands (Fig. 29) were previously synthesized in our group to explore their scope of reactivity towards silanes, stannanes or organic compounds.

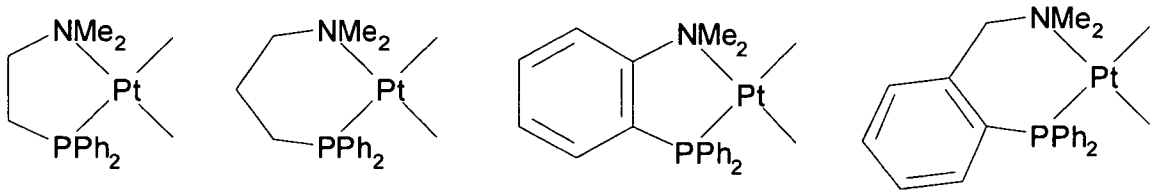

A1 **A2** **A3** **A4**

Fig. 29: *P,N* coordinated platinum complexes

The complexes **A1-A4** were reacted at 60°C with 1,2-bis(dimethylsilyl)benzene in a molar ratio of 1:2[58]. Reactions with the complexes **A1**, **A3** and **A4** yielded square planar complexes with bis(dimethylsilyl)benzene ligands as well as methane and 1-dimethylsilyl-2-trimethylsilylbenzene (Fig. 30). Reaction with **A2** led to formation of four different complexes that were not identified.

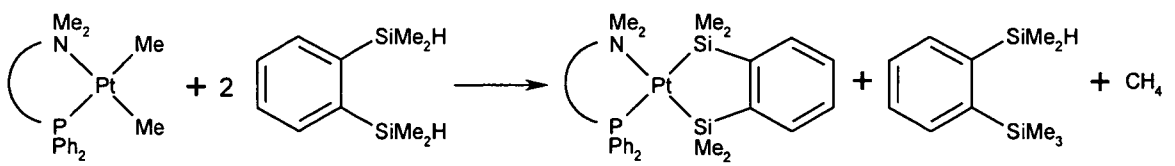

Fig. 30: Reaction with 1,2-bis(dimethylsilyl)benzene

On reaction with trimethoxysilane, complex **A1** was transformed into a methyl-trimethoxysilyl complex and a bis-trimethoxysilyl complex. Methyltrimethoxysilane, tetramethoxysilane, and small amounts of pentamethoxydisiloxane and hexamethoxydisiloxane were identified as by-products (Fig. 31)[68].

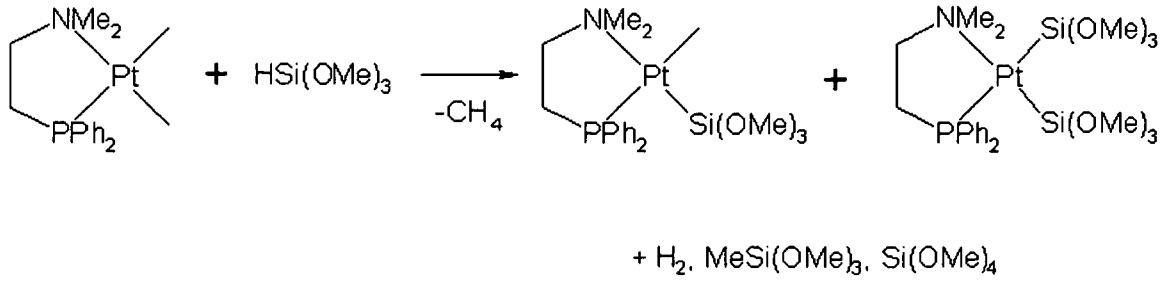

Fig. 31: Reaction of A with trimethoxysilane

Two reactions with silyl halides have been performed. Reaction of the compounds **A1-A4** with iodo-trimethylsilane yielded tetramethylsilane and [(κ^2-*P*,*N*)-$Ph_2PCH_2CH_2NMe_2$]PtMeI[58] (**D3**, Fig. 32). With chloro-dimethylphenylsilane, the complex [(κ^2-*P*,*N*)-$Ph_2PCH_2CH_2NMe_2$]PtMeCl (**D1**) and dimethyl-tetraphenyldisilane was formed, as well as methyl chloride, which adds to the starting compound **A1** likewise (Fig. 33)[60]. The resulting complex [(κ^2-*P*,*N*)-$Ph_2PCH_2CH_2NMe_2$]$PtMe_3Cl$ (**B1**) can be transformed into **D1** by elimination of ethane.

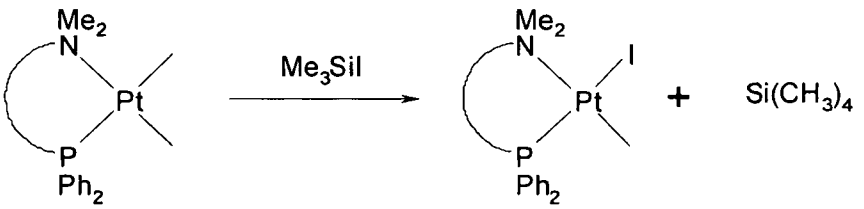

Fig. 32: Reaction of **A1** with iodotrimethylsilane

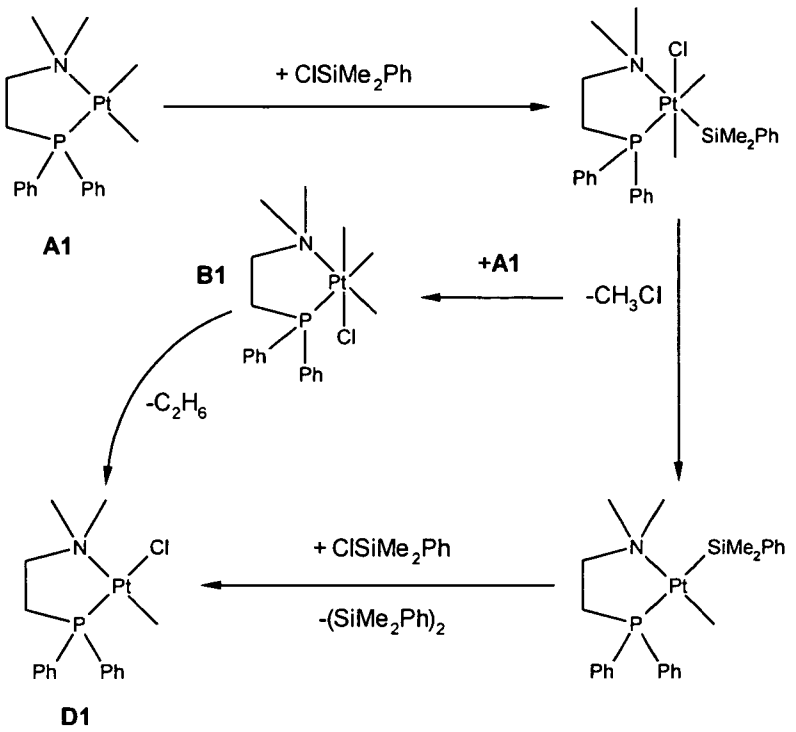

Fig 33: Reaction of **A1** with $ClSiMe_2Ph$

Studies of the reaction rate of different complexes showed clearly, that the reactivity correlates with the ability of nitrogen decoordination, which is the highest for complex **A1**[69]. The complex $[(\kappa^2\text{-}P,N)\text{-}Ph_2PCH_2CH_2NMe_2]PtMeCl$ proved to act as catalyst for transformation of hydrosilanes into chlorosilanes via dechlorination of chlorinated hydrocarbons[70].

Complex **A1** has also been reacted with small chlorinated hydrocarbons, namely CCl_4, $CHCl_3$, CH_2Cl_2 and CH_3Cl, where it proved its ability to activate the C-Cl bond by oxidative addition[60]. The reaction was the fastest with CCl_4, what may be due to the fact, that the bond strength between C and Cl is the lowest in that molecule, what renders oxidative addition easier.

1.3 Motivation and Objectives

As mentioned above, complex **A1** shows the highest reactivity in oxidative addition reactions. While the reactivity of this compound with different hydrosilanes and stannanes has been extensively investigated, only few experiments have been conducted with halogenated

hydrocarbons. The used compounds were only methane derivatives, thus no information about the influence of different types of substituents in the β-position or steric influences on the rate and the outcome of a reaction was obtained. The starting point of the current work was thus to investigate the effect of the organic halide on the processes.

Another goal of the work was to investigate the influence of different halogens on the oxidative addition and the subsequent reactions. An important issue was to find out, whether reactions of complex **A1** are only specific for these compounds or whether they represent more general pathways for type **A** complexes with halogenated compounds (Fig. 34).

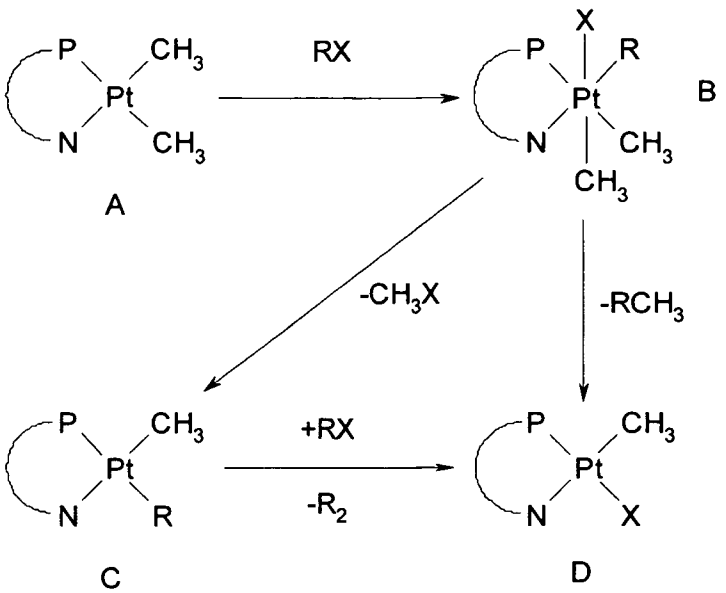

Fig. 34: The possible general reaction pattern

Only one experiment was previously conducted with silyl chlorides, this reaction yielded a disilane (Fig 33). Reactions between silyl chlorides and compound **A1** could offer new possibilities for the formation of Si-Si bonds and the formation of silicon backbones in inorganic polymers. In this work, reactions between **A1** and a variety of silyl monochlorides and dichlorides were to be investigated, with the focus on the formation of bonds between silicon, dechlorinated by the oxidative addition reaction, and other molecules in the coordination sphere.

2. Results and Discussion

2.1 Experimental Conditions

The experiments described in this thesis were carried out as NMR experiments. The starting complexes (20mg if not mentioned otherwise) were dissolved in deuterated benzene in a Young tube under argon, then the organic compounds were added to this solution from a Schlenk vessel. In case of solid reactants they were dissolved in 0.1ml of deuterated benzene under argon. This solution was then added to the solution of the complex. The reactions were left to subside for five minutes, then NMR spectra were taken. All reaction mixtures were left at room temperature for 18 hours. If no reaction took place they were then heated to 70°C. NMR spectra were regularly taken.

For GC/MS analysis the reaction mixtures were passed through silica gel to remove the complexes that would otherwise spoil the column. They were then diluted with CH_2Cl_2 to obtain a concentration of less than 1mg/ml for the measurement. Since the silyl chlorides described in chapter 2.6 could not pass the silica, the reaction mixtures containing these compounds were treated with methanol to transform the silyl chlorides to methoxysilanes, which were then detected by GC/MS.

2.2. Reactions with Halogenated Hydrocarbons with CH_x-Groups in the β-Position

2.2.1 Chlorides

2.2.1.1 1,3-Dichloropropane

The reactions between complex **A1** and 1,3-dichloropropane were carried out at molar ratios of 1:1 and 1:2. At room temperature no reaction was visible at both ratios. After heating to 70°C a very slow reaction was monitored by NMR. Only 30% of **A1** were converted into **D1** within three weeks. In the ^1H NMR spectrum CH_4 was visible, but no signals of 1,6-dichlorohexane and 1-chlorobutane, the products of dehalogenative coupling or methylation of the starting halide. In the GC/MS spectrum only the signal of the starting compound could be observed. No new

complexes were identified as well. During the reaction an amorphous precipitate was formed, that could not be dissolved in any standard NMR solvent. Closer examination of the ^{1}H NMR spectrum between 4 and 6 ppm revealed weak signals that seem to belong to allyl chloride (Fig. 35).

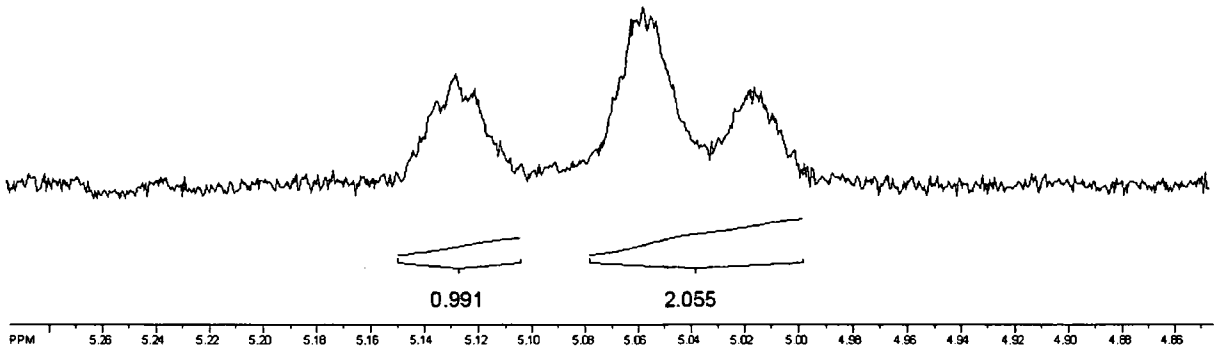

Fig. 35: Section from the ^{1}H NMR spectrum of the reaction of complex **A1** with 1,3-dichloropropane

Obviously β-elimintion of allyl chloride takes place through abstraction of a proton from the coordinated CH_2 group of the chloropropyl ligand after oxidative addition of one C-Cl group of the starting halide. The abstracted proton is then transferred to one CH_3 ligand and methane is subsequently eliminated from the complex, leaving behind complex **D1** (Fig. 36). Since no octahedral species could be identified in the NMR spectrum, the oxidative addition of the C-Cl bond appears to be the rate-determining step. The amount of of allyl chloride visible in the NMR spectra cannot explain the conversion of about 30% of complex **A1**, since the reaction conditions (heat, no oxygen) support radical polymerization reactions the amorphous precipitate could consist of polymerized allyl chloride.

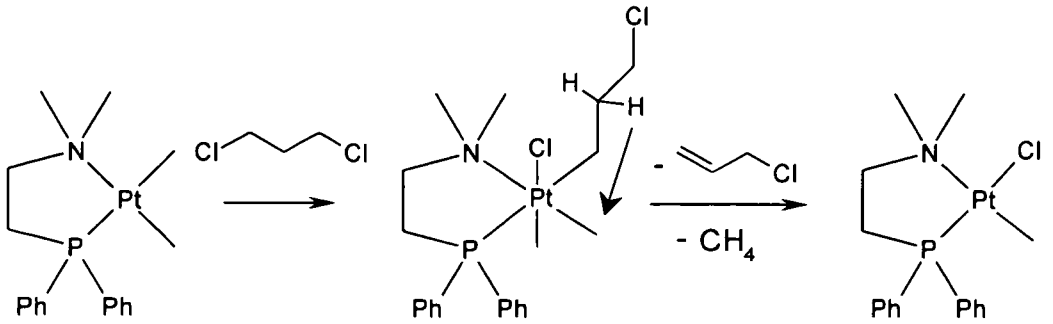

A1 **D1**

Fig. 36: Addition of 1,3-dichloropropane and elimination of allyl chloride

2.2.1.2 (3-Chloropropyl)trimethylsilane

(3-Chloropropyl)trimethylsilane was reacted with complex **A1** at the stoichiometric ratios of 1:1, 1:2 and 1:4. No reaction was visible at room temperature and also after heating up to 70°C only very slow formation of signals of complex **D1** could be monitored. The reaction was stopped after one week, no signals in the vinylic region of the ^{1}H NMR spectrum were visible.

2.2.2 Bromides

2.2.2.1 1,3-Dibromopropane

The reactions with 1,3-dibromopropane were performed at molar ratios 1:1, 1:2, 1:4 and 1:24. At room temperature no reaction was observable at any ratio. After heating at 70°C **A1** was completely consumed within 65 hours at a 1:1 ratio, within 48 hours at a 1:2 ratio, within 32 hours at a 1:4 ratio and within one hour at a 1:24 ratio. In the ^{1}H NMR spectrum, signals of the same appearance like those of **D1** were visible, but at slightly different chemical shifts (Fig. 37) as well as two double triplets at 0.61 (J= 7.6 and 70,3 Hz) and 2.0ppm (J= 6.9 and 72 Hz) and a singlet with satellites at 2.68ppm. In the ^{31}P NMR spectrum a new signal with platinum satellites emerged at 6.55ppm. According to the data known about chemical shifts and coupling constants in the platinum complexes used in that work (see table 4, p. 23) they belong to two methyl

groups in *trans* position to nitrogen and halogen, what renders it possible to define this complex as [(κ^2-*P*,*N*)-$Ph_2PCH_2CH_2NMe_2$]Pt((CH_2)$_2$Br)Me_2Br (**B3**, Fig. 38). The signal at 6.55ppm in the ^{31}P NMR spectrum is in the region of the octahedral complexes and is therefore apparently the signal of complex **B3**. A precipitate was formed, consisting of crystals and an amorphous phase.

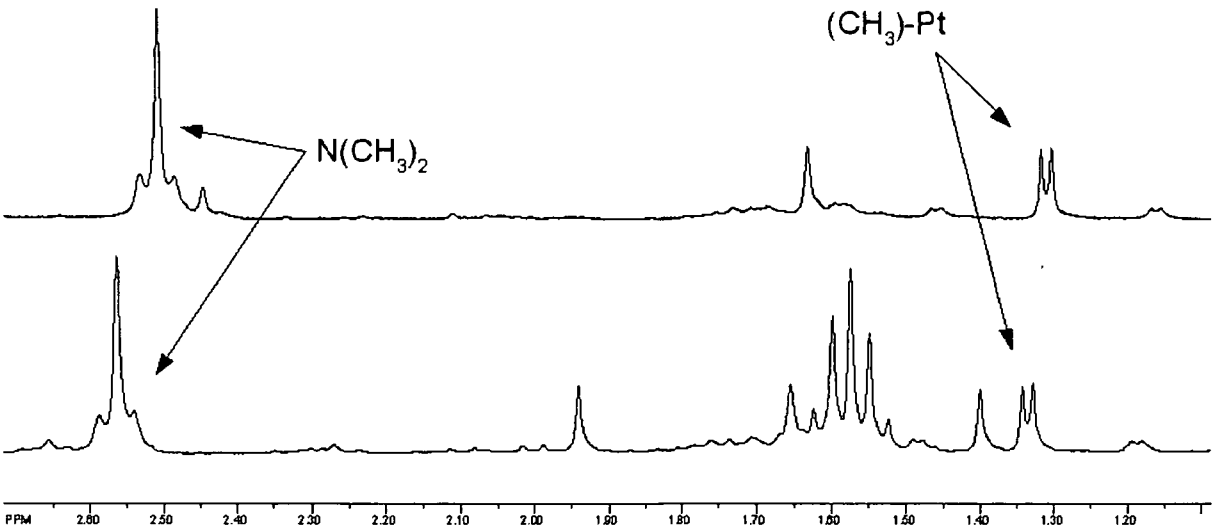

Fig. 37: Section from the ^{1}H NMR spectra of complex **D1** (top) and complex **D2** (below)

The crystals were identified as [(κ^2-*P*,*N*)-$Ph_2PCH_2CH_2NMe_2$]PtMeBr (**D2**, Fig. 39). Since the NMR analysis also showed the presence of allyl bromide and methane, β-elimination alsp appears to take place (Fig. 38). In comparison to the chlorinated compounds with CH_2-groups in the β-position oxidative addition takes place much faster with brominated compounds (as expected due to the bond dissociation energy that is about 10 kcal/mol lower for the C-Br bond compared to the C-Cl bond[28]) and it is obviously also much faster than the elimination of the allyl bromide. Therefore, the octahedral complex became and stayed visible in the ^{31}P NMR spectrum. Due to its low boiling point, allyl bromide was not detected in the GC/MS-analysis.

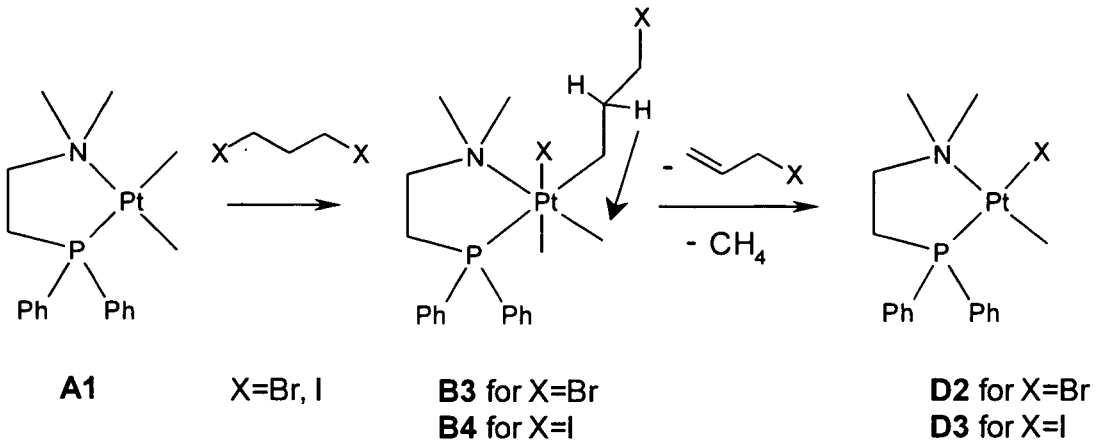

Fig. 38: Reaction of **A1** with 1,3-dibromopropane and 1,3-diiodopropane

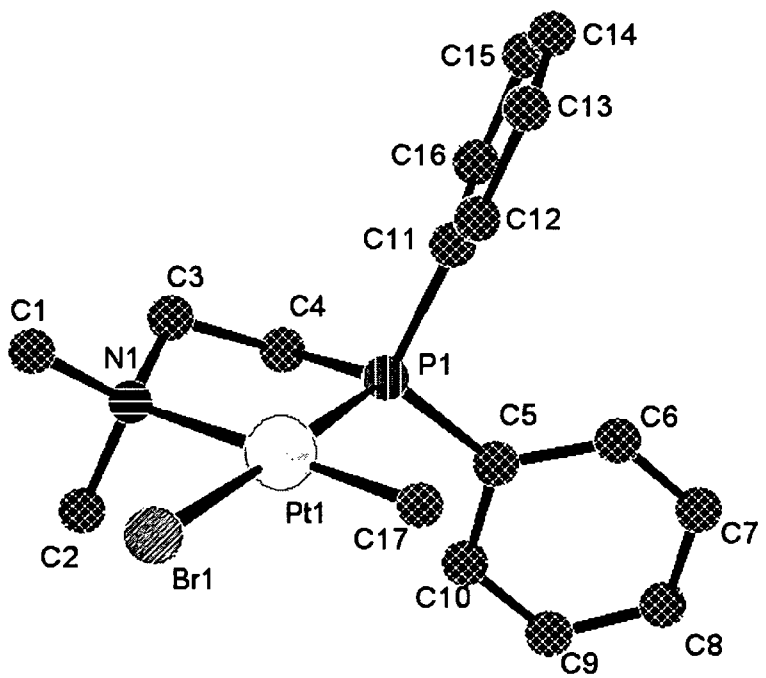

Fig. 39: Molecular structure of [(κ^2-*P*,*N*)-$Ph_2PCH_2CH_2NMe_2$]PtMeBr (**D2**)

Table 5: Selected bond lengths and angles of complex **D2**

Bond lengths (Å)	
Pt-C	2.017(14)
Pt-Br	2.491(19)
Pt-P	2.180(4)
Pt-N	2.213(13)
Bond angles (°)	
P(1)-Pt(1)-N(1)	85.6(4)
C(17)-Pt(1)-P(1)	92.3(4)
C(17)-Pt(1)-Br(1)	89.3(4)
N(1)-Pt(1)-Br(1)	92.8(4)

Additionally a group of non assignable signals was found around 6ppm in the ^{1}H NMR spectrum (Fig. 40). These signals will be discussed in chapter 2.5.6.

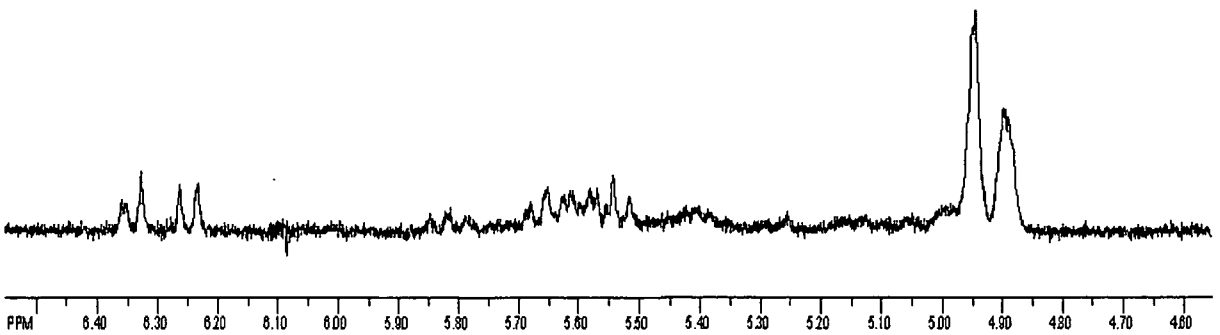

Fig. 40: Unknown signals in the reaction of A1 with 1,3-dibromopropane

2.2.2.2 1,6-Dibromohexane

1,6-Dibromohexane was reacted with **A1** at molar ratio 1:2. At room temperature no reaction

was visible, at 70°C the reaction was finished after 4 days. Also here complex **D2** was formed and clear signals of methane and 6-bromo-1-hexene were visible in the ^{1}H NMR as well as in the GC/MS-analysis, thus β-elimination also took place. An octahedral intermediate could not be monitored, apparently it is converted much faster than complex **B3** in the reaction with 1,3-dibromopropane. A precipitate was formed, but no crystals could be extracted from that. Signals similar to the ones in Fig. 40 were also found in the ^{1}H NMR spectrum (see chapter 2.5.6).

2.2.3 Iodides

2.2.3.1 1,3-Diiodopropane

The reactions with 1,3-diiodopropane were carried out at molar ratios 1:0.25, 1:1, 1:2, and 1:4. At room temperature no reaction took place. After heating to 70°C the reactions proceeded very fast, **A1** was completely consumed after one hour at any ratio, [(κ^2-*P*,*N*)-$Ph_2PCH_2CH_2NMe_2$]PtMeI, **D3** was identified as reaction product by ^{1}H NMR spectroscopy (Fig. 41).

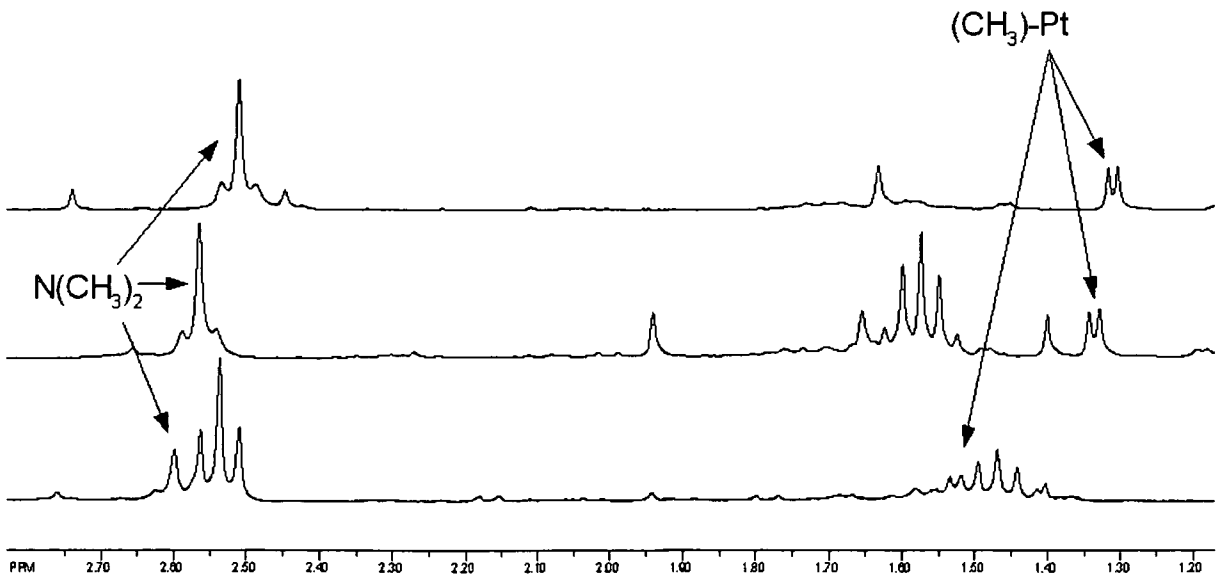

Fig. 41: Section from the ^{1}H NMR spectra of complex **D1** (top), **D2** (middle) and complex **D3** (below)

Complex **D3** crystallized from the reaction solution together with an amorphous phase. The molecular structure could be determined by X-ray diffraction of the crystals (Fig. 22).

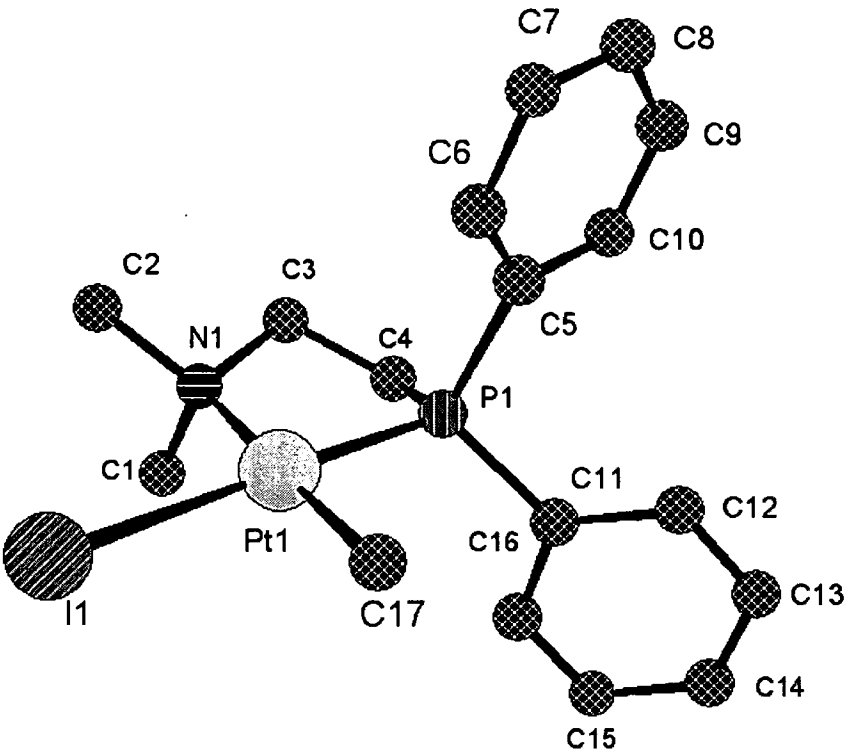

Fig. 42: Molecular structure of [(κ^2-*P*,*N*)-$Ph_2PCH_2CH_2NMe_2$]PtMeI (**D3**)

Table 6: Selected bond lengths and angles of complex **D3**

Bond lengths (Å)	
Pt-C	2.065(4)
Pt-I	2.6694(4)
Pt-P	2.1776(13)
Pt-N	2.217(4)
Bond angles (°)	
P(1)-Pt(1)-N(1)	85.31(11)
C(17)-Pt(1)-P(1)	91.04(12)
C(17)-Pt(1)-I(1)	89.76(11)
N(1)-Pt(1)-I(1)	93.87(11)

In this reaction the octahedral intermediate [(κ^2-*P*,*N*)-$Ph_2PCH_2CH_2NMe_2$]Pt($(CH_2)_3I$)IMe_2 (**B4**) was also observed, its methyl signals were found at 0.78ppm ($^2J_{PtH}$= 68.8 Hz) and 2.17ppm ($^2J_{PtH}$= 71.2 Hz) in the ^1H NMR spectrum. It also undergoes β-elimination (Fig. 38), but its stability is much higher than that of the brominated octahedral intermediate **B3**, so only very little allyl iodide, as elimination product, was visible, while the signal of **B4** disappeared very slowly. In the ^1H NMR spectrum signals similar to the ones in Fig. 40 were found and will also be discussed in chapter 2.5.6.

2.2.3.2 1,6-Diiodohexane

Reactions with 1,6-diiodohexane were performed at molar ratios 1:1, 1:2 and 1:4. As with 1,3-diiodopropane no reactions were observed at room temperature. After heating to 70°C **A1** was completely consumed within 24 hours at all ratios. Also this reaction proceeded via β-elimination, **D3**, [(κ^2-*P*,*N*)-$Ph_2PCH_2CH_2NMe_2$]Pt($(CH_2)_6I$)IMe_2 (**B5**) and 6-chloro-1-hexene were identified as reaction products, signals similar to the ones in Fig. 40 (p. 36) were also present here (to be discussed in chapter 2.5.6).

2.2.4 Conclusions

This chapter shows, that the main reaction pathway of halogenated hydrocarbons with CH_2-groups in β-position is β-elimination of an unsaturated compound. The rate of the elimination reaction seemingly does not very much depend on the nature of the halogen, the main factor that influences this reaction is the rate of oxidative addition to the platinum atom, that is, very slow for C-Cl bonds, so the reactions do not take place easily. With bromides and iodides the addition takes place very fast. Since the elimination is very slow, the octahedral intermediate, formed by this addition reaction can be monitored very well by NMR spectroscopy. In no case a binuclear complex, formed by activation of both C-X bonds of the same starting compound by two complexes was monitored. The reactions also yielded amorphous precipitates that could possibly be formed by polymerisation of the eliminated halogenated olefins.
A halogen-methyl complex is the main product with all compounds, the complexes **D2** and **D3** were synthesized for the first time.

Table 7: NMR signals of the complexes D**1**, D**2** and D**3**

Complex	^{31}P [ppm]	^{1}H of $N(CH_3)_2$ [ppm]	^{1}H of Pt-CH_3 [ppm]
D1	27.15	2.51	1.31
D2	28.17	2.54	1.33
D3	28.9	2.62	1.52

2.3 Reactions with Halogenated Hydrocarbons without CH_2- Groups in the β-Position

As seen in chapter 2.1, halogenated hydrocarbons with CH_2 groups in the β-position tend to yield 1-alkenes and methane by β-elimination while there is no evidence for methylation or coupling of the dehalogenated compounds. Compounds without a CH_2 group neighbouring the halogenated carbon cannot undergo such an elimination reaction. This raises the question, what can happen to this group of halogenated hydrocarbons after activation of the C-X bond.

2.3.1 Chlorides

2.3.1.1 Chlorocyclohexane

Chlorocyclohexane was reacted with **A1** at a molar ratio of 1:2. Since no spectroscopic evidence for a reaction was visible at room temperature, the reaction mixture was heated to 70°C, with nearly no effect at all. After one week at 70°C only a tiny signal for complex **D1** was visible in the ^{31}P NMR spectrum, in the ^{1}H NMR spectrum no new signal big enough to be distinguishable from the educts was visible.

2.3.1.2 Chlorobenzene

Chlorobenzene was added to **A1** at a molar ratio of 1:2. Here also no reaction could be monitored in the NMR spectra at room temperature. Heating to 70°C did not change the picture, after one week a signal for **D1** even smaller than for the reaction with chlorocyclohexane was visible in the ^{31}P NMR spectrum, the ^{1}H NMR spectrum showed no new signals at all.

2.3.1.3 2,2-Dichloropropane

2,2-Dichloropropane was reacted with complex **A1** at a ratio of 1:2. No evidence for a reaction was visible at room temperature in the NMR spectra, so the reaction mixture was heated to 70°C. Here also nearly no reaction could be observed by NMR spectroscopy, after one week the experiment was finally stopped. Only a small signal of complex **D1** was visible in the ^{31}P NMR spectrum, the ^{1}H NMR spectrum only showed the starting complex.

2.3.1.4 Chloroacetic Acid

To find out whether C-Cl bond activation is strong enough to compete with an acid for coordination sites, complex **A1** was reacted with chloroacetic acid. The reactions were performed at a molar ratio of 1:2. The reaction with the acid took place immediately. In the

^{31}P NMR spectrum two signals became visible, a small one for complex **D1** and an intense signal at 20.82 ppm. Methane, a very small signal for complex **D1** and several new signals became visible in the ^{1}H NMR spectrum (Fig. 43). Two of these signals (at 4.17 and 0.97ppm) could be assigned to platinum-coordinated carboxylate by means of EXSY measurement. The signal at 20.82ppm in the 31P NMR spectrum was correlated to these signals in a P/H HMBC spectrum. No other complexes could be identified, apparently the main reaction mechanism with chloroacetic acid is formation of complex $[(\kappa^2P,N)Ph_2PCH_2CH_2NMe_2]Pt(OOCCH_2Cl)Me$ (**C1**) by coordination of the oxygen to platinum through elimination of one methyl ligand as methane with the acid's proton (Fig. 44).

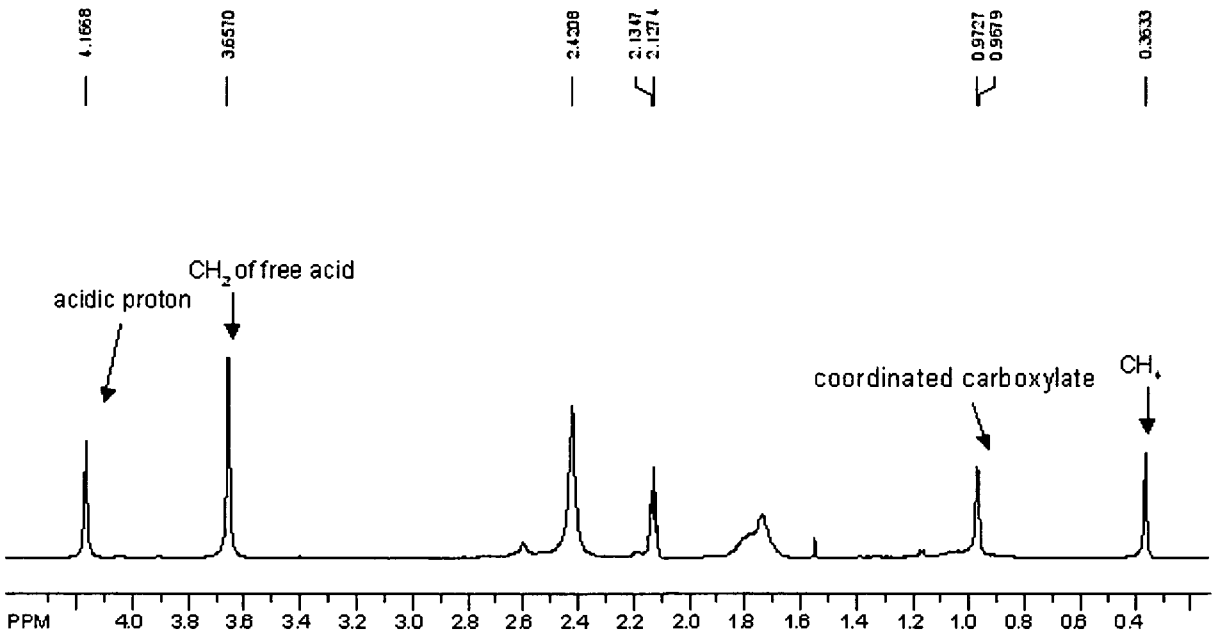

Fig. 43: Section from the ^{1}H NMR spectrum of the reaction of **A1** with chloroacetic acid

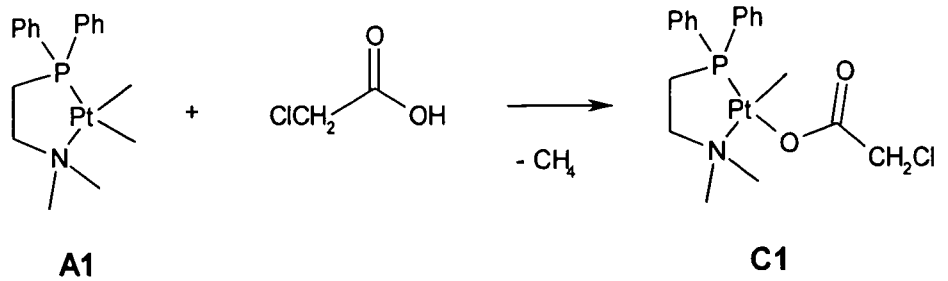

A1 **C1**

Fig. 44: Reaction of **A1** with chloroacetic acid

As in the experiments with bromides and iodides carrying β-CH_2 groups also here a group of non assignable signals was found around 6ppm in the ^{1}H NMR spectrum (Fig. 45). These signals will also be discussed in chapter 2.5.6.

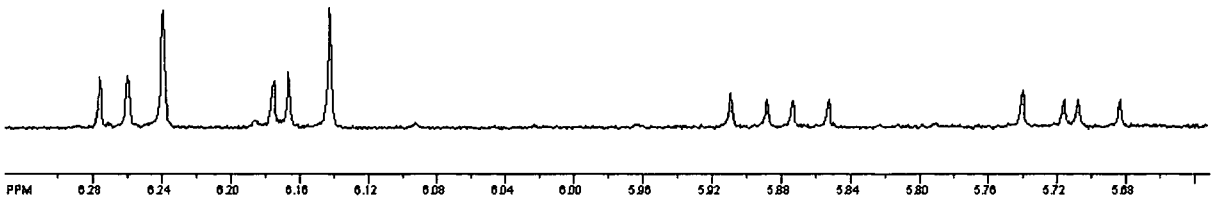

Fig. 45: Non-assignable signals in the reaction of **A1** with chloroacetic acid

2.3.1.5 Propargyl Chloride

Propargyl chloride was added to complex **A1** at a molar ratio of 1:2. The reaction with this compound proceeded very fast at 70°C, after 20 hours complex **A1** was completely consumed. During the reaction two new signals were visible in the ^{31}P NMR spectrum at 12.49 and 9.79 ppm. In the ^{1}H NMR spectrum methane was observed and several signals appeared in the range of the double bond signals around 6 ppm (Fig. 46), similar to the ones found for the reactions with bromides and iodides with β-CH_2 groups and chloroacetic acid. These signals will be discussed in chapter 2.5.6. Only a small amount of complex **D1** was detected in the NMR spectra.

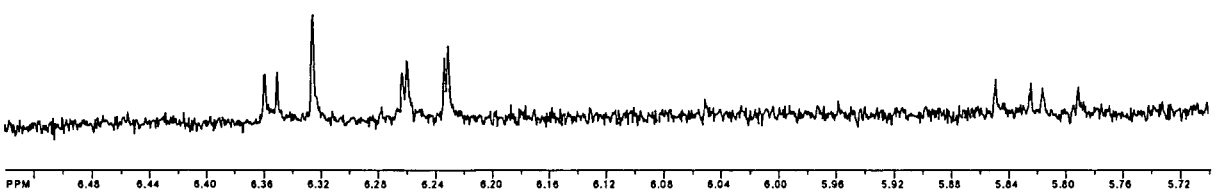

Fig. 46: Non-assignable signals in the reaction of **A1** with propargyl chloride

In this reaction a brown solid precipitated from the solution. Its mass was 18mg, what nearly equals the mass of complex **A1** used. It was not soluble in any common solvent for NMR

measurement, so no spectrum was obtained.

The precipitate was dried on high vacuum, and TGA under N_2 as well as an elemental analysis were performed. The TGA measurement in N_2 revealed a residue of 40%, the elemental composition was quantified as C: 42.34, H: 4.7, N: 1.72, Cl: 4.92 [w%]. According to these values the solid consists of a *P,N*-chelated platinum complex. Closer examination revealed some problems: The values for chlorine and nitrogen indicate, that the ratio of these two elements in the compound is 1:1. Considering this, the unknown complex appears to carry one P,N ligand and one chlorine ligand, its elemental composition is $C_xH_yClNPPt$. The closest match of the value of x to the results of the elemental analysis would be 18, together with a value of 20-23 for y. This would mean, that besides the hemilabile ligand ($C_{16}H_{20}PN$) only two additional carbons only two additional carbons and less then four hydrogens are part of this complex (Fig. 47). Considering the presence of vinylic signals in the ^1H NMR spectrum, it is possible that polymerisation of the propargyl group takes place here. If the precipitate is a polymer it could also incorporate different impurities, what could spoil the elementary analysis.

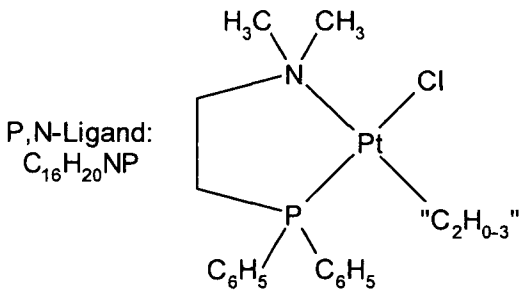

Fig. 47: A complex with the formula $C_{16}H_{20-23}PN$

2.3.2 Bromides

2.3.2.1 2,2-Dibromopropane

2,2-Dibromopropane was reacted with **A1** at molar ratios of 1:1, 1:2 and 1:4. At room temperature no reaction took place, after heating up to 70°C, complex **A1** was consumed within

two days at all three ratios. A small signal for a potential octahedral intermediate was monitored at 6.48ppm in the ^{31}P NMR spectrum during the reaction, in the ^{1}H NMR spectra no signals could be assigned to that peak. **A1** was completely converted into **D2** after three days. In the ^{1}H NMR spectrum a new signal signal became visible at 1.56ppm. According to reference spectra this is the methyl signals of 2,3-dibromo-2,3-dimethylbutane , the coupling product (Fig. 48). In GC/MS no new signal was visible, possibly because of the high boiling point of the organic dibromides.

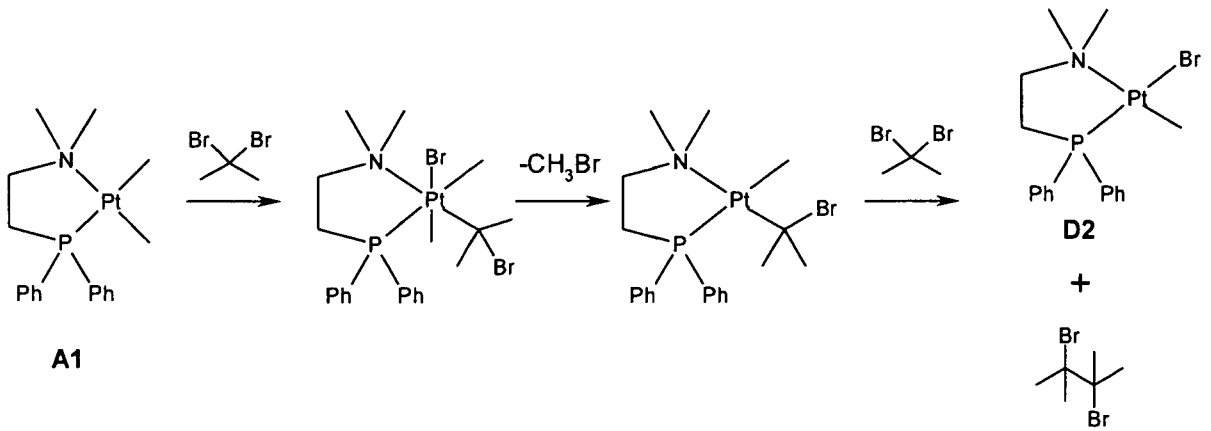

Fig. 48: Reaction of A1 with 2,2-dibromopropane

2.3.2.2 Bromobenzene

The experiments with bromobenzene were performed at molar ratios of 1:1, 1:2 and 1:4. At room temperature no reaction took place, therefore the reaction mixtures were heated to 70°C. In contrast to the experiments with chlorobenzene, reactions were observed, but also at a very slow rate. At a ratio of 1:1 nearly no conversion of **A1** was visible after ten days, at ratio of 1:2 and 1:4 about half of complex **A1** was converted into **D2** after that time. In the GC/MS analysis biphenyl was identified as organic product (Fig. 49). An octahedral intermediate could not be monitored in that reaction.

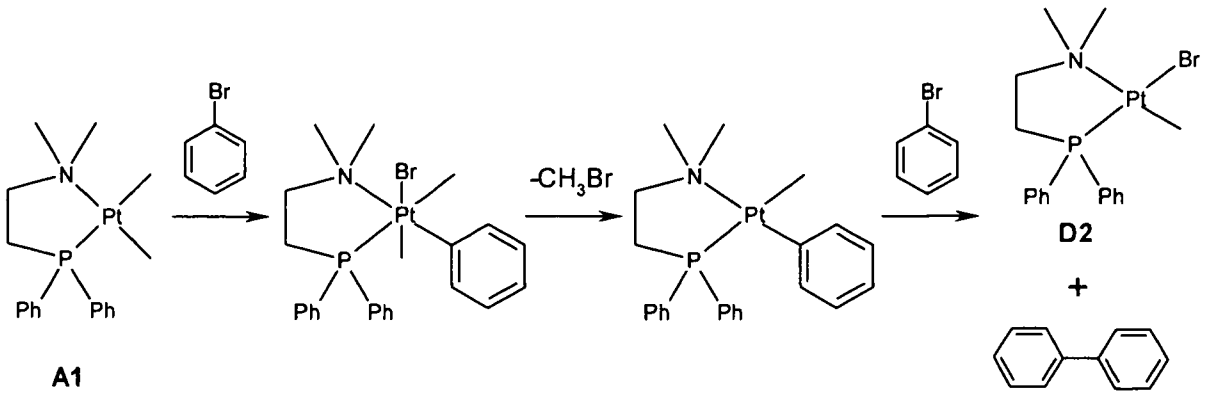

Fig. 49: Reaction of **A1** with bromobenzene

2.3.2.3 1,4-Dibromobenzene

Since bromobenzene reacts with complex **A1** by formation of biphenyl, 1,4-dibromobenzene was added to complex **A1** at a molar ratio of 1:15, to see if longer chains of phenyl groups can be formed. At room temperature no conversion was monitored in the NMR spectra, so the reaction mixture was heated to 70°C. After two weeks about 65% of **A1** was converted into **D2**. The reaction was then stopped. 4-Bromotoluene could be identified as reaction product in the ^{1}H NMR spectrum and in the GC/MS analysis, seemingly no coupling or even chain formation of the phenyl groups takes place here (Fig. 50).

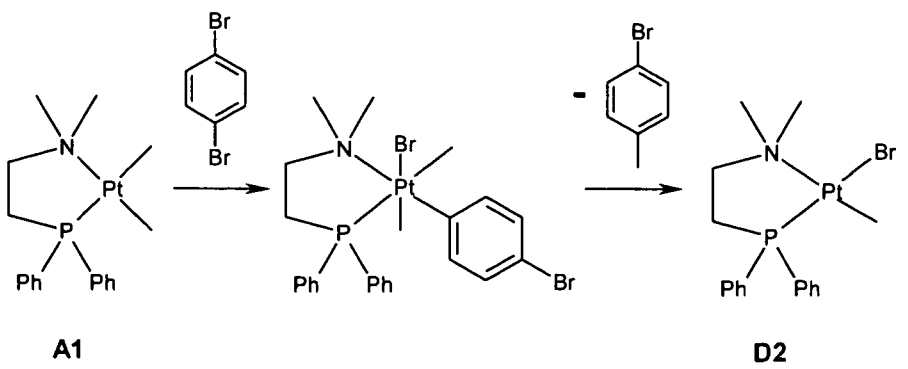

Fig. 50: Reaction of **A1** with 1,4-dibromobenzene

2.4 Fast Reactions with Halogenated Hydrocarbons without CH_2-Groups in the β-Position

2.4.1 Benzyl Chloride

Benzyl chloride was added in the ratio of 1:1, 1:2 and 1:15 to a d_6-benzene solution of the starting complex **A1**. After standing overnight at room temperature no reaction was visible in the NMR spectra at any ratio. At 70°C, all starting complex was converted to complex **D1** after two days at ratio 1:15 and after four days at ratio 1:1 and 1:2. No signal of octahedral intermediates was detected during the reactions, after consumption of **A1, D1** was the only visible metal-organic compound at any ratio. In the ^1H NMR spectrum a new signal was detected at 2.72ppm that was assigned to bibenzyl, the coupling product of the dehalogenated organic moiety, by comparison with an original spectrum of that compound. Also small signals for toluene were found. The formation of bibenzyl was confirmed by GC/MS analysis (Fig. 51), where also a small signal for ethylbenzene was discovered. Thus, seemingly both dehalogenative coupling and methylation take place in that reaction, with coupling being the prevalent reaction (Fig. 52).

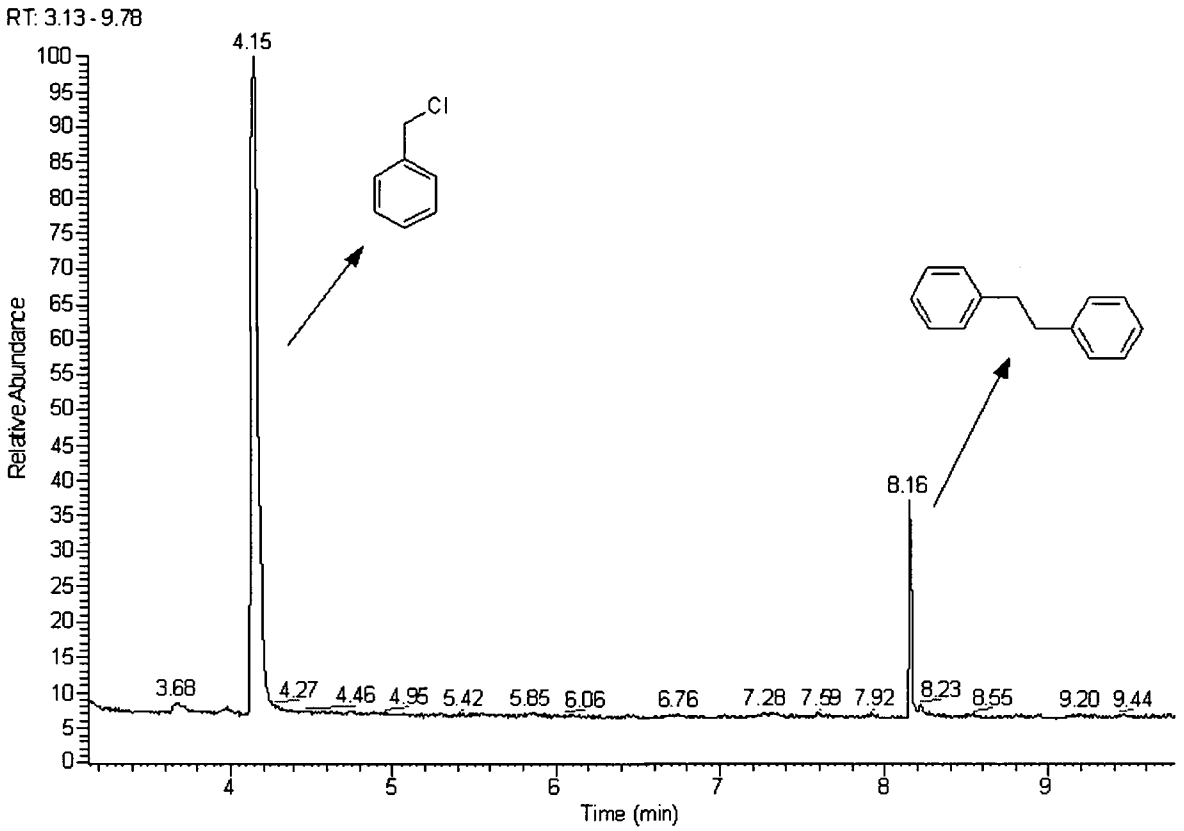

Fig 51: GC of the reaction with benzyl chloride, T_{3min} = 90°C, dT = 20°C/min

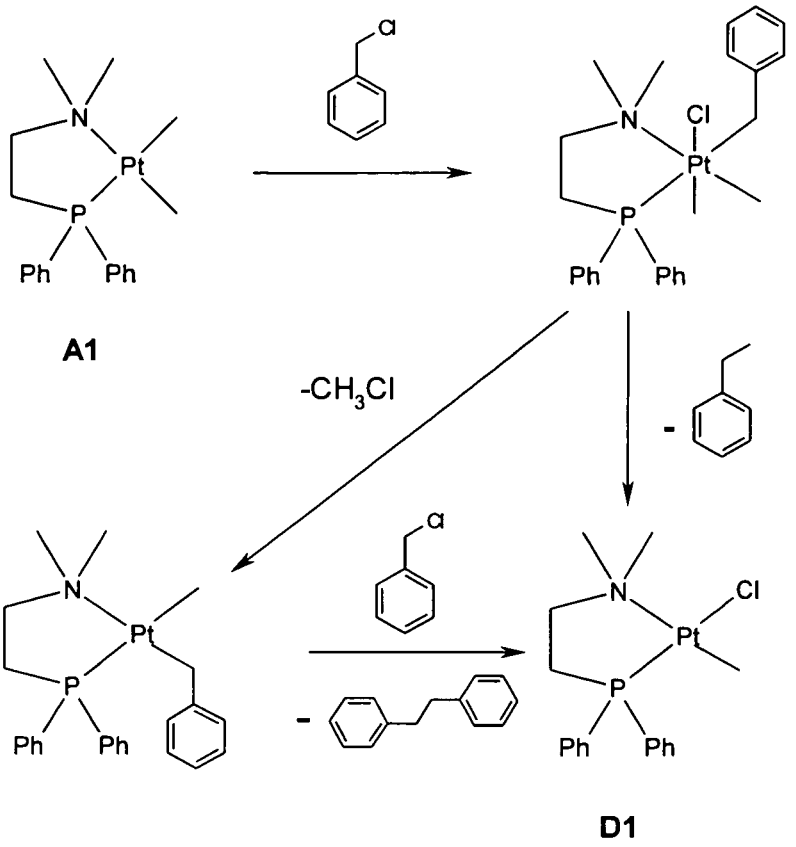

Fig. 52: Reaction of **A1** with benzyl chloride

Apart from the signals mentioned above two other features were found in the NMR spectra, that could not be assigned: A group of signals around 6ppm in the ^{1}H NMR spectrum, similar to the signals found in the spectra of the reaction mixtures with bromides and iodides with β-CH_2 groups, propargyl chloride and chloroacetic acid, as well as a single peak at 20.19ppm in the ^{31}P NMR spectrum.

2.4.2 Benzyl Bromide

Considering the easier activation of the C-Br bond compared to the C-Cl bond (see chapters 2.1 and 2.2) experiments were performed with benzyl bromide in anticipation of higher reactivity than benzyl chloride. First, benzyl bromide was added to **A1** at molar ratios of 1:0.5, 1:1, 1:2, and 1:4. There was no reaction at room temperature, but after heating to 70°C complex **A1** was completely consumed within six hours at all ratios except 1:0.5. As usual for brominated

compounds, activation of the C-Br bond took place easily. An octahedral compound (**B6**) was clearly visible in the NMR spectra within 10 minutes of heating, while conversion into **D2** was much slower. At a ratio of 1:0.5, **D2** was the only clearly visible reaction product in the NMR spectrum, while **B6** was still present after nine days at the other three ratios. At ratio 1:4 its signal was even stronger than that of **D2**.

These results showed, that higher educt concentrations obviously stabilize the octahedral intermediate. Therefore, the experiments were repeated at molar ratios 1:12 and 1:24 to investigate this complex. After five minutes of heating at these ratios **B6** was nearly the only visible compound in the ^{31}P NMR spectrum. It was crystallized by diffusion of petroleum ether into the solution. The crystal structure was determined by X-ray diffraction (Fig. 53), revealing its composition as $[(\kappa^2\text{-P,N})\text{-}Ph_2PCH_2CH_2NMe_2]PtMe_2BzBr$, existing as two isomers **B6a** and **B6b**, one with the benzyl group in *trans* position to the phosphorus atom, one with a methyl group in that position.

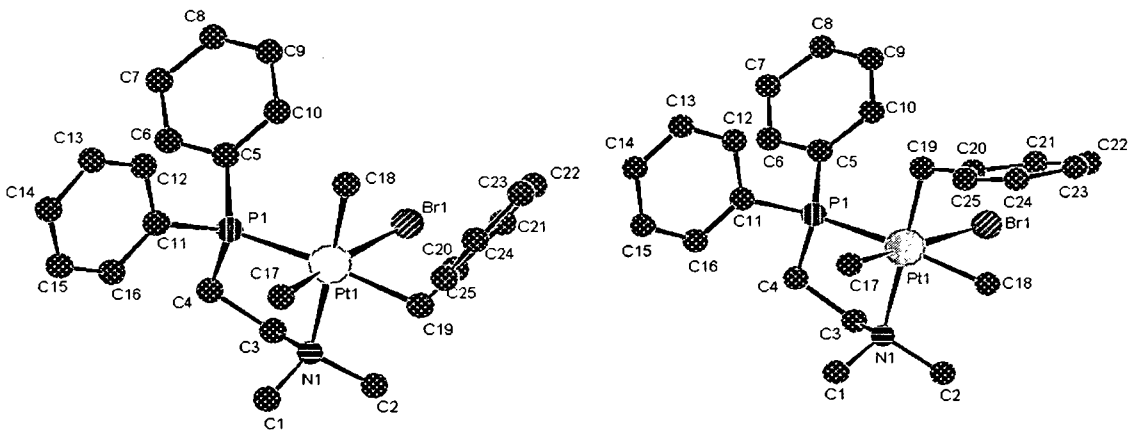

Fig. 53: Molecular structures of the two isomers of $[(\kappa^2\text{-}P,N)\text{-}Ph_2PCH_2CH_2NMe_2]PtMe_2BzBr$ (left: **B6a**, right: **B6b**)

Table 8: Selected bond lengths and angles of the complexes **B6a** and **B6b**

	B6a	**B6b**
Bond lengths (Å)		
Pt-C(17)	2.072(3)	2.072(3)
Pt-C(18)	2.065(3)	2.063(3)
Pt-C(19)	2.119(3)	2.122(3)
Pt-Br	2.6207(4)	2.6206(4)
Pt-P	2.3480(7)	2.3479(7)
Pt-N	2.287(2)	2.287(2)
Bond angles (°)		
N(1)-Pt(1)-P(1)	82.99(6)	82.98(6)
C(18)-Pt(1)-P(1)	93.61(7)	170(3)
C(18)-Pt(1)-C(19)	92.31(10)	92.39(17)
C(19)-Pt(1)-N(1)	91.10(9)	176(4)
C(17)-Pt(1)-P(1)	93.13(8)	93.12(8)
C(18)-Pt(1)-C(17)	85.51(10)	85.70(19)
P(1)-Pt(1)-Br(1)	92.023(18)	92.024(18)
C(18)-Pt(1)-Br(1)	91.91(7)	91.73(18)

Considering the organic products, traces of ethyl benzene, directly eliminated from complex **B6** were found by GC/MS and NMR (Fig. 55), while no evidence for the formation of bibenzyl via elimination of methyl bromide was detected (Fig. 54). During the reaction signals of toluene emerged in the ^{1}H NMR spectrum as well as the unusual signals at around 6ppm as known from chapter 2.2.2, 2.2.3 and 2.4.1. Like in the reaction with benzyl chloride a new signal in the ^{31}P NMR spectrum was visible, in this case at 21.23 ppm, no platinum satellites could here be determined, too.

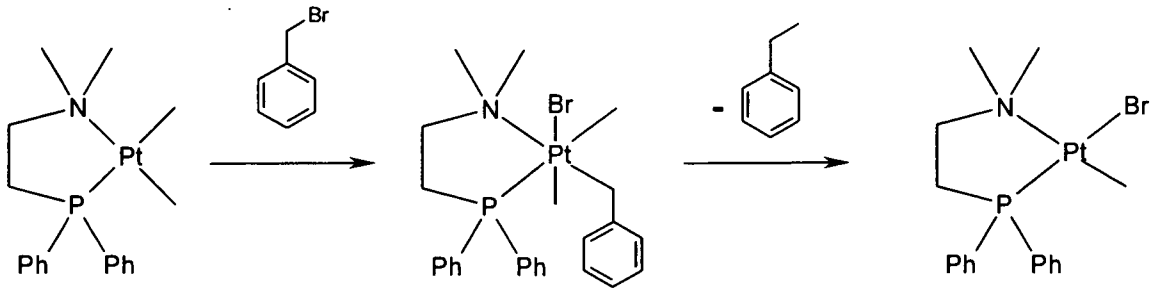

A1 **B6** **D2**

Fig. 54: Reaction of **A1** with benzyl bromide

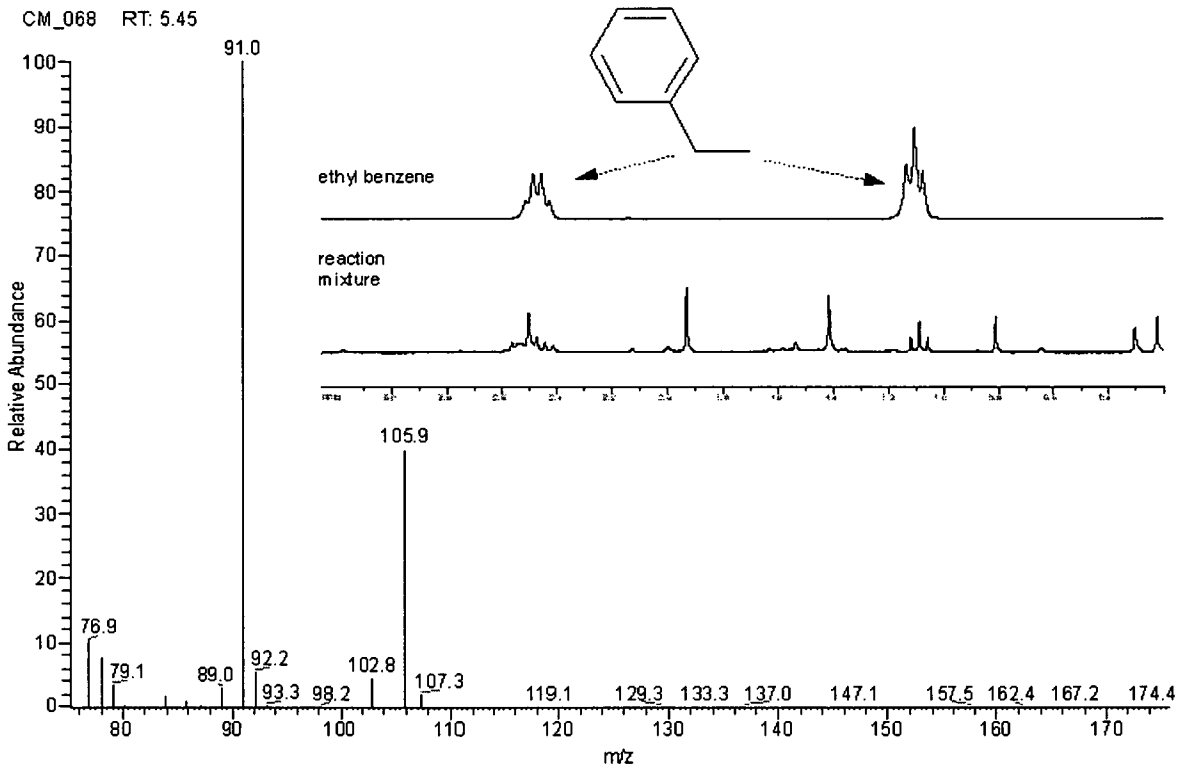

Fig. 55: MS and ^{1}H NMR spectum of ethyl benzene, formed by reaction with benzyl bromide

Another signal of an octahedral intermediate was found in the ^{31}P NMR spectrum at 1.65ppm (Fig. 56)

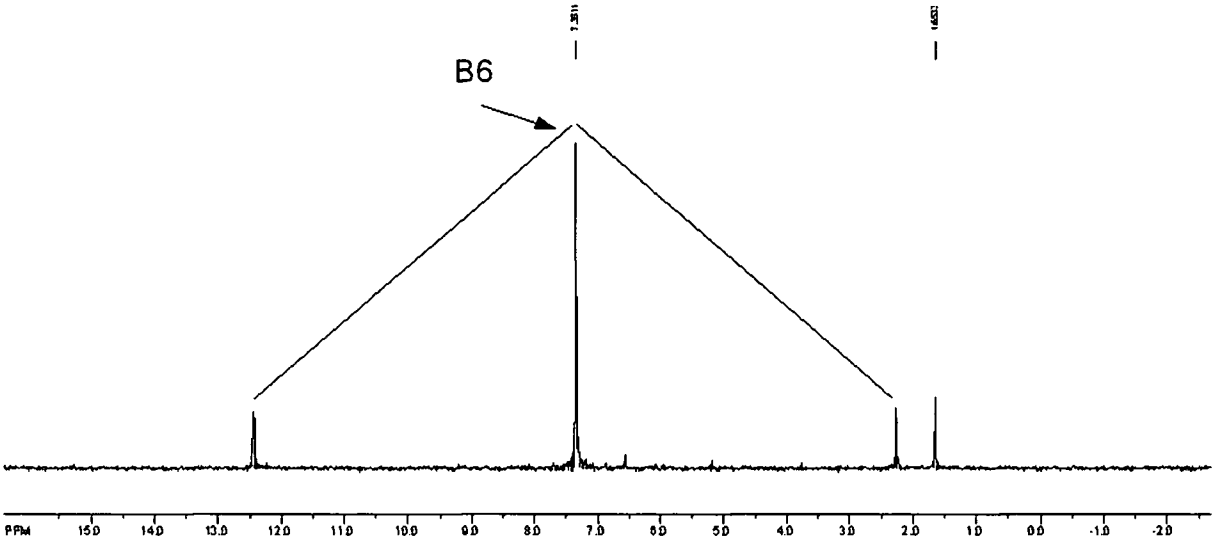

Fig. 56: ^{31}P NMR spectrum of complex **B6** and the unknown octahedral complex

This signal was more closely examined by correlation NMR measurements. In the P/H correlation three ligands were found at 0.88, 1.49 and 4.51ppm (Fig. 57).

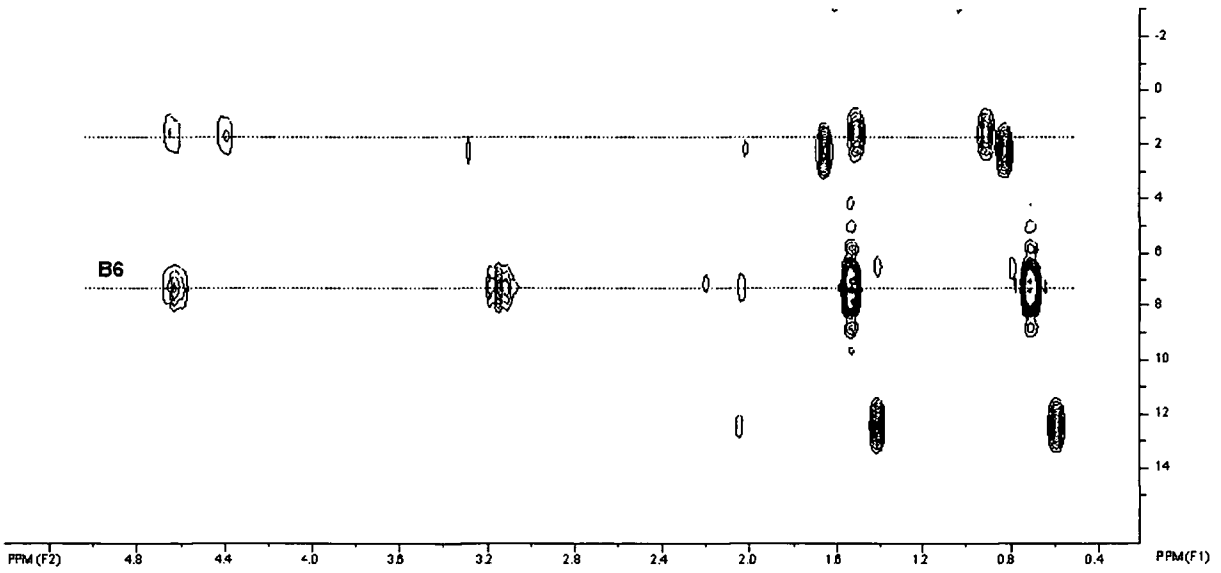

Fig. 57: Ligands of complex **B6** and the complex at 1.65ppm in the ^{31}P NMR spectrum in the P/H HMBC measurement

Considering the coupling constants the signal at 0.88ppm was identified as a CH_3 group out of

the P-Pt-N plane in *trans* position to bromine ($^2J_{PtH}$ = 71Hz), the signal at 1.49ppm ($^2J_{PtH}$ = 60Hz) looks like a methyl group in *trans* position to phosphorus. The signals at 4.43pm look similar to the ones of the CH_2Ph ligand in complex **B6** but with a much lower coupling constant $^2J_{PtH}$ of only 71Hz, compared to 443Hz for complex **B6** (Fig. 58). Apparently these signals belong to the isomer **B6b**, the different coupling constant could be the result of steric hindrance of the phenyl which is much closer to the phenyl groups of the phosphorus donor in that isomer.

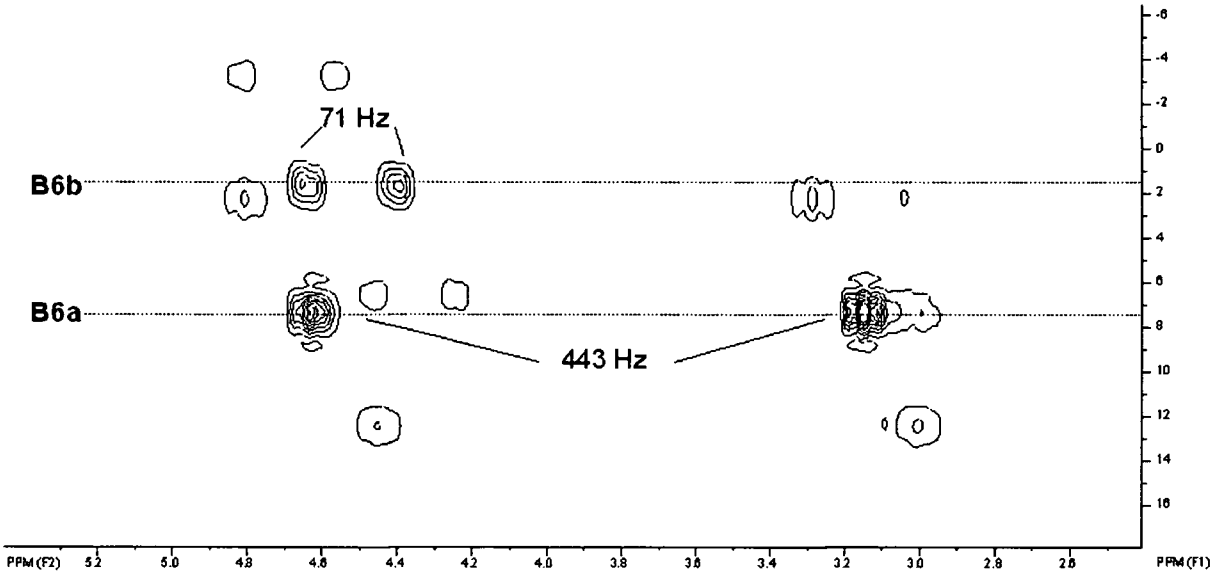

Fig. 58: The CH_2 groups of the phenyl ligands in the P/H correlation spectrum of the reaction of complex **A1** with benzyl bromide

2.4.3 Ethyl Chloroacetate

Ethyl chloroacetate was reacted several times with **A1** at a molar ratio of 1:2. Since no reaction was monitored at room temperature in the NMR spectra, the reaction mixtures were heated to 70°C, where complex **A1** was consumed after about two days. After three to four days no further changes occurred, and signals of complex **D1** and another complex at 35ppm were visible in the ^{31}P NMR spectrum, as well as a signal at 21.16ppm without platinum satellites. The latter two could not be assigned in the first place. In the region of the octahedral complexes three signals were visible but too small to determine coupling constants. No ethyl propionate, the methylation

product, and diethyl succinate, the coupling product, were found but signals for ethyl acetate became visible in the ^{1}H NMR spectrum and also here the unknown signals around 6ppm appeared.

2.5 New Reaction Mechanisms

2.5.1 Unusual Reaction Yields, Speed and Products

As described in chapter 2.4.3, no products of dehalogenative coupling or methylation were found in the reaction with ethyl chloroacetate, although the boiling points of diethyl succinate (218°C) and ethyl propionate (99°C) are both within the measurement range of GC/MS (60-280°C). Still complex **A1** was completely consumed and the chloro-methyl complex **D1** was formed, as well as ethyl acetate.

The reactions with benzyl chloride and benzyl bromide yielded organic products (mainly bibenzyl in the first and ethyl benzene in the latter case as well as toluene in both cases), but the proportion of these products was not high enough to explain the complete conversion of complex **A1** into **D1** or **D2**, as can be calculated from integration of the ^{1}H NMR spectra, e.g. the molar ratio between bibenzyl and **D1** should be 1:2, but it is 1:8 (Fig. 59).

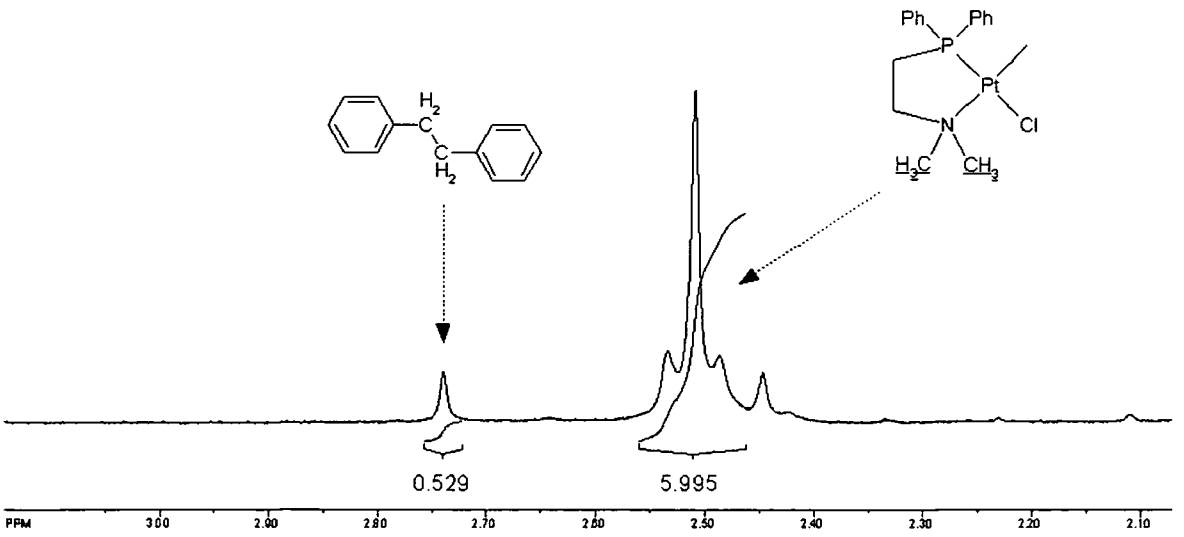

Fig. 59: Integration of ^{1}H NMR signals, showing the mismatch of **D1** and bibenzyl proportion after reaction with benzyl chloloride

What is furthermore interesting is the reaction rate: While the reactions with chlorinated compounds with β-CH_2 groups are extremely slow and reactions with chlorinated hydrocarbons with the chlorine on a non-terminal group (chlorocyclohexane and chlorobenzene) do not take place at all, the reactions with benzyl chloride and ethyl chloroacetate are completely finished after three to four days. Together with the small amount or even non-existence of compounds formed by dehalogenative coupling or methylation and the impossibility of β-elimination this suggests, that a fourth, hitherto unknown reaction mechanism takes place here.

Closer examination of the NMR spectra revealed three unusual features not observed in the previous cases (Fig. 60):

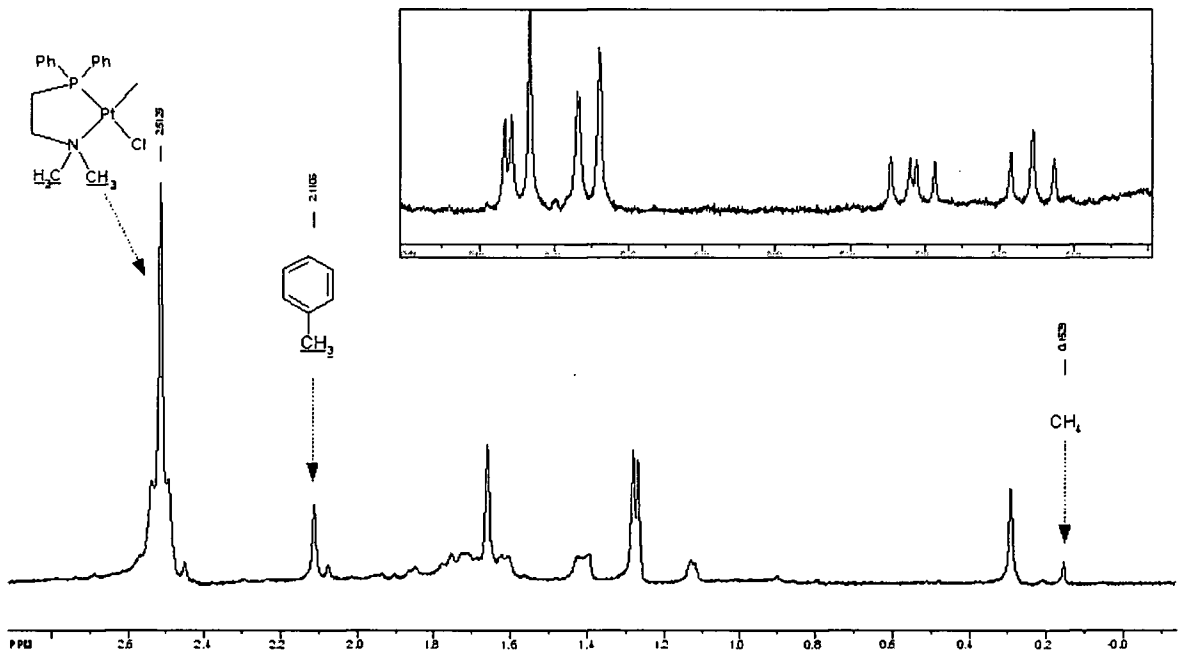

Fig.60: Unusual signals in the ^{1}H NMR spectrum after reaction with benzyl chloride

- A methane peak in the ^{1}H NMR spectra
- Signals for toluene in the reactions with benzyl chloride and bromide, signals for ethyl acetate in the reaction with ethyl chloroacetate in the ^{1}H NMR spectra
- Two groups of signals in the olefinic region of the ^{1}H NMR spectra (See insert in fig. 60)
- A single signal at around 21ppm in the ^{31}P NMR spectra

Considering the formation of methane the only reaction in this context that could yield this compound is the reaction of a methylated complex with hydrogen halides. Toluene and ethyl acetate are possibly formed by reaction of a **C**-type complex with HCl as well (Fig. 61).

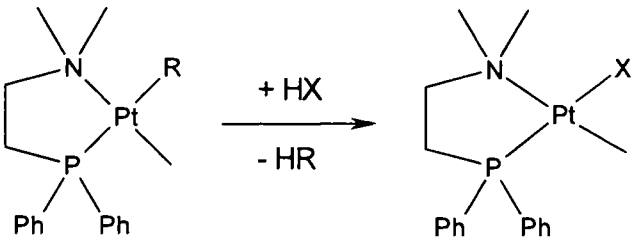

C **D1**

R = Bz or CH_2COOEt

Fig. 61: Formation of toluene or ethyl acetate by reaction of a **C** type intermediate with HX

This raises the question, where HCl and HBr originate from. The two easiest explanations would be that either the halogenated educts or of the starting complex are impure. The first possibility can be ruled out because:

- The educts are degassed prior to reaction, thus they cannot contain enough hydrogen halogenide to convert the whole amount of **A1**.
- An own experiment carried out between complex **A1** and HCl dissolved in C_6D_6 showed an extremely high reaction rate, **A1** is converted to **D1** or **D2** within seconds even at room temperature, while the reactions described here require three to four days

The starting complex cannot be the source of the acids, since then the reaction with benzyl bromide should also yield the chloro-methyl complex **D1**, but it yields the bromo-methyl complex **D2**. In consideration of these facts the only possibility is, that HCl and HBr are formed during the unknown reaction. The halogen of the starting compound must abstract a proton from another group in the reaction mixture. Since it is rather unlikely that it is taken from the solvent C_6D_6 (since CH_3D should be formed then) or the organic moiety connected to the CH_2Cl or

CH_2Br group (in the case of benzyl chloride and bromide these residues are phenyl groups that do not claeve protons easily), the proton must originate from either the CH_2 group of the organic starting compound or the complex itself (Fig. 62)

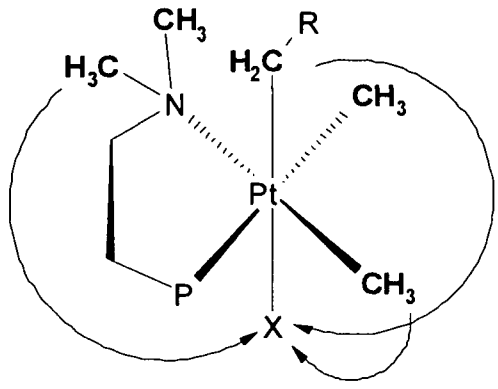

Fig. 62: Possible proton sources

The olefinic peaks exhibit a very strange pattern: They are split in four groups (Fig. 63) from which group 1 and 3 appear to represent protons that couple with each other as well as groups 2 and 4. Considering the integration values, these signals appear to represent two vinyl groups, but the patterns do not look like this.

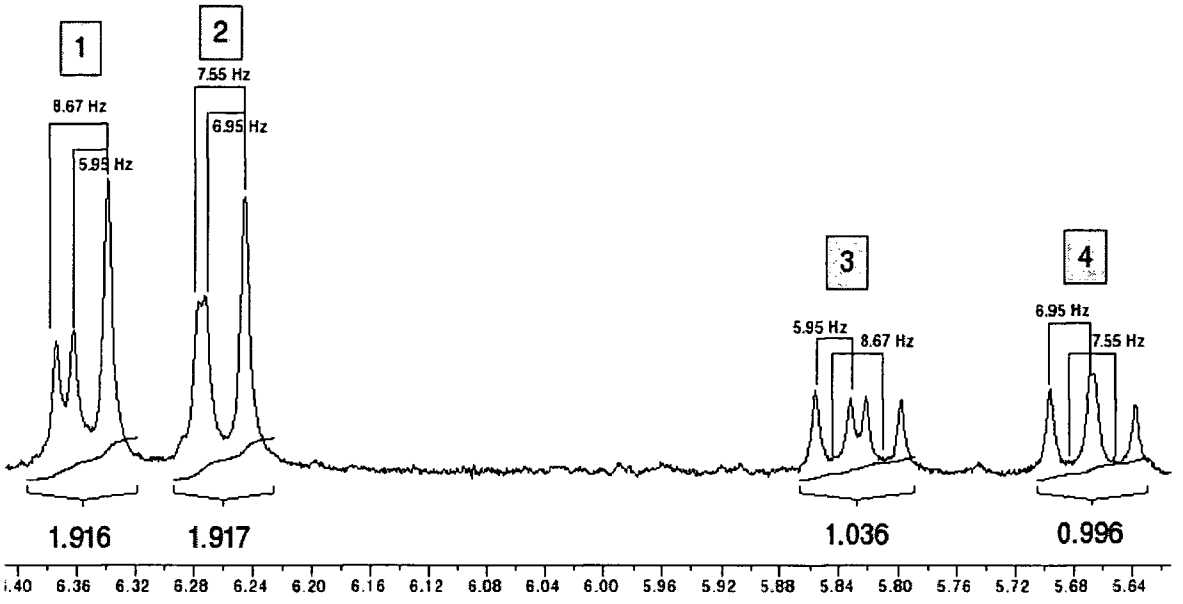

Fig. 63: Closer examination of the vinylic signals in the ^{1}H-NMR spectrum of the reaction between **A1** and ethyl chloroacetate

When the solvent is changed to deuterated acetone the signal pattern appears even more complicated (Fig. 64). Considering the integration values, the largest signal group consists of three doublets. If these signals represent two olefinic protons of a vinyl group as suggested above, the signals are once more split by the atom the group is connected to.

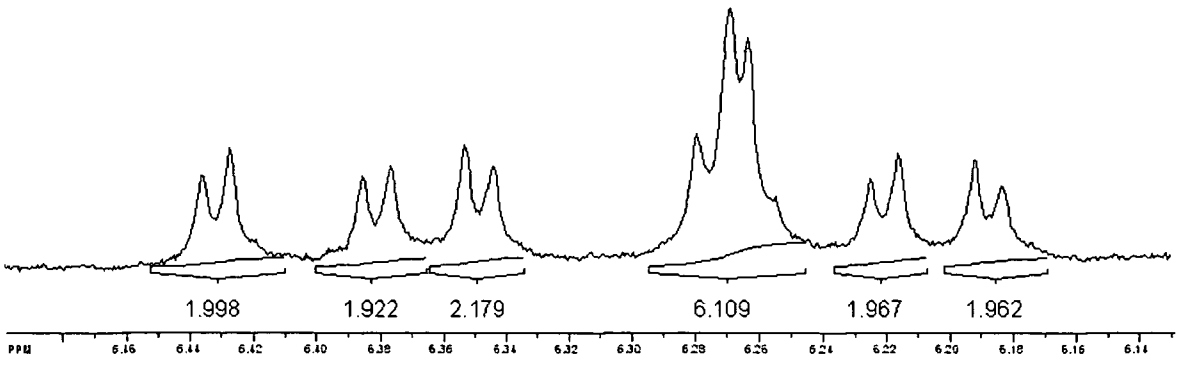

Fig. 64: Section of the ^{1}H NMR spectrum of the reaction between **A1** and ethyl chloroacetate, showing the signal of group 1 and 2 in fig. 63 in deuterated acetone

2.5.2 Closer 1D and 2D-NMR Investigations

To gain deeper insight in the apparently new reactions taking place in this case another experiment was started with ethyl chloroacetate at molar ratio of 1:2. The mixture was only heated to 70°C for one hour to investigate the reaction at an early stage, where the signals of the different unknown octahedral intermediates are much better visible than at the end of the reaction. This sample was then investigated at a NMR device with a carrier frequency of 500 MHz.

The ^{31}P NMR spectrum shows three signals with platinum satellites in the region of the octahedral complexes (0-12ppm, Fig. 65) as well as the single peak at 21.16ppm, that could not be assigned in the first place (see chapter 2.4.3)

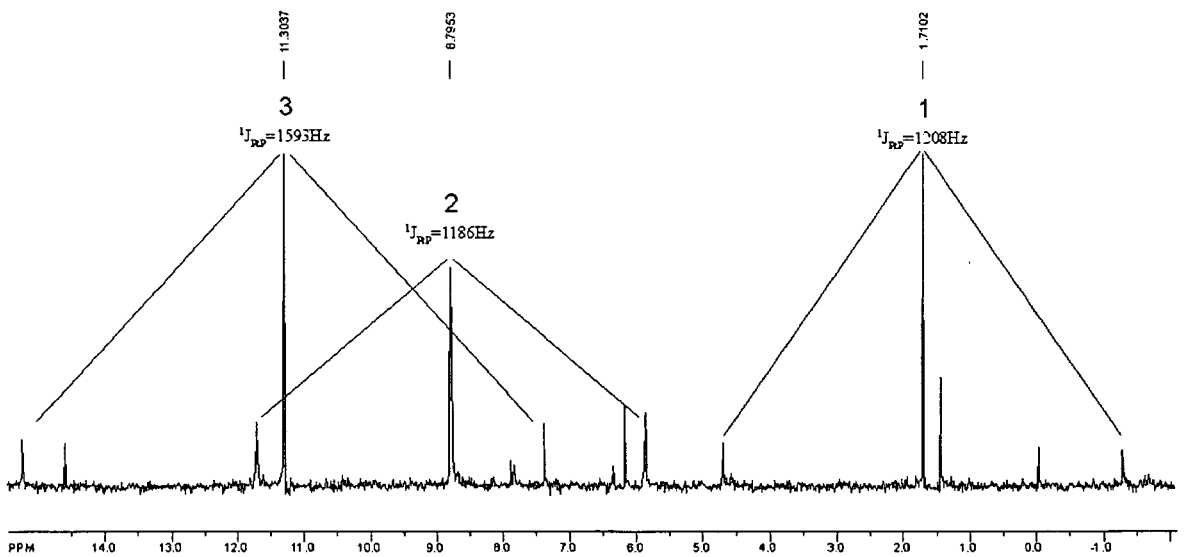

Fig. 65: ^{31}P NMR signals of the unknown octahedral complexes formed by reaction of **A1** with ethyl chloroacetate

First, the olefinic signals were investigated. As mentioned above, they look like a vinyl group connected to an atom or group that splits the signals. This could possibly be phosphorus, since it is part of the *P,N*-ligand. Therefore, a phosphorus-decoupled ^1H NMR spectrum was measured. The spectrum shows, that the signals are indeed split by phosphorus (Fig. 66), so apparently some transformation of the *P,N*-ligand took place.

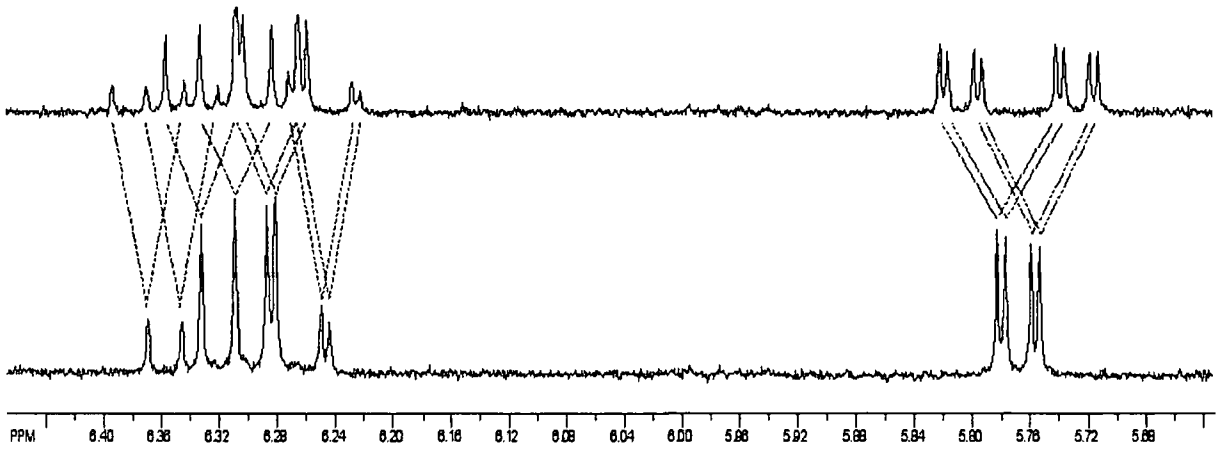

Fig. 66: Signal splitting by phosphorus as seen in the 500MHz ^{1}H NMR spectrum, ^{31}P-coupled (top) and ^{31}P-decoupled (bottom)

In order to determine the composition of the unknown complexes that appeared in the ^{31}P NMR spectrum, two-dimensional NMR measurements were performed.

Since the signals in the ^{31}P NMR spectrum are easiest to distinguishable, they were used as starting point for the investigation of the two-dimensional spectra. These signals can be divided into three groups, that were treated separately: The region of octahedral complexes (0-12ppm), the region of square planar complexes (26-40ppm) and the peak of the unknown vinylphosphine at around 21ppm.

- Octahedral Complexes:

As seen in Fig. 65, three unknown complexes were found here, named 1, 2 and 3. In the P/H-HMBC measurement, signals of other ligands of these complexes appeared (Fig. 67).

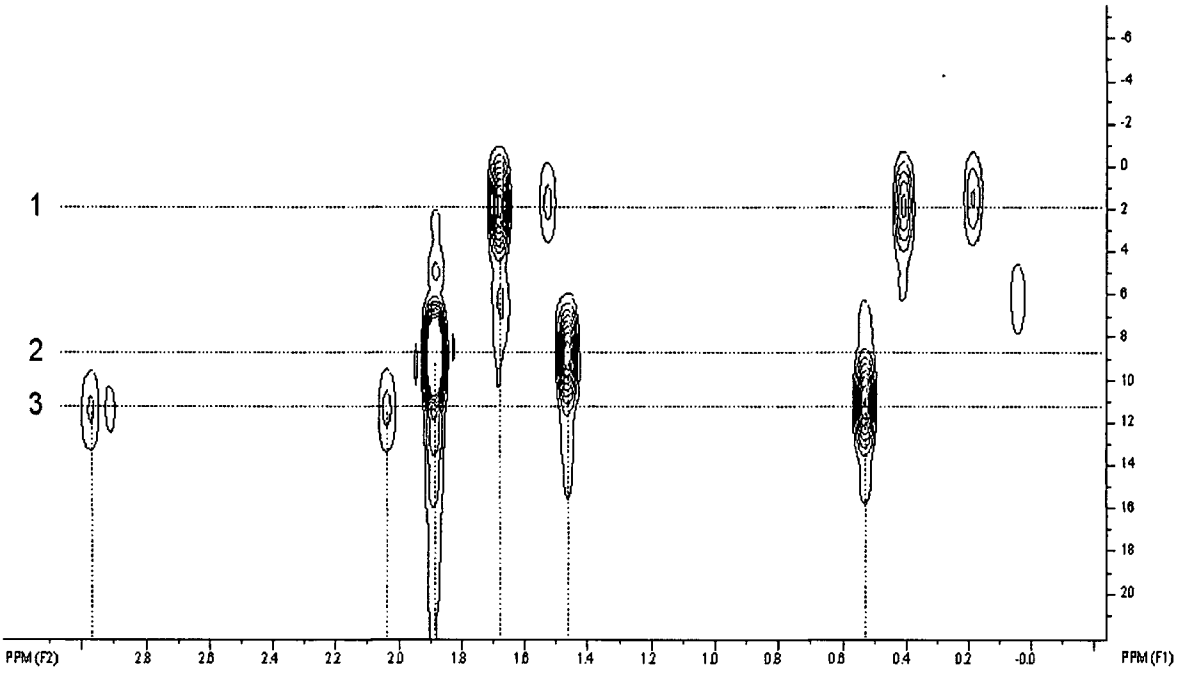

Fig. 67: P/H-correlation NMR of the region showing the octahedral ^{1}H signals of the complexes 1-3 at the following positions:

Complex 1: 0.41 and 1.68ppm

Complex 2: 1.47 and 1.89ppm

Complex 3: 0.53, 2.04 and 2.98ppm

Complex 1:

According to an APT NMR measurement, the two ligands of complex 1 are CH_3 groups. No additional correlated signals could be found for that complex. According to its chemical shift, the signal at 0.41ppm appears to be a CH_3 group out of the P-Pt-N plane. The peak at 1.68 has a second order coupling of $^{2}J_{PtH}$= 73Hz, typical for a CH_3 ligand in *trans* position to the nitrogen of the P,N ligand (see the data of complex **B1**, fig. 27, p. 23). No other ligand signals than these two were identified. Its ^{31}P NMR signal is shifted upfield compared to the signal of complex **B1**, this is typical for replacing a ligand in *trans* position with a group with lower *trans* influence[53]. Since there is obviously no organic ligand in *trans* position to the phosphorus, the ligand in that position could be chlorine, which has a very weak *trans* influence[11] so complex 1 appears to be [(κ^2-*P*,*N*)-$Ph_2PCH_2CH_2NMe_2$]$PtMe_2Cl_2$ (**B2**), formed by reaction of [(κ^2-*P*,*N*)-$Ph_2PCH_2CH_2NMe_2$]$PtMe_3Cl$ (complex **B1**) with HCl (Fig. 68). As there is no vacant

coordination site on complex **B1** for coordination of chlorine, this reaction could be achieved by decoordination and recoordination of the nitrogen.

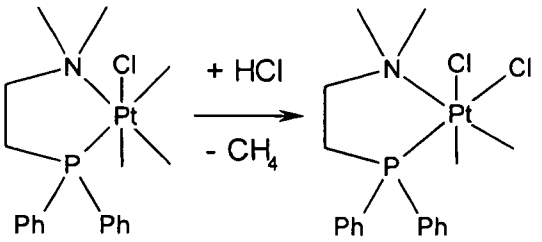

B1 **B2**

Fig. 68: Formation of complex **B2**

Complex 2:

This compound has two ligands that appear at 1.57 and 1.89ppm, they are also CH_3 groups. According to literature[70], this could be **B1** , formed by addition of CH_3Cl to **A1** (Fig. 69), but the signal for the third methyl ligand is missing. To gain more information, a Pt/H-correlation experiment was performed (Fig. 70)

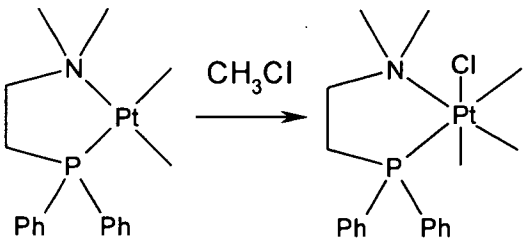

A1 **B1**

Fig. 69: Formation of complex **B1**

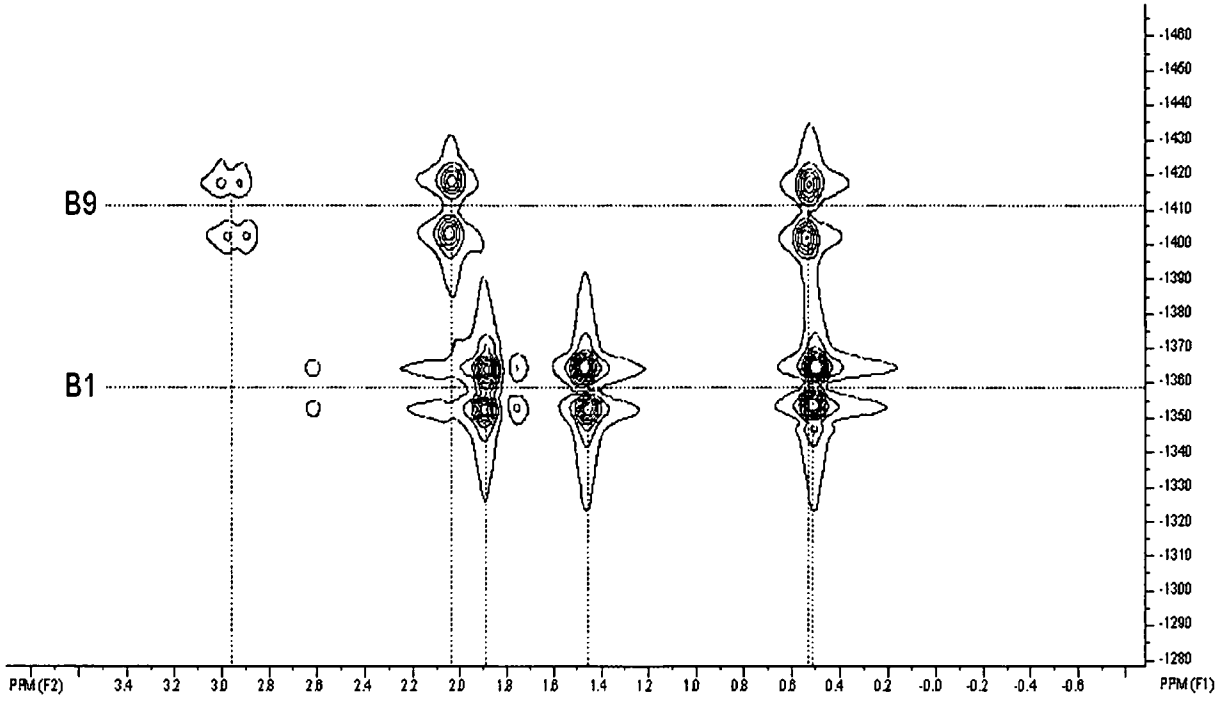

Fig. 70: Pt/H-correlation NMR of the region showing the octahedral ^{1}H signals

Here complex 2 is detected at -1358ppm and a third ligand can be seen at 0.50ppm, the position of the third methyl ligand of **B1** according to literature[11]. This shows that this complex is **B1**.

Complex 3:

Another octahedral complex is visible in the two-dimensional NMR spectrum in Fig. 70 at -1410ppm with methyl signals at 0.53 and 2.04ppm and another signal at 2.98ppm. This appears to be the octahedral complex 3. The first two signals are methyl ligands according to APT measurement: The one at 0.53ppm apparently belongs to a CH_3 group out of the P-Pt-N plane, the other signal at 2.04ppm has a Pt-P coupling constant of $^{2}J_{PtH}$=70Hz and is therefore in *trans* position to the nitrogen of the P,N ligand. The peak at 2.98ppm belongs to a CH_2 group. At a first look, complex 3 could be [(κ^2-*P*,*N*)-$Ph_2PCH_2CH_2NMe_2$]$PtMe_2Cl(CH_2COOEt)$ (**B7**, Fig. 71), the product of C-Cl bond activation.

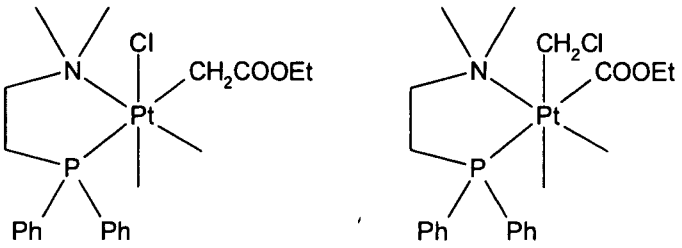

Fig. 71: Complex **B7** (left) and **B8** (right)

This would be rather exceptional: The ligand in *trans* position to the phosphorus can definitely not be chlorine, because this would shift the ^{31}Pt signal upfield from the signal of complex **B1**, but actually it is found about 2.5ppm downfield (see Fig. 70). Also the Pt-P coupling constant of 1593Hz is remarkably high compared to the Pt-P coupling constant of 1208Hz in complex **B2**, where the chlorine is situated opposite to the phosphorus. It also cannot be -CH_2COOEt, since this ligand has a lower *trans* directing effect and should therefore also shift the ^{31}P NMR signal upfield compared to complex **B1**. A possible explanation for these unusual observations could be, that here the ClH_2C-CH_2 bond is activated, yielding the complex [(κ^2-*P*,*N*)-$Ph_2PCH_2CH_2NMe_2$]$PtMe_2(CH_2Cl)(COOEt)$ (**B8**, fig. 71). The -COOEt group is a strong-field ligand with a high *trans* influence[11] and since it is part of a π-bond it is also a weaker σ-donor than chlorine or CH_3. This explains both the higher shift and coupling constant. Another hint for that structure was found in a C/H HMBC measurement, where the protons of the CH_2Cl group of the unreacted ligand exhibit coupling with the CH_2 carbon of the ethyl group, while no coupling can be seen between the protons of the CH_2 ligand and the ethyl CH_2 carbon, these two groups are separated by Pt in complex **B8**. This reaction pathway would be similar to the reaction pathway described by Suggs and Jun[40] (Fig. 16, p. 15), also here one of the carbons involved is a C=O carbon and also here a nitrogen ligand is present.

- Square Planar Complexes

In the region of planar Pt(II) complexes three compounds were visible in the ^{31}P NMR spectrum (Fig. 72): Complex **A1**, complex **D1** and an unknown planar complex P1.

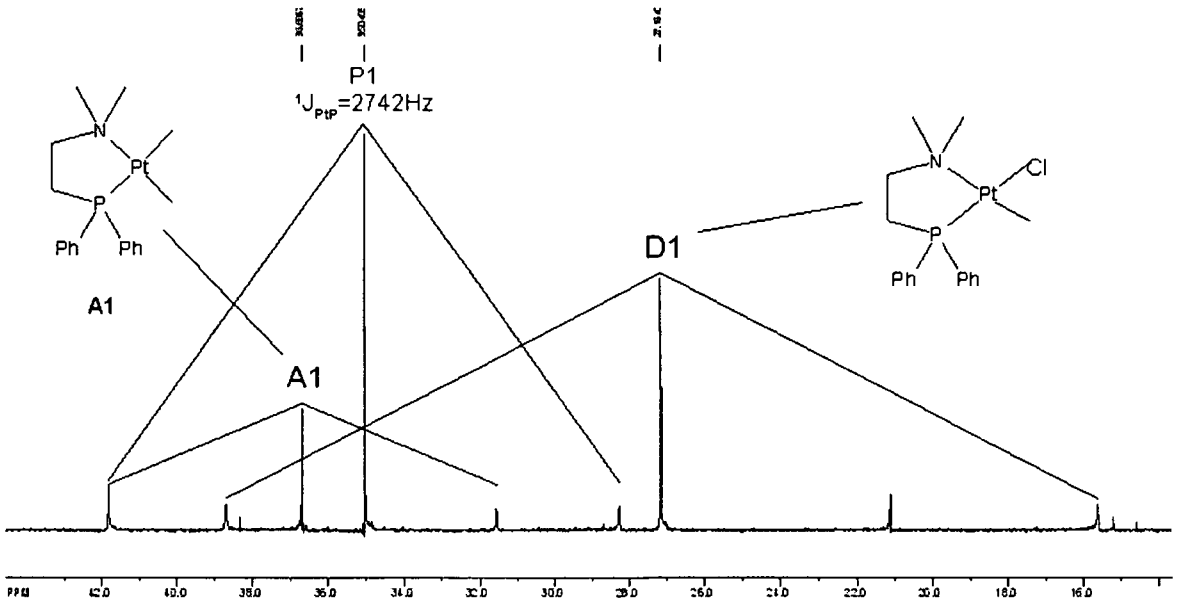

Fig. 72: ^{31}P-NMR signals in the shift range of the planar complexes in the reaction mixture of **A1** with ethyl chloroacetate

To determine the composition of complex P1 a Pt/H correlation spectrum was measured (Fig. 73)

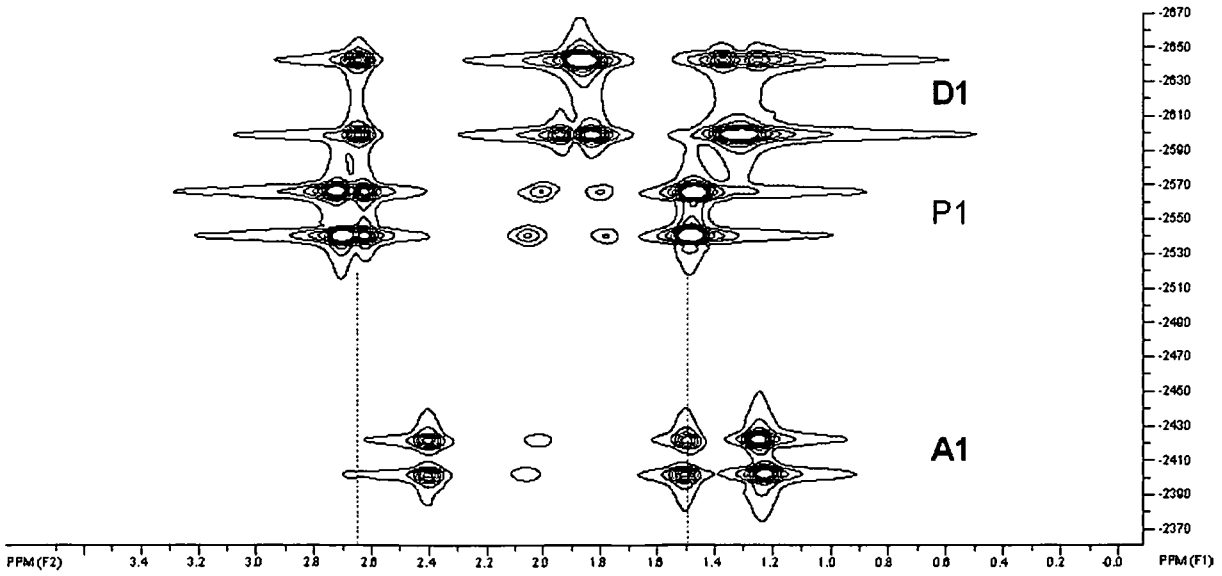

Fig. 73: Pt/H correlation measurement of the planar complexes yielded by the reaction of **A1** with ethyl chloroacetate

Here two new ligand signals appeared at 1.38 and 2.52ppm. According to APT NMR the first is a methyl group, the second a CH_2 group. Since the Pt-P coupling constant in the ^{31}P NMR spectrum is increased from 2070 to 2742Hz, the ligand opposite to the phosphorus apparently has been modified by the the formation of the unknown complex. In a 2D C/H spectrum the CH_2 group shows correlations with COO, CH_2 and CH_3 groups. Therefore, this signal appears to belong to a ethoxycarbonyl-methyl ligand, and the composition of P1 is $[(\kappa^2\text{-}P,N)\text{-}Ph_2PCH_2CH_2NMe_2]PtMe(CH_2COOEt)$ (complex **C2**, Fig. 74), formed by elimination of methyl chloride from the octahedral intermediate **B7**. This complex was very stable during the reaction, therefore oxidative addition of another ethyl chloroacetate molecule and subsequent elimination of diethyl succinate is not favourable. Thus, reaction with HCl, formed by the unknown mechanism, yielding complex **D1** and ethyl acetate appears to be the main reaction pathway of the intermediate **C2**.

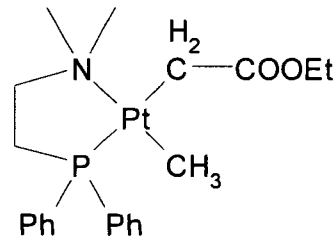

Fig. 74: Complex **C2**

- Vinylic compound

A P/H-HMBC measurement was performed to collect more information about the vinylic protons that couple with phosphorous. Although the signals of these protons were very weak, correlations could be found (Fig. 75)

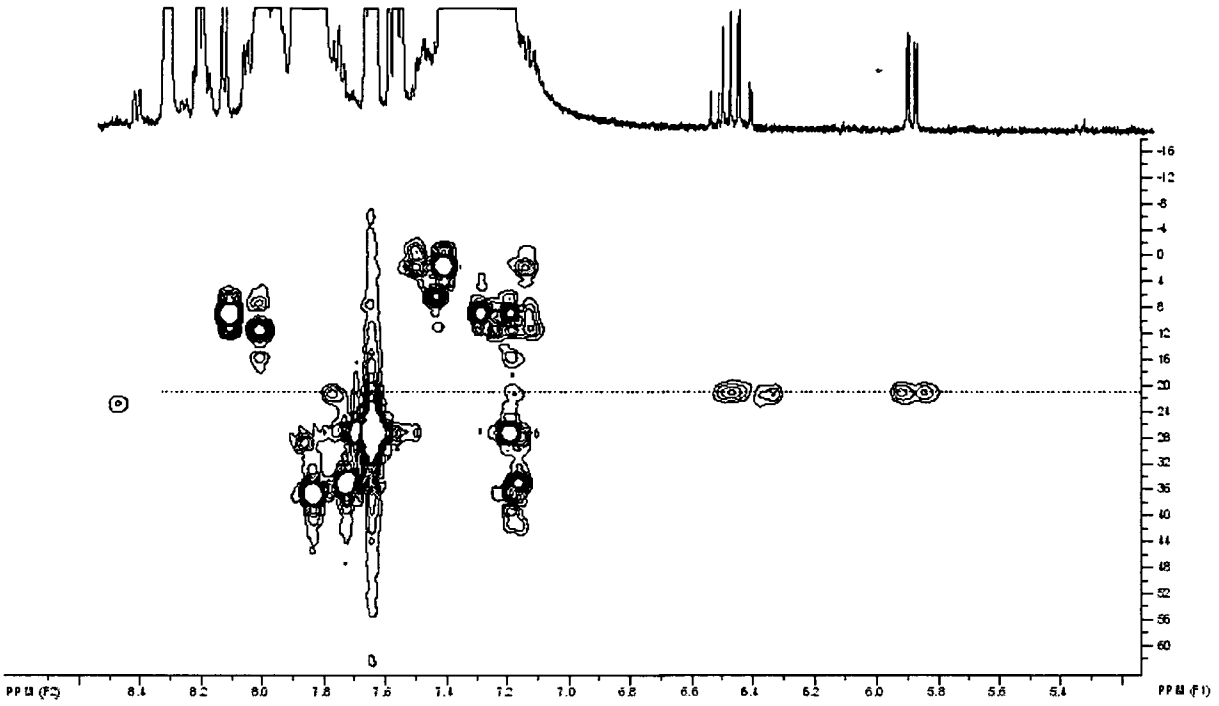

Fig. 75: P/H HMBC measurement of the vinylic protons

The first obvious feature in that spectrum is that the vinylic protons correlate with the unknown signal at 21.6ppm in the ^{31}P NMR spectrum. In the P/H correlation in Fig. 75 it can also be seen, that this signal correlates with two signals in the aromatic region of the ^{1}H NMR spectrum. In the region below 5ppm no correlated signals were identified, since the multitude of much stronger signals in that region made detection virtually impossible.

A possible explanation for those signals could be, that they are signals of diphenylvinylphosphine, produced by the unknown mechanism. A spectrum of that compound was measured and compared with the unknown vinylic signals, showing that they are not identical compounds (Fig. 76). There was also no similarity when diphenylvinylphosphine was oxidized.

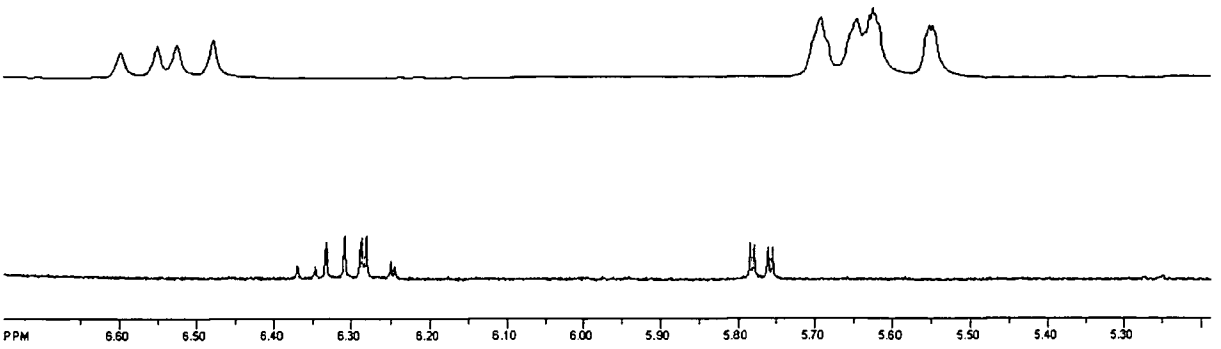

Fig. 76: Section of the P-decoupled ^{1}H NMR spectra of diphenylvinylphosphine (top) and the unknown vinylic protons (below)

Since HX is formed during the unknown reaction, it appears logical to assume that this is the elimination step that forms the vinylic compound.. According to Fig. 62 (p. 58) the proton source can be the NCH_3 groups, the CH_2 of the activated educt, the methyl ligands, and the CH_2 groups between N and P. Since the first two possibilities could not really explain the correlation between the resulting vinylic signals and the phosphorus atom, the protons should be either eliminated from the methyl ligands or the CH_2 groups of the *P,N* ligand. To rule one possibility or the other out by ^{1}H NMR measurement, a new deuterated starting complex [(κ^2-*P,N*)-$Ph_2PCH_2CH_2NMe_2$]Pt(CD_3)$_2$ (complex **A5**) was synthesized and reacted with benzyl chloride (Fig. 77).Due to the low amount of complex **A5** the experiment could not be performed with ethyl chloroacetate.

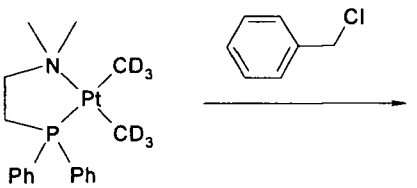

(A5)

Fig. 77

In the ^{1}H NMR spectrum of that reaction mixture the vinylic signals were visible without any change, showing clearly that the methyl ligands are not changed by this reaction. The reaction mixture was treated with petroleum ether, where the complex [(κ^2-*P,N*)-$Ph_2PCH_2CH_2NMe_2$]Pt(CD_3)Cl (**D4**) precipitated completely. The solvent was then evaporated

and the residue dissolved in deuterated benzene. A ^{1}H NMR spectrum was measured, revealing the vinylic signals as well as a triplet with the right shape to belong to a $N(CH_3)_2$ group coordinated to platinum (Fig. 78).

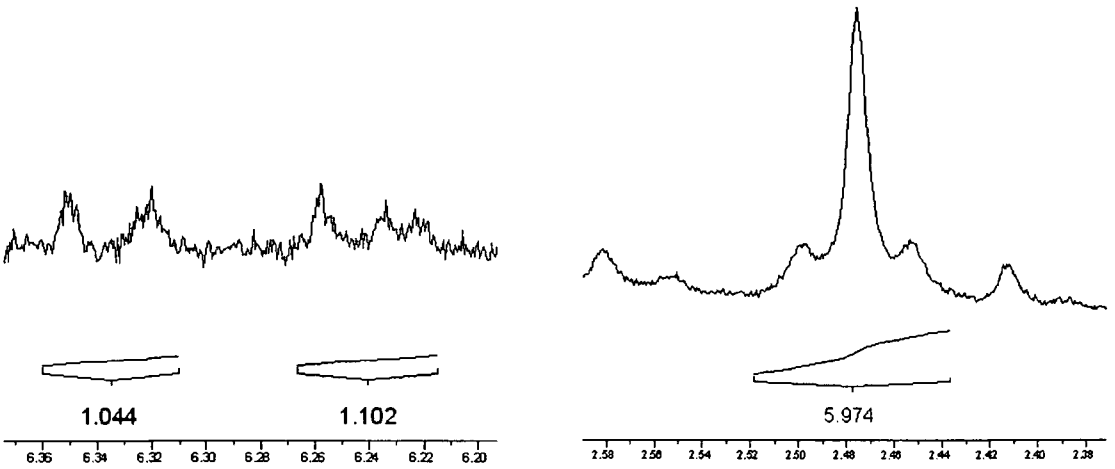

Fig. 78: ^{1}H NMR signals of the $N(CH_3)_2$ group and the double bond, formed by reaction of **A5** with benzyl chloride

The fact is remarkable that according to the integration values, the double bond appears to belong to the same complex and not to an organic compound produced by the unknown reaction. Unfortunately, complete removal of petroleum ether was not possible even at high vacuum, so no signals of other ligands of the new complex could be determined at chemical shifts lower than 2ppm.

2.5.3 Phosphonium Ylide Complexes

The experiments discussed in the last chapter show, that the HX-producing reaction yields a complex containing a nitrogen donor and a vinyl group connected to a phosphorous with a chemical shift of 21.6ppm in the ^{31}P NMR spectrum. Evidence for an activation of the ClH_2C-CH_2 bond and therefore presence of a CH_2Cl ligand was also found in the reaction with ethyl chloroacetate. As chapter 1.2.5 shows, these observations can also be made in reactions that yield phosphorus ylide complexes[15,16](Fig 6, p. 7). The ^{31}P NMR signal at 21.6ppm is in

accordance with data described in literature for the ylidic P atom, as well as the fact that this kind of complexes can be formed by addition of CH_2ICl to a Pt(II) complex. If such a reaction would take place here, the remaining chlorine could be eliminated as HCl with a proton that should originate from one of the CH_2 groups between the donor groups of the *P,N*-ligand.

2.5.4 Mass Spectroscopy

To determine the composition of the possible ylide complex, mass spectroscopy with chemical ionisation was used. This method was chosen to generate complex ions with low fragmentation, since several building blocks of all the complexes in the reactions investigated here are identical. The measurements were performed on the reaction mixtures of complex **A1** with benzyl chloride and ethyl chloroacetate. Although also showing signals that could belong to a phosphorus ylide ligand the reaction with benzyl bromide was not investigated that way, since the addition of the C-Br bond is thermodynamically much more favourable than the C-Cl activation. Therefore, as mentioned before, the main coordination compound in this reaction mixture is complex **B6**, rendering detection of any other compound in the mass spectrum too difficult, since fragments of that complex would appear in the same range as square planar compounds.

- Benzyl Chloride

A reaction was set up at molar ratio 1:2. The solution was heated until the complexes **A1**, **D1** and the potential ylide complex, appearing at 20.11ppm in the ^{31}P NMR spectrum of the reaction mixture of **A1** with benzyl chloride, were visible in the ^{31}P NMR spectrum (Fig. 79).

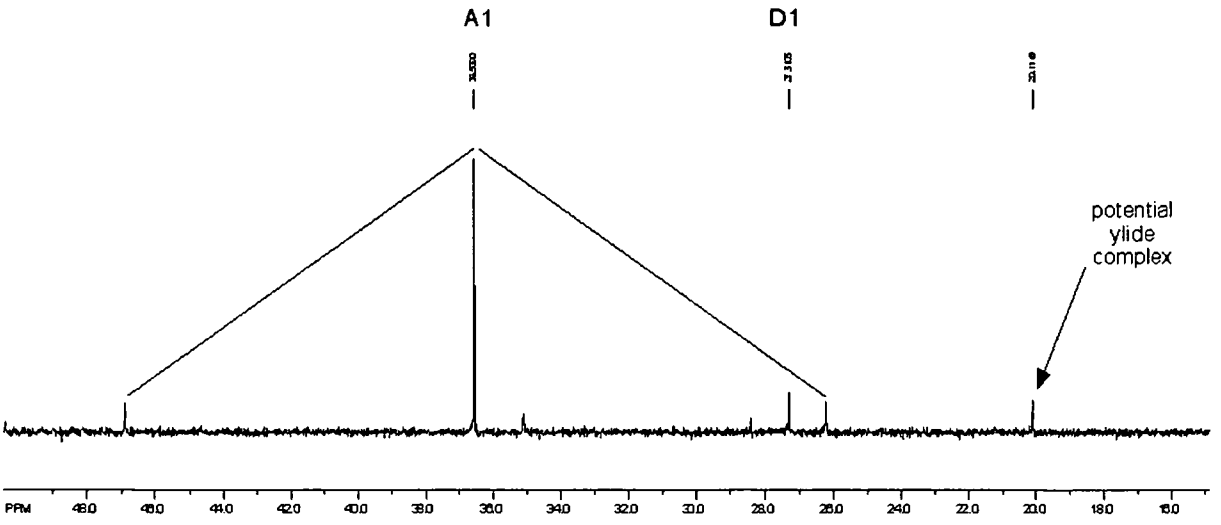

Fig. 79: ^{31}P-NMR spectrum of the reaction mixture with benzyl chloride prior to mass spectroscopy

The crude mass spectrum showed four signal groups: Complex **A1**, complex **D1**, complex **A1** minus one CH_3 group and a group of unknown signals, possibly belonging to the ylide complex (Fig. 80):

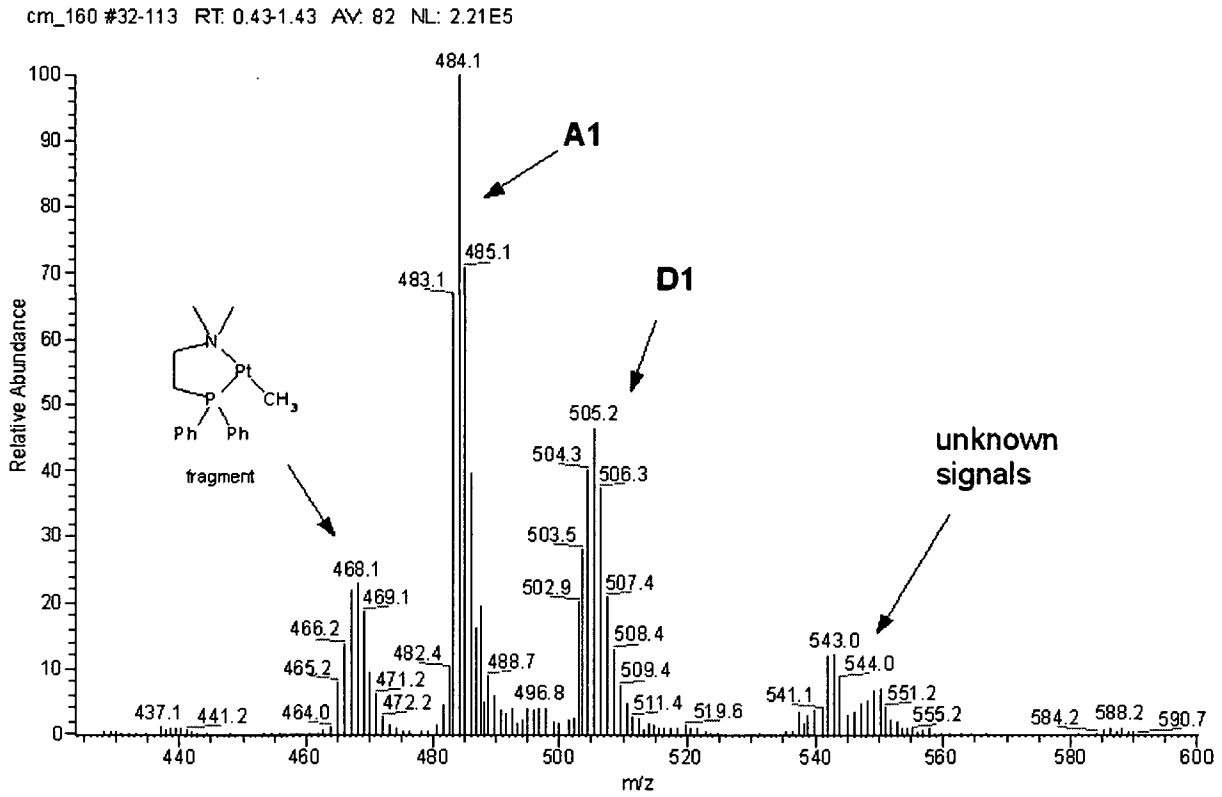

Fig. 80: Mass spectrum of the reaction mixture with benzyl chloride

A background file, containing of the spectrum of the complexes **A1** and **D1** was measured and subtracted from the spectrum to reveal the isotope pattern of the unknown signal. This rendered elucidation of the elemental composition as $C_{23}H_{26}NPPt$ possible (Fig. 81):

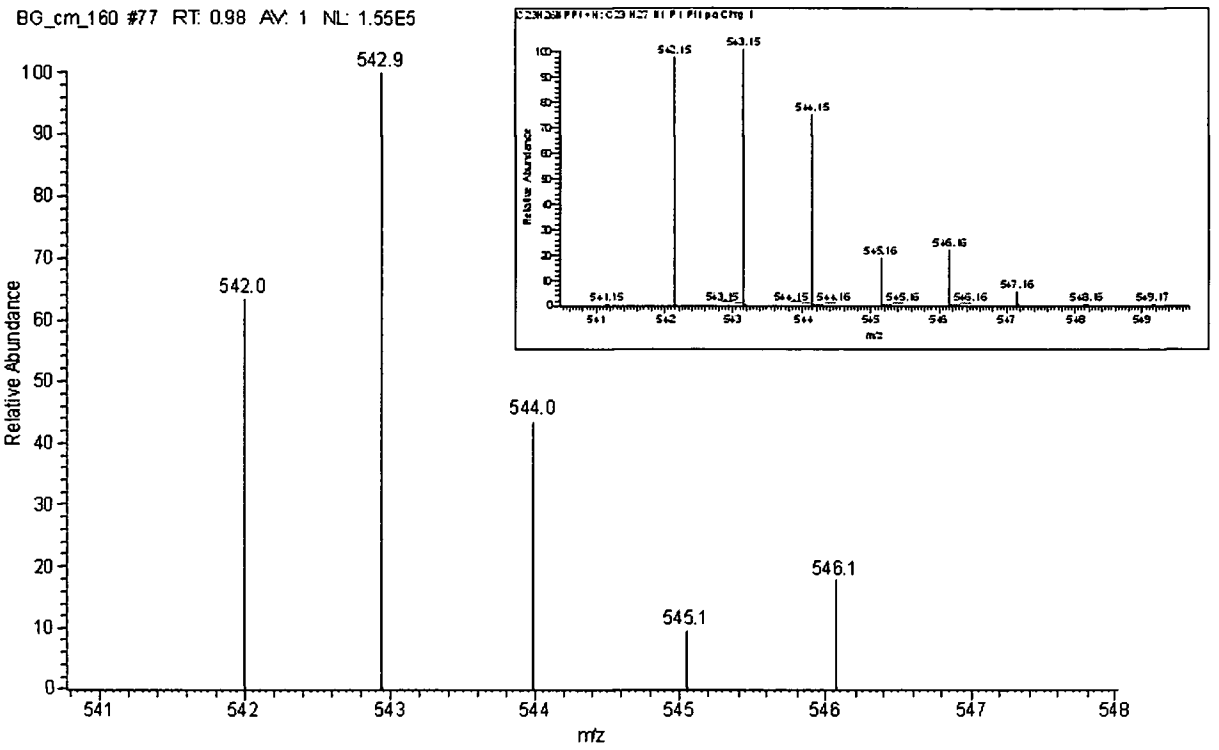

Fig. 81: Isotope pattern of the unknown signal and calculated pattern of $C_{23}H_{26}NPPt + H^+$ (insert)

Considering all the facts known about the unknown reaction so far, a molecular structure was postulated for this isotope pattern, demonstrating the signal to belong to a two-fold demethylated fragment of the ylide complex $Pt(CH_2PPh_2(C_2H_3))(NMe_2Ph)(CH_3)_2$ (**F1**, Fig. 82):

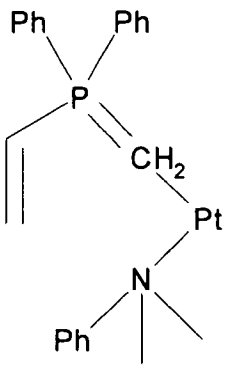

Fig. 82: Fragment of complex **F1**

- Ethyl Chloroacetate

A new reaction mixture was prepared at molar ratio of 1:2 and heated, until here also **A1**, **D1** and the possible ylide complex were visible. The mass spectrum of that reaction looked only slightly different (Fig 83):

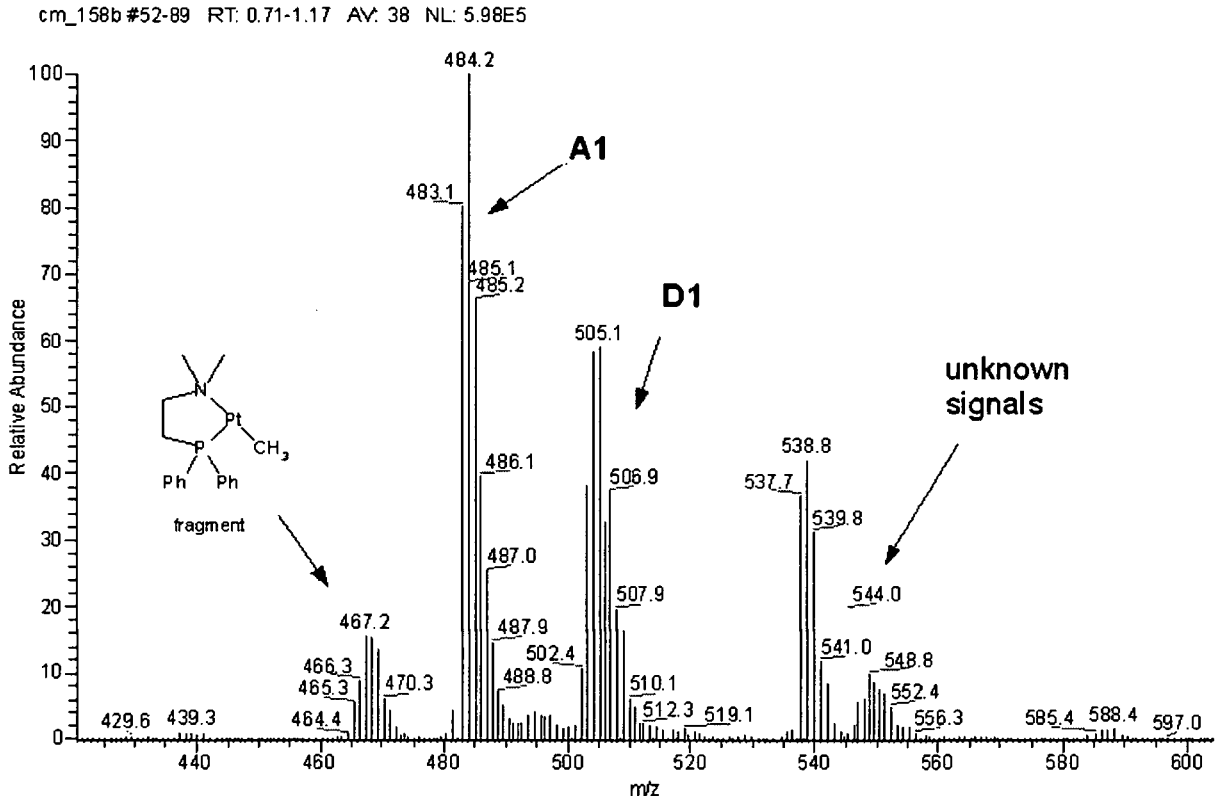

Fig 83: Mass spectrum of the reaction mixture with ethyl chloroacetate

Here also the background file was subtracted rendering it possible to calculate the elemental composition as $C_{20}H_{26}NO_2PPt$ (Fig. 84):

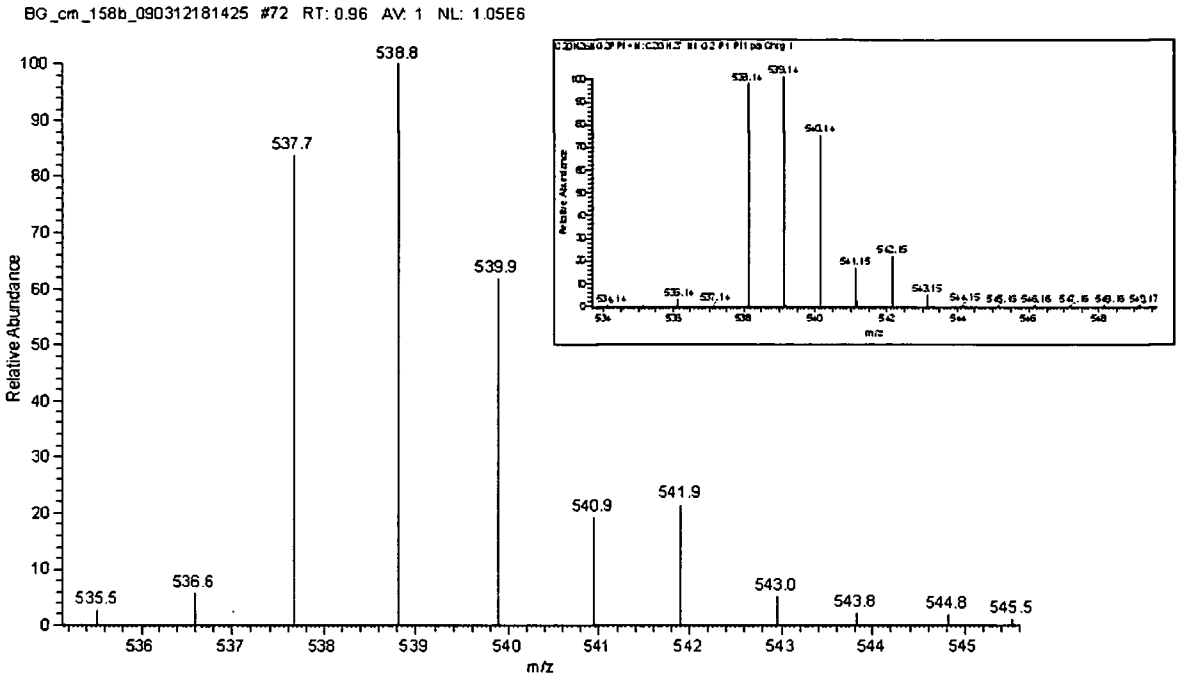

Fig. 84: Isotope pattern of the unknown signal and calculated pattern of $C_{20}H_{26}NO_2PPt + H^+$ (insert)

$Pt(CH_2PPh_2(C_2H_3))(NMe_2COOEt)(CH_3)_2$ (**F2**) was postulated here as a molecular structure similar to the structure from the reaction with benzyl chloride (Fig. 85):

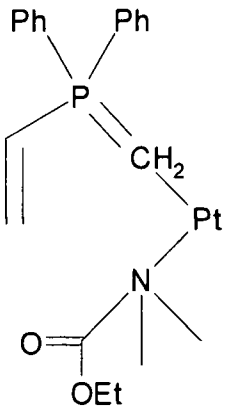

Fig. 85: Fragment of complex **F2**

To collect more data about complex **F2**, another experiment with ethyl chloroacetae was started

and heated to a point, where complex **D1** and **F2** were the two most abundant complexes. A P/H HMBC spectrum was measured, where the signals of two methyl groups at 1.11 and 1.69ppm were visible (Fig 86):

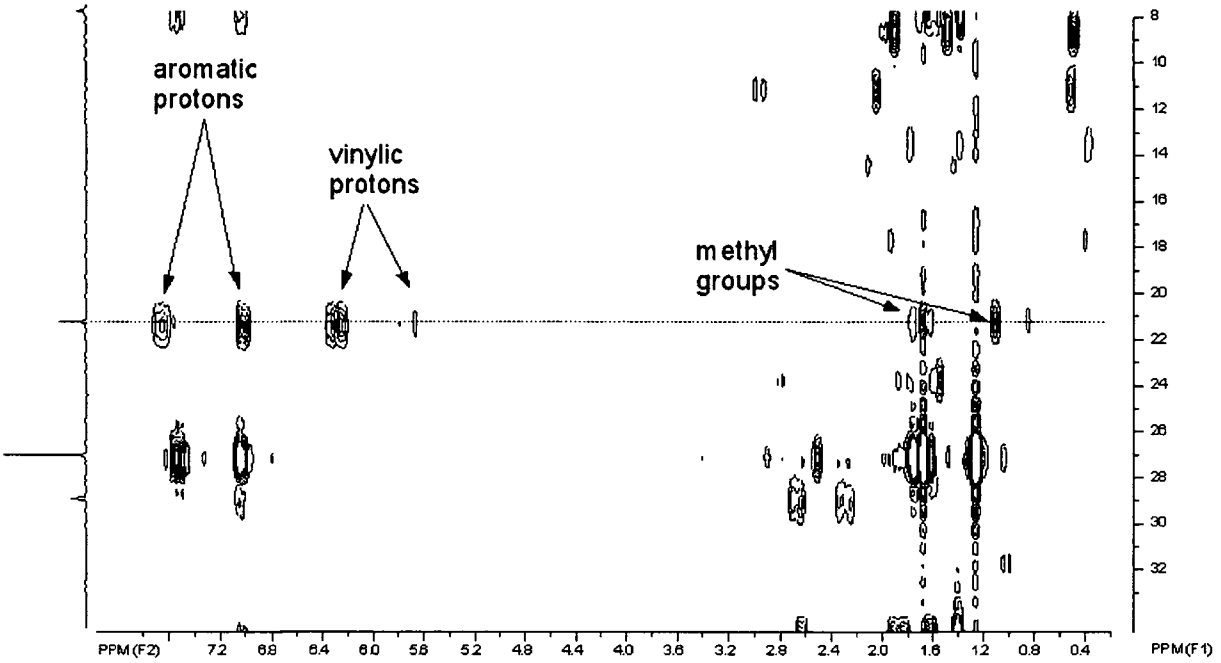

Fig 86: P/H hmbc measurement of complex **F2**

2.5.5 Mechanism

With all the data collected above it was now possible to postulate a reaction mechanism to explain all the transformations and products observed (Fig. 87):

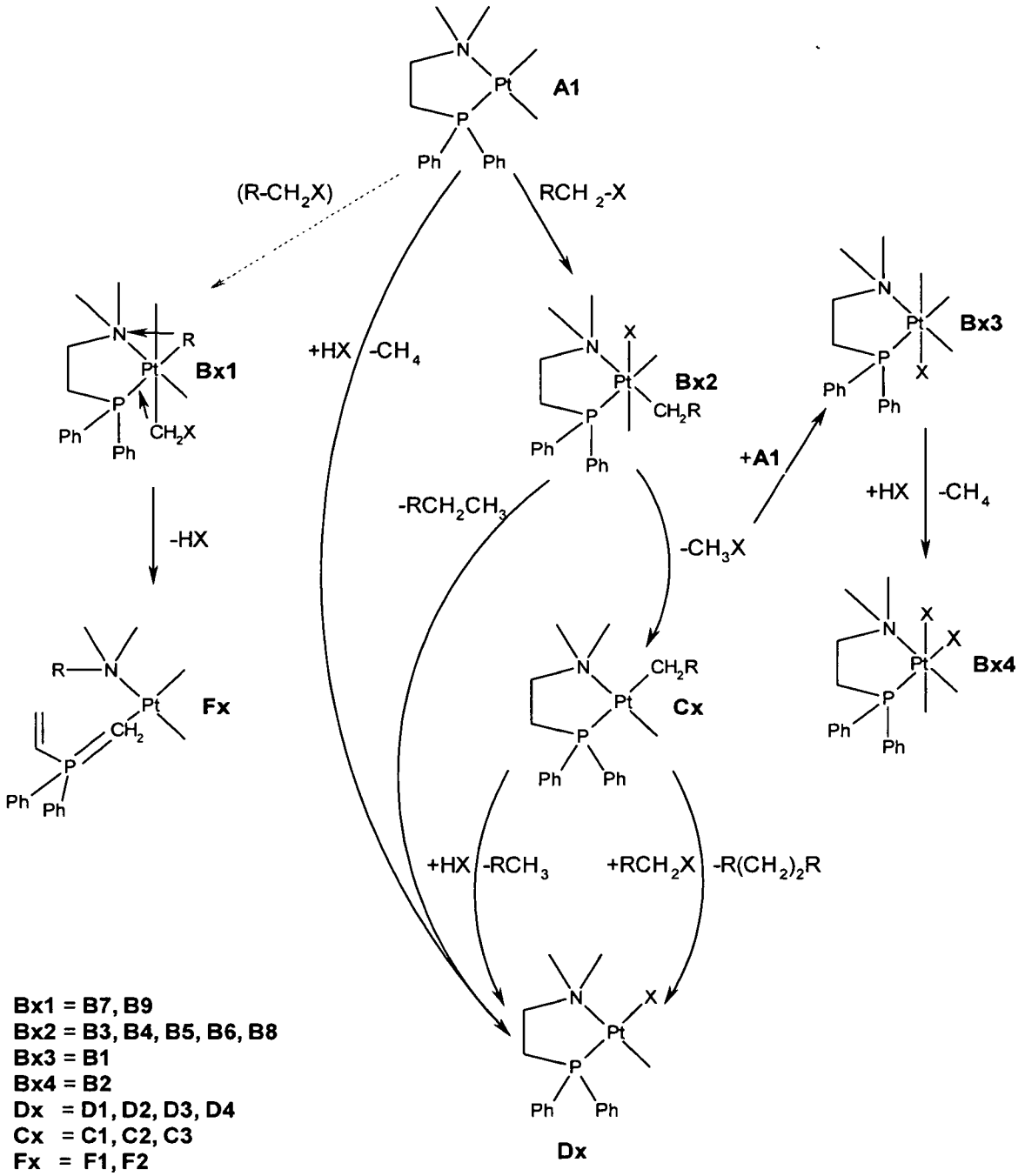

Fig. 87: Summary of the possible reaction mechanisms for halogenated hydrocarbons.

On the one hand the starting complex **A1** reacts through the same pathway already postulated before: Activation of the C-X bond and then formation of a **D**-type complex by either

elimination of methyl halide (which subsequently reacts with complex **A1** to form a trimethyl-halide complex) from the octahedral **B**-type intermediate (**Bx2** in Fig. 87) and reaction of the now remaining **C**-type complex with another RX molecule or by elimination of RCH_3 directly from the octahedral intermediate.

The new reaction mechanism starts from complex **Bx1** in Fig. 87. The mechanism of formation of this complex is not clear. Although C-C bond activation is the most probable pathway, it could also be formed by rearrangement of the octahedral intermediate **Bx2**. The CH_2X group now present in complex **Bx1** is now able to form an ylide with the phosphine ligand, as reported by Sbovata *et al*[15] The remaining halide now eliminates a hydrogen from the ethylene bridge of the *P,N*-ligand. This reaction could be facilitated by unfavourable geometry of a six-membered chelate ring in a possible intermediate compound (Fig. 88).

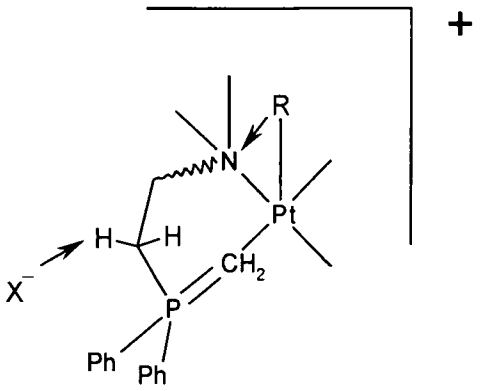

Fig. 88: Possible intermediate species of **Fx** formation

The group R could now migrate from the metal to the nitrogen atom, forming the **F**-type phosphonium ylide complexes observed in the reactions with benzyl chloride, -bromide and ethyl chloroacetate. During this reaction HX is developed, which now reacts with the starting complex **A1** and the trimethyl-halogen complex (**Bx3** in Fig. 107) through formation of methane as well as with **C**-type complexes through formation of CH_3R (toluene and ethyl acetate).

2.5.6 Review of Earlier Experiments

As described in the chapters 2.2 and 2.3 the NMR spectra of the reactions with propargyl chloride, bromides and iodides with β-CH_2-groups and chloroacetic acid showed signals in the vinylic region as well as the formation of methane. Since the vinylic signals in these experiments were similar to the ones found in chapter 2.4, the data were revised and additional NMR measurements were performed.

- Propargyl Chloride

Despite the fact that the largest proportion of the complexes formed in that reaction precipitated from the solution as an insoluble compound that could not be identified, signals for complex **D1** and two unknown complexes with signals at 12.49 and 9.79ppm in the octahedral region of the ^{31}P NMR spectrum were observed. As with the three compounds discussed in chapter 2.4, the formation of methane was also observed in the spectrum. Furthermore, no reaction product in an amount that could explain the complete conversion of complex **A1** was seen. From its chemical shift and its coupling constant, the signal at 12.49ppm was very similar to that of complex **B7** and also the signals of the vinylic protons of the ylide ligand were visible in the ^1H NMR spectrum of that reaction. A P/H correlation NMR measurement was performed and the ligands of the complex at 12.49ppm in the ^{31}P NMR spectrum became visible (Fig. 89): Two of them are methyl groups, the third ligand is seemingly connected to the platinum through a CH_2 group. Its chemical shift is very similar to the one of the -CH_2Cl ligand in complex **B8**. It thus appears that here the C-C bond between the -CH_2Cl group and its neighbouring carbon was also activated, yielding the complex [(κ^2-*P*,*N*)-$Ph_2PCH_2CH_2NMe_2$]$PtMe_2(CH_2Cl)(C{\equiv}CH)$ (**B9**, Fig. 90). Complex **B9** can now be transformed into a F-type complex by ylide formation, as described in chapter 2.5.5. This would then be the origin of the vinylic signals in the ^1H NMR spectrum.

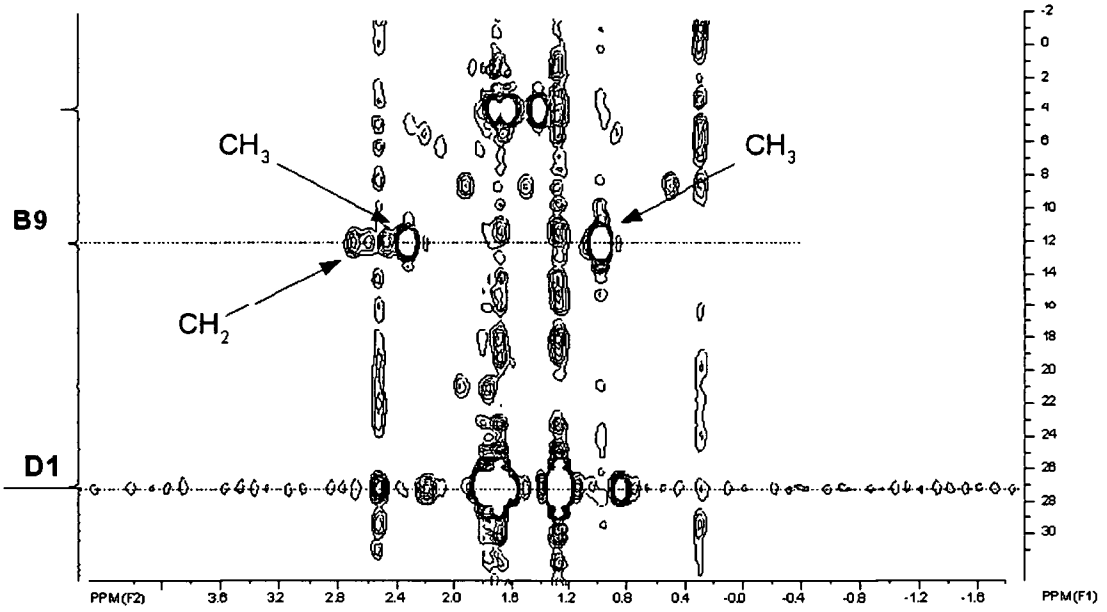

Fig. 89: P/H correlation NMR of the reaction with propargyl chloride

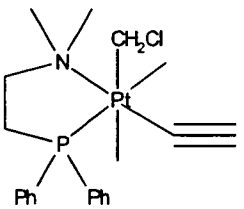

Fig. 90: Complex **B9**

- Bromides and Iodides with β-CH_2-Groups

As described in chapter 2.2, β-elimination is the main reaction pathway of these compounds with complex **A1**. Nevertheless also here the typical signals of the ylide ligand's vinylic protons were visible in the ^{1}H NMR spectrum (Fig 91).

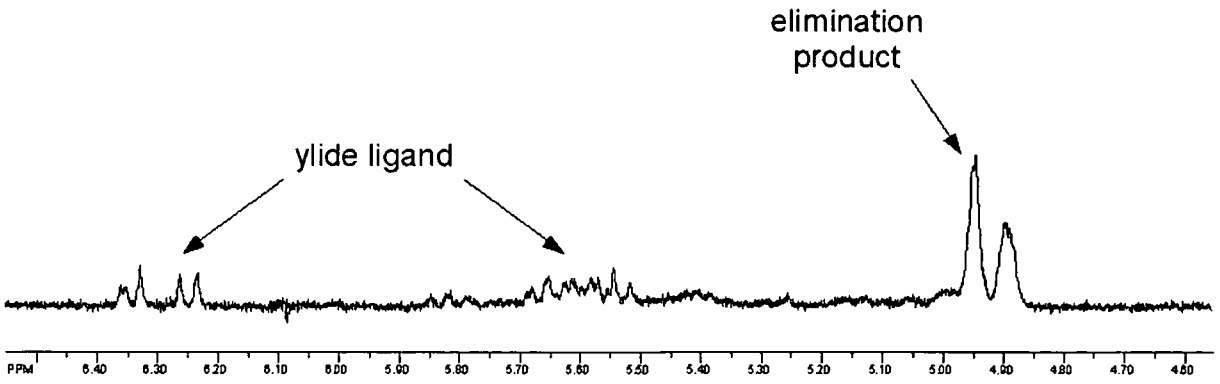

Fig 91: Signals of the ylide ligand in the ^{1}H NMR spectrum of the reaction with 1,6-dibromohexane

The bromide and iodide appear to affect the C-C bond in a similar way than phenyl and COOR groups do, so that this bond can be activated by complex **A1**, yielding a **F** type complex.

- Chloroacetic Acid

As seen in chapter 2.3.1.4, the activation of C-Cl bonds is not strong enough to compete with the coordination of an acid to complex **A1**. Since it was shown in chapters 2.4.1 and 2.4.3, that reactions of β-CH_2-less chlorinated compounds over ylide formation are faster than the reactions of these compounds via the reaction pathways described in Fig. 34 (p.30) and the ^{1}H NMR spectrum of the reaction of chloroacetic acid with complex **A1** showed vinylic signals (Fig. 45, p. 43), obviously also part of the chloroacetic acid reacts by ylide formation.

2.6 Reactions with Silyl Chlorides

In a previous experiment[32] (described in chapter 1.2.12.2) complex **A1** was reacted with iodotrimethylsilane in a molar ratio of 1:1. In this reaction complex **D3** and tetramethylsilane was formed (Fig. 32, p. 28). In another experiment with dimethylphenylsilane[32] a Si-Si bond was formed (Fig 33, p. 29), showing that also with silyl halides dehalogenative coupling or methylation of the dehalogenated moiety is basically possible. To see if this applies to a broader range of silyl halides, experiments with silyl mono-, di- and trichlorides were performed.

2.6.1 Silyl Monochlorides

2.6.1.1 Chlorotrimethylsilane

The first compound of this group investigated was chlorotrimethylsilane. The reactions were carried out at stoichiometric ratios of 1:1 and 1:2.

On addition of the reactant at a 1:1 ratio no reaction wasobserved at room temperature. Heating of the reaction mixture to 70°C resulted in slow consumption of **A1**. At this time 60% of **A1** were converted to **D1**, according to the ^{31}P and ^{1}H NMR spectra. In the ^{1}H NMR spectra two new signals emerged at 0.0ppm and 0.12ppm (Fig. 60).

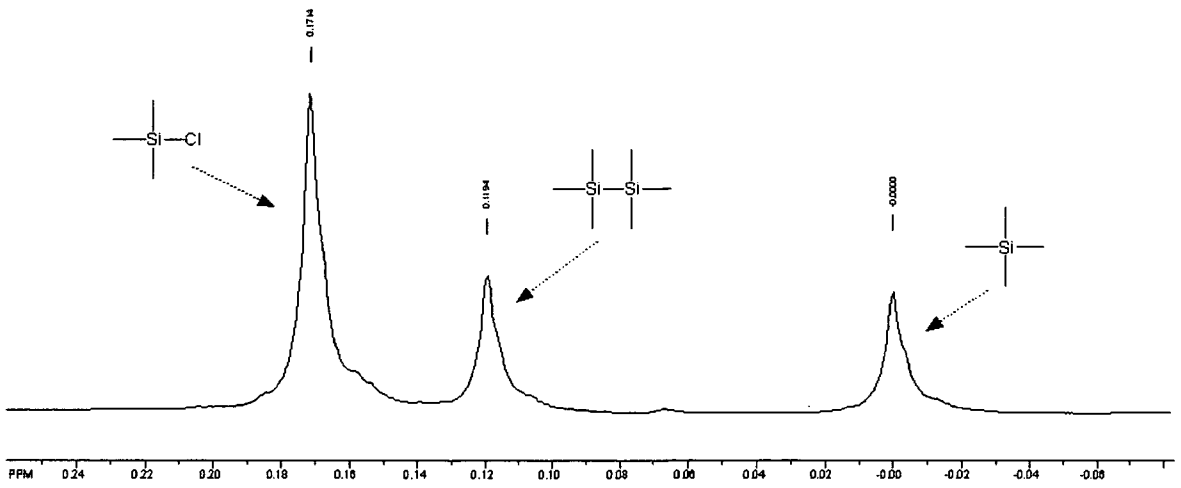

Fig. 92: Section from the ^{31}P-NMR spectrum of the reaction mixture of **A1** with chlorotrimethylsilane

The first could be easily assigned to tetramethylsilane, apparently formed by elimination from the octahedral intermediate $[(\kappa^2\text{-}P,N)\text{-}Ph_2PCH_2CH_2NMe_2]PtMe_2((CH_3)_3Si)Cl$ (**B10**, Fig. 93) as described by Pfeiffer *et al*[32], the second to hexamethyldisilane, produced by coupling of two trimethylsilyl groups similar to the reaction with chloro-dimethylphenylsilane. No other products were observed, and the amount of silanes formed is in good accordance with the amount of **D1**

formed.

In the reaction with a 1:2 ratio at room temperature 30% of the starting complex **A1** were converted into **D1** within 12 hours. The main product at this temperature was hexamethyldisilane. Upon heating to 70°C tetramethylsilane was produced, too. **A1** was completely consumed within four days. No other organosilanes or complexes were observed.

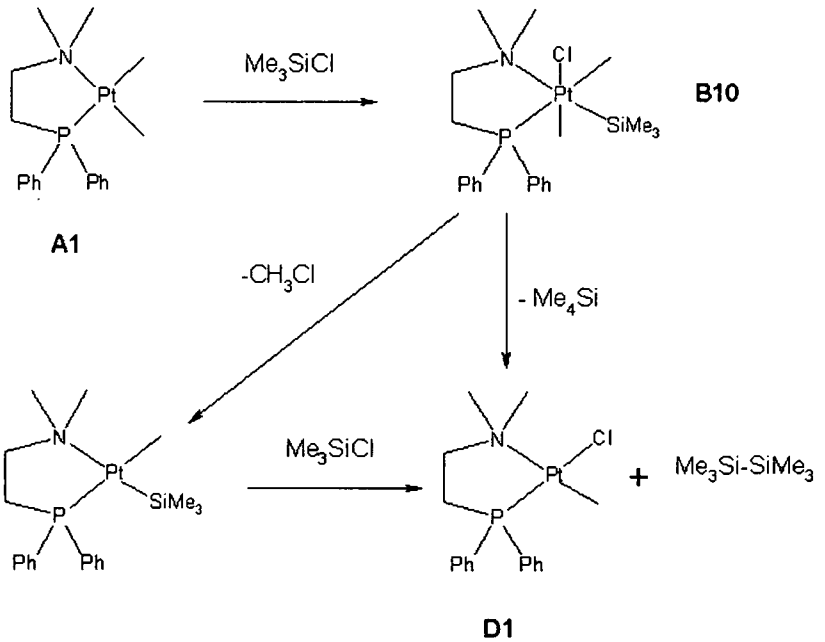

Fig. 93: Reaction of chlorotrimethylsilane with complex **A1**

In contrast to the reaction with iodotrimethylsilane as described in chapter 1.2.12.2 (p. 28) elimination of a methyl halogenide from the octahedral intermediate **B10** also takes place here. This can be explained by the fact, that the C-Si bond strength is very similar to that of the of C-Cl (89.4 kcal/mol for $(CH_3)_3Si\text{-}CH_3$[51] vs 83.7 kcal/mol for $CH_3\text{-}Cl$[28]) so both possible elimination reactions from complex **B10** are energetically nearly equally favourable. In contrast, the difference between the bond strengths of C-Si and C-I amounts to about 32 kJ/mol (89.4 kcal/mol for $(CH_3)_3Si\text{-}CH_3$[51] vs 57.6 kcal/mol for $CH_3\text{-}I$[28]), what renders elimination of MeI rather unfavourable. A methyl-silyl complex, the proposed intermediate formed by elimination of methyl chloride, was not monitored.

2.6.1.2 Chlorodimethylvinylsilane

The reactions with chlorodimethylvinylsilane were performed in stoichiometric ratios of 1:1, 1.2 and 1:4. The reactivity of that compound was much higher than that of chlorotrimethylsilane (see Fig. 94). When the experiment was carried out in a ratio of 1:1 a reaction was observed even at room temperature. Half of the starting complex **A1** was converted into **D1** after about 80 hours. At a 1:2 ratio it took about 70 hours for 50% conversion and at ratio 1:4 50% of **A1** were converted after about 50 hours. The starting complex was fully converted into **D1** after about 90 hours of reaction at room temperature at this ratio.

Besides **D1** no further platinum compounds could be identified in the ^{31}P and ^{1}H NMR spectra. In the ^{1}H NMR spectrum another signal appeared at 0.19ppm, 12Hz upfield from the peak of chlorodimethlvinylsilane that can be assigned to tertramethyldivinyldisilane. This product was also identified by GC/MS analysis, no further organosilanes were found. In contrast to the experiment with chlorotrimethylsilane, heating of the reaction mixture did not change the range of products, the methylation product trimethylvinylsilane was not observed.

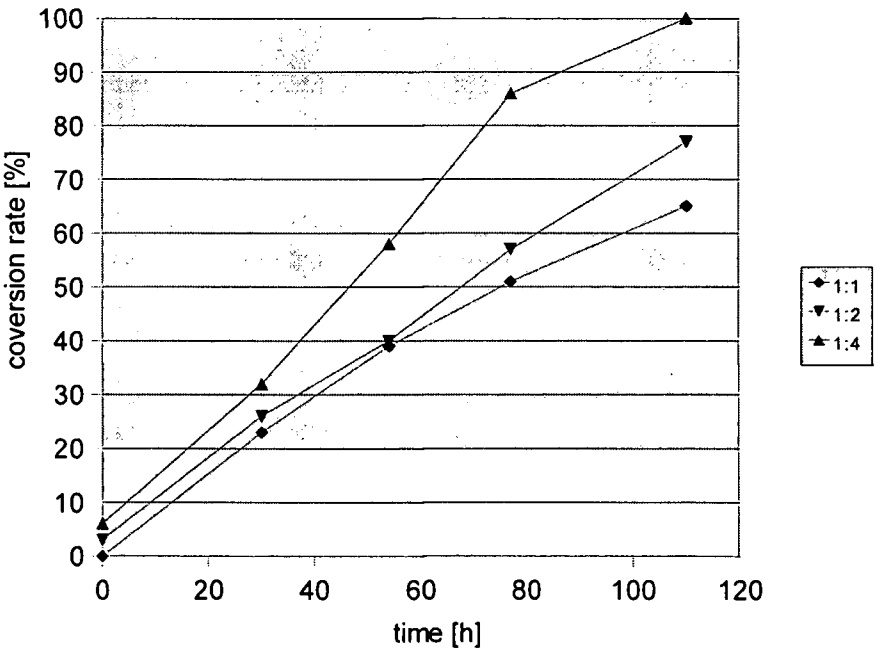

Fig. 94: Conversion rate of **A1** into **D1** by reaction with chlorodimethylvinylsilane at room temperature and different ratios

2.6.1.3 Chlorotriethylsilane

Chlorotriethylsilane was reacted with complex **A1** in the stoichiometric ratios of 1:1, 1:2 and 1:4. At all three ratios no change was visible after 24 hours at room temperature, therefore the reaction mixtures were heated.

At a molar ratio of 1:1 80% of **A1** was transformed into **D1** after 48 hours at 70°C. At ratios 1:2 and 1:4 the conversion rate after this time was 90%. In the ^{1}H NMR spectra the formation of new organosilanes was monitored. 22Hz upfield from the CH_2-Si peak of the starting compound a new quartet signal emerged at 0.52ppm, and 14Hz downfield from the CH_3 peak of the ethyl group of the starting compound a new triplet became visible at 0.97ppm (Fig. 95).

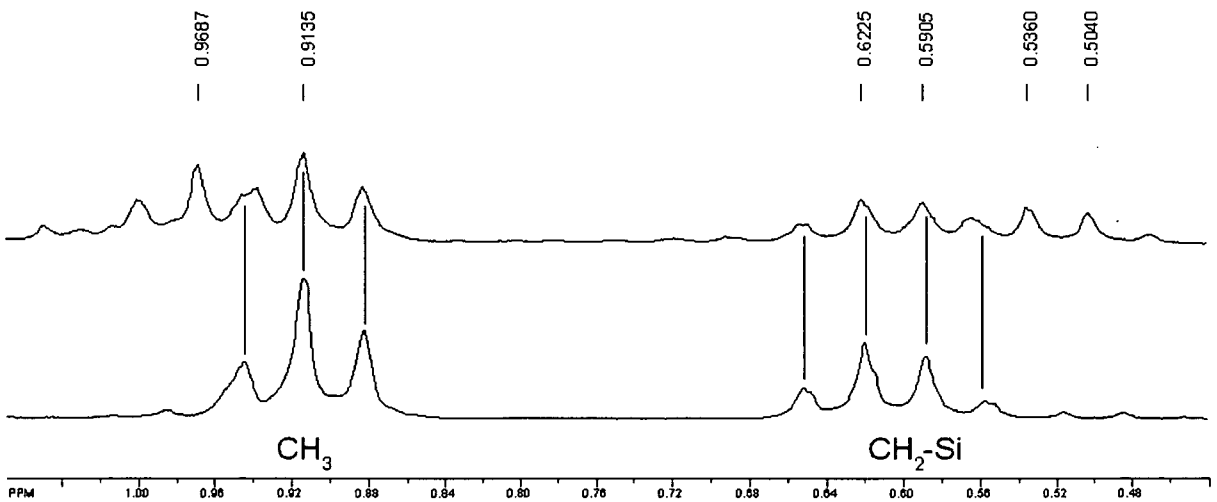

Fig. 95: Section of the ^{1}H NMR spectra of triethylchlorosilane (below) and the reaction mixture with complex **A1** (top)

Since no new signals with a chemical shift lower than 0.5ppm (the area where CH_3-Si signals can usually be found) could be identified at any molar ratio, formation of Et_3MeSi, formed by methylation of the dechlorinated moiety, can be ruled out. Therefore the new signals appear to belong to hexaethyldisilane, the product of dehalogenative coupling (Fig. 96). In the GC/MS spectrum no signal for the coupling product was found. Since no experimental data for that

compound are available, it could be, that its boiling point is out of range of the GC/MS method. In the ^{31}P NMR spectrum a weak signal at 8.6ppm was found, being typical for the octahedral complex **B1**. This complex is formed by addition of methyl chloride to **A1**. Methyl chloride is eliminated during the formation of a **C**-type complex (Fig. 96). Upon reaction with another Et_3SiCl molecule and elimination of Si_2Et_6 this complex is then converted transformed into complex **D1**. So the observation of complex **B1** supports the possibility of dehydrogenative coupling in this reaction.

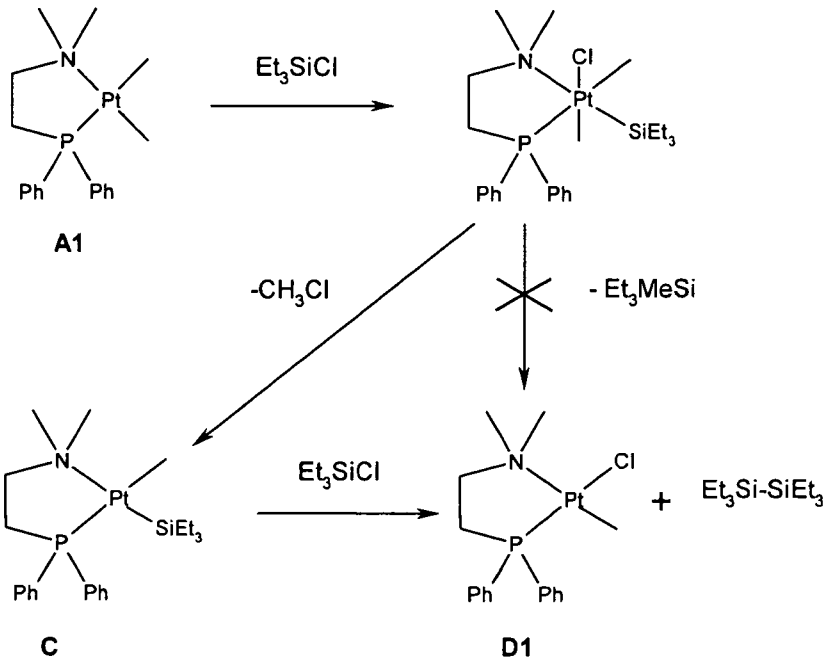

Fig. 96: Reaction of chlorotriethylsilane with complex **A1**.

2.6.2 Silyl Di- and Trichlorides

2.6.2.1 Dichlorodiphenylsilane

The basic experiments with dichlorodiphenylsilane were performed in the molar ratios of 1:1, 1:2 and 1:4.

At molar ratio of 1:1 or 1:2 21% of **A1** was converted into **D1** within 12 hours at room temperature. At molar ratio 1:4 the conversion rate after 12 h was 28%. After heating the

reaction solution to 70°C, **A1** was completely converted into the chloro-methyl complex **D1** within five hours at all three ratios.

The only organic product identified was chloro-methyldiphenylsilane, which could be identified in the GC/MS analysis as well as by its methyl peak at 0.69ppm in the ^{1}H NMR spectrum.

During the reaction a white solid with very low solubility in the most common solvents precipitated. It was possible to measure a ^{1}H NMR spectrum of that compound in deuterated acetone (Fig. 97).

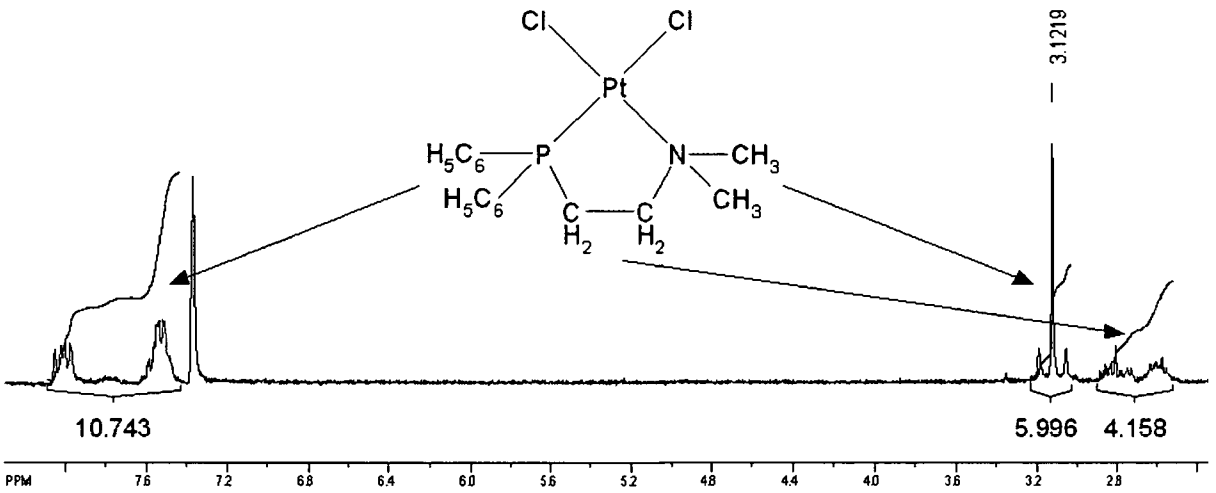

Fig. 97: ^{1}H NMR spectrum of complex **E1** in deuterated acetone

A triplet at 3.1ppm, two signals for aromatic groups at about 7.5 and 8ppm and two multiplets at 2.6 and 2.8ppm were observed. Considering their integration values and the kind of observed protons, these signals appear to belong to a the P,N-ligand coordinated to platinum. The precipitate exhibited good crystallinity, therefore the structure could be determined by X-ray diffraction. The precipitate turned out to be the dichloro complex [(κ^2-*P*,*N*)-$Ph_2PCH_2CH_2NMe_2$]$PtCl_2$ (**E1**, Fig. 98).

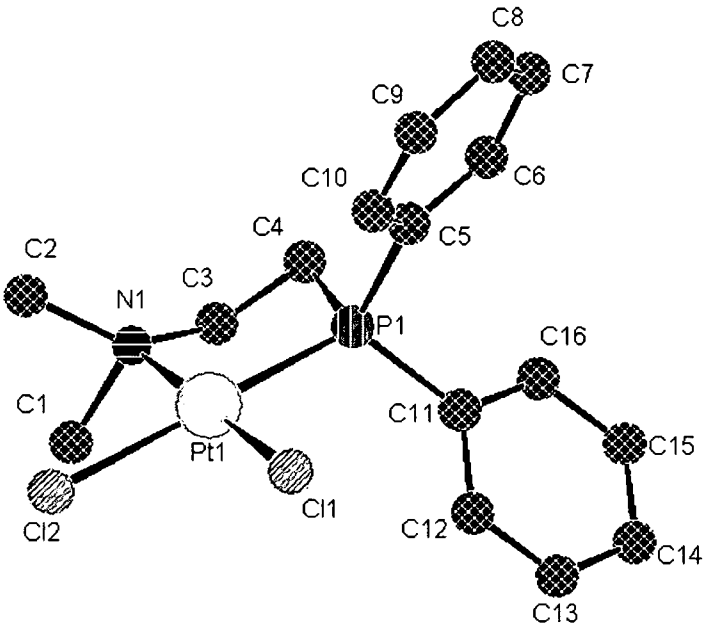

Fig. 98: Molecular structure of $[(\kappa^2\text{-}P,N)\text{-}Ph_2PCH_2CH_2NMe_2]PtCl_2$ **(E1)**

Table 9: Selected bond lengths and angles of complex **E1**

Bond lengths (Å)	
Pt-Cl(1)	2.257(2)
Pt-Cl(2)	2.367(2)
Pt-P	2.194(2)
Pt-N	2.124(6)
Bond angles (°)	
P(1)-Pt(1)-N(1)	86.16(15)
P(1)-Pt(1)-Cl(1)	93.82(6)
Cl(1)-Pt(1)-Cl(2)	88.23(6)
N(1)-Pt(1)-Cl(2)	91.79(15)

Assuming that complex **E1** is formed by reaction of a platinum complex with the starting compound through an oxidative addition reaction, the reactive platinum species in that reaction could only be a square planar Pt(II) complex, since the octahedral intermediates do not offer the

possibility to activate the Si-Cl bond. A reaction of an **A** or **C** type intermediate with a dichlorosilane would require the transfer of both chlorines from the starting compound to the complex in one step or through formation of a short-lived intermediate. Furthermore the dechlorinated silane would either have to be coordinated to the platinum or to bind to two new groups. Since neither any unknown complex nor any dechlorinated silane was identified in any reaction with a dichlorosilane such a mechanism is rather unlikely. An easier reaction mechanism would proceed through addition of the dichlorosilane to complex **D1** and methylation or coupling of the dechlorinated ligand similar to methylation or coupling by coordination to **A1**. To verify this theory, dichlorodiphenylsilane was reacted with isolated complex **D1**. The reaction was finished after 20 hours at room temperature and in fact complex **E1** could be identified as reaction product (Fig. 99).

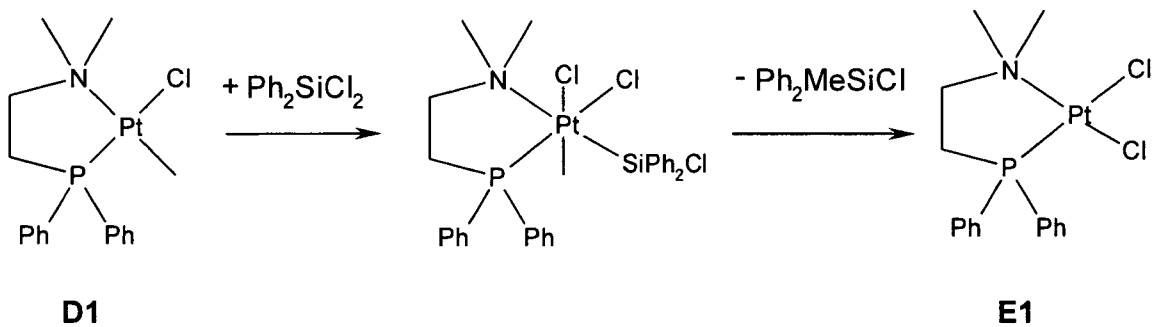

Fig. 99: Formation of complex **E1** by oxidative addition of a dichlorosilane to complex **D1**

2.6.2.2 Dichlorodimethylsilane

The experiments with dichlorodimethylsilane were carried out in the stoichiometric ratios 1:1, 1:2 and 1:4.

At a ratio of 1:1, the reaction proceeded very slowly at room temperature, only about 10% of **A1** were converted into **D1** after 24 hours. The reaction mixture was then heated, which led to complete consumption of **A1** after three days. The situation was the same for a molar ratio of 1:2. At ratio 1:4 the reaction was comparably slow at room temperature, but at 70°C it was finished after only two days.

^{1}H NMR analysis showed the formation of a small amount of chlorotrimethylsilane and a new signal about 5ppm upfield from the CH_3-Si signal. In the GC/MS analysis tetramethyl-dichloro-disilane could be identified and assigned to the new signal in the ^{1}H NMR spectrum (Fig. 100).

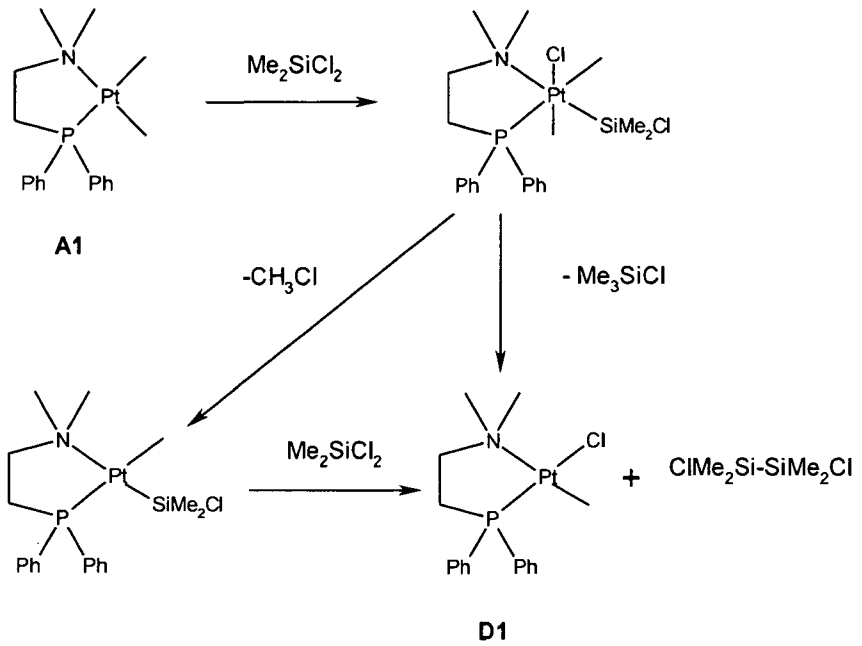

Fig. 100: Reaction of dichlorodimethylsilane with complex **A1**

Also in this reaction a signal of **B1**, formed by addition of methyl chloride, was found in the ^{31}P NMR spectrum (Fig. 101). Complex **E1** precipitated from the reaction solution and was identified by ^{1}H NMR in deuterated acetone.

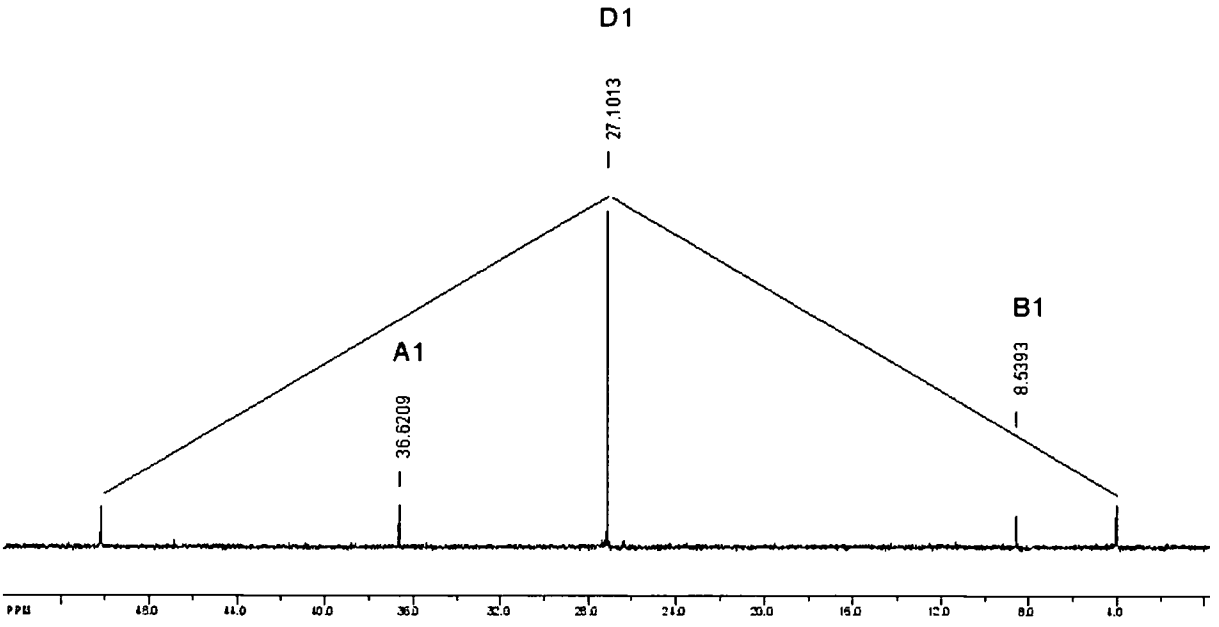

Fig. 101: ^{31}P NMR spectrum of the reaction mixture of **A1** with dichlorodimethylsilane

2.6.2.3 Cyclohexylmethydichlorosilane

The reactions with cyclohexyl-methyldichlorosilane were performed in the stoichiometric ratios of 1:1, 1:2 and 1:4. At all three ratios the formation of a slightly yellow precipitate was observed after only a few hours at room temperature. After five days at room temperature no signals of platinum complexes were detectable in the ^{1}H and ^{31}P NMR spectra any more, all platinum species had seemingly precipitated quantitatively.

In the ^{1}H NMR spectra of the reaction solutions a new signal at 0.27ppm was visible, it apparently belongs to cyclohexyl-dimethylchlorosilane. The yellow precipitate turned out to be a mixture of the complexes **D1** and **E1** at a molar ratio of 1:2 in the ^{1}H NMR analysis. Since no traces of **D1** were visible in the reaction solution (normally **D1** is completely soluble in the concentration range used at my experiments, usually between 20 and 40 mg/ml) complex **D1** appears to cocrystallize with complex **E1** when **E1** is produced in a high yield.

2.6.2.4 Trichlorophenylsilane

The experiments with trichlorophenylsilane were set up at the stoichiometric ratios 1:1, 1:2 and 1:4. At a ratio of 1:1 21% of **A1** was converted into **D1** after 12 hours at room temperature. At ratios of 1:2 and 1:4 the conversion rate was 50%. After heating the reaction mixtures to 70°C, complete conversion was obtained within 30 minutes at ratios of 1:2 or 1:4, while at ratio 1:1 it took 24 hours.

Considering the reaction products, the results differed depending on the ratio of the starting compounds (Fig. 102). At ratio 1:1 two new peaks in the ^{1}H NMR analysis appeared at 0.42 and 0.59ppm. In GC/MS, three products were visible at that ratio: Dichloro-methyl-phenylsilane (P1), chloro-dimethyl-phenylsilane (P2) and 1,2-dichloro-1,2-dimethyl-1,2-diphenyldisilane (P4), where P1 was the main product. At ratios of 1:2 and 1:4 P2 and P4 could not be found but the new compound 1,1-dichloro-2,2-dimethyl-1,2-diphenyldisilane (P3) was detected together with P1 as the main product. In the ^{1}H NMR analysis only the peak at 0.59ppm was visible in this case. This appears to be the signal of the CH_3-Si protons of P1, while the the methyl protons of P2 are responsible for the signal at 0.42ppm. The dichloro complex **E1** was not found in these reactions, no precipitate was observed.

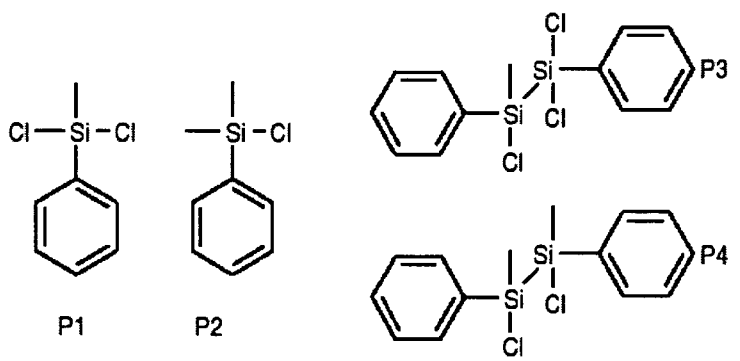

Fig. 102: Products of the reaction with trichlorophenylsilane

At a 1:1 ratio, P4 was obvioulsy obtained by dehalogenative coupling of P1, while P3 is formed by oxidative addition of trichlorophenylsilane to complex **C3** (and subsequent elimination of P3) which is more likely than the coordination of another P1 molecule at molar ratio of 1:2 or 1:4 (Fig. 103).

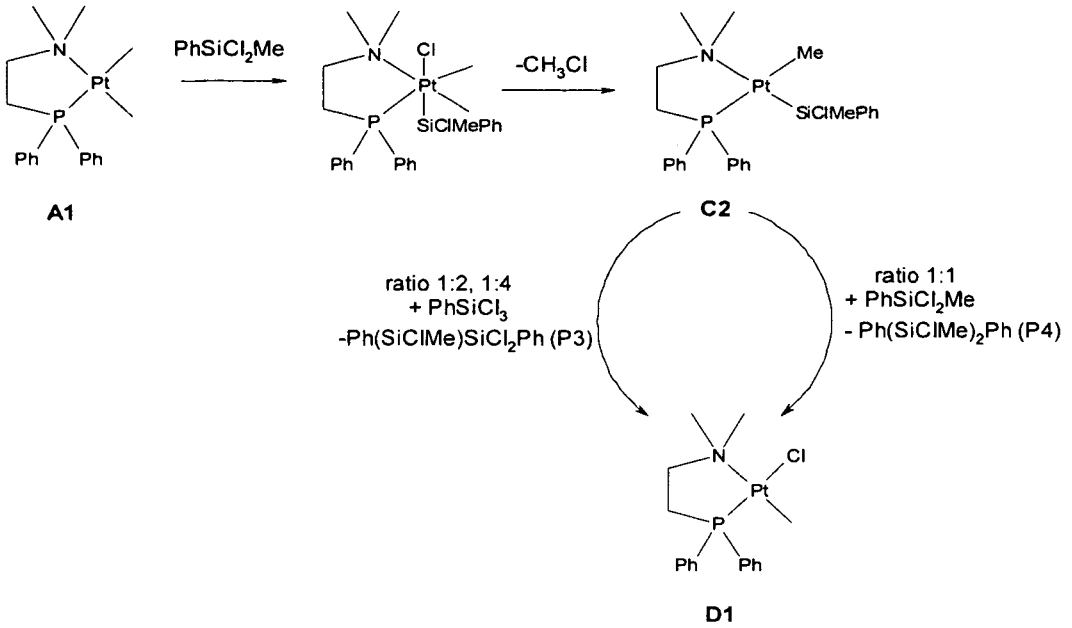

Fig. 103: Reaction pathways for the formation of products P3 and P4

2.6.3 Conclusions

The experiments with different silyl chlorides show that in fact these compounds react in a similar way than halogenated hydrocarbons do, but at a much higher reaction rate. Dichlorosilanes were even able to add to the complex **D1**, with subsequent elimination of a chlorosilane and formation of a dichloro complex.

3. Experimental Section

3.1 Reaction Conditions

All reactions were carried out under inert conditions. Argon 5.0 (O_2 < 2.0ppm, H_2O <3.0ppm) was used as inert gas. The solvents and liquid reactands used were distilled once under argon and made oxygen-free by the use of the freeze-pump-thaw methode prior to every reaction. The NMR solvents were stored over molecular sieve (4Å). The NMR tubes were treated with dichlorodimethylsilane to prevent the SiOH groups from reacting with the educts and the complexes.

NMR experiments were performed on Bruker Avance 250 MHz and 300 MHz spectrometers and on a Bruker Avance III 500 MHz device spectrometer. The measurements took place at room temperature, Tetramethylsilane, H_3PO_4 and $Na_2Pt(H_2O)_6$ were used as external standards for ^{1}H, ^{13}C, ^{31}P and ^{195}Pt NMR respectively. ^{13}C, ^{31}P and ^{195}Pt NMR spectra were proton decoupled. All pulse programs were obtained from the Bruker software library.

The NMR data listed here include signals that were visible throughout the reactions as well as signals that only appeared temporarily. Signals of unreacted educts are not listed.

GC/MS data was obtained on a Finnigan Voyager GC/MS device and a Thermo scientific Focus GC / DSQ II device with an EI ion source, an achiral capillary and a quadrupole analyser.
Mass spectra were measured on a Thermo Scientific ITQ 1100 with chemical ionistation. Signals of unreacted educts are not listed.

3.2 Reactant Synthesis

3.2.1 N-[2-(Diphenylphosphino)ethyl]-N,N-dimethylamine (*P,N*-chelated Ligand)

The P,N-chelated ligand was prepared by the following procedure[71]:

(A) $Cl(CH_2)_2NMe_2 * HCl \xrightarrow{KOH} Cl(CH_2)_2NMe_2$

(This compound was then extracted into diethyl ether)

(B) $4\ Li + ClP(C_6H_5)_2 \xrightarrow{THF} 2\ LiP(C_6H_5)_2$

(C) $LiPPh_2 + Cl(CH_2)_2NMe_2 \xrightarrow{DEE / THF} Ph_2P(CH_2)_2NMe_2$

3.2.2 $[(\kappa^2\text{-}P,N)\text{-}Ph_2P(CH_2)_2NMe_2]PtMe_2$ (**A1**)

The starting complex was prepared as follows:

(A)[72] $K_2PtCl_4 + nbd \xrightarrow{AcOH,\ HCl,\ H_2O} nbdPtCl_2$

(B)[73] $nbdPtCl_2 + 2LiMe \xrightarrow{DEE} nbdPtMe_2$

(C) $nbdPtMe_2 + Ph_2P(CH_2)_2N(CH_3)_2 \xrightarrow{cyclohexane} (Ph_2P(CH_2)_2NMe_2)PtMe_2$

3.3. Reactions of Complex A1 with Halogenated Hydrocarbons with CH_x-Groups in the β-Position

3.3.1 1,3-Dichloropropane

(A) An amount of 2.37 mg (0.021 mmol) of 1,3-dichloropropane was added at room temperature to 10 mg (0.021 mmol) of **A1** in 0.6 ml of C_6D_6. NMR spectra were taken at regular intervals. Only about 10% of the starting complex were consumed after 10 days at 70°C, the reaction was stopped after three weeks.

(B) An amount of 9.84 mg (0.084 mmol) of 1,3-dichloropropane was added at room temperature to 20 mg (0.042 mmol) of **A1** in 0.6 ml of C_6D_6. NMR spectra were taken at regular intervals. Only about 10% of the starting complex were consumed after 10 days at 70°C, the reaction was stopped after three weeks.

^1H NMR: δ (ppm): 0.16 (s, CH_4), 1.31 (d, with satellites, $^3J_{PH}$= 3.3 Hz, $^2J_{PtH}$= 74 Hz, $CH_3\text{-}Pt_{D1}$), 2.51 (s, with satellites, $^3J_{PtP}$=11.5 Hz, $CH_3\text{-}N_{CMK}$), 5.00-5.14 (m, CH_2=$CHCH_2Cl$) 7.04 (m, $C_{arom\ D1}$), 7.53 (m, $C_{arom\ D1}$)

^{31}P NMR: δ (ppm): 27.12 (s with satellites, $^1J_{PtP}$= 4676 Hz, **D1**)

3.3.2 (3-Chloropropyl)trimethylsilane

(A) An amount of 4.2 mg (0.021 mmol) of 1,3-dibromopropane was added at room temperature to 10 mg (0.021 mmol) of **A1** in 0.6 ml of C_6D_6. NMR spectra were taken at regular intervals. The reaction was stopped after one week with no product formation visible in the NMR spectra.

(B) An amount of 8.4 mg (0.042 mmol) of 1,3-dibromopropane was added at room temperature to 10 mg (0.021 mmol) of **A1** in 0.6 ml of C_6D_6. NMR spectra were taken at regular intervals. The reaction was stopped after one week with no product formation visible in the NMR spectra.

(C) An amount of 16.8 mg (0.084 mmol) of 1,3-dibromopropane was added at room temperature to 10 mg (0.021 mmol) of **A1** in 0.6 ml of C_6D_6. NMR spectra were taken at regular intervals. The reaction was stopped after one week with no product formation visible in the NMR spectra.

^{31}P NMR: δ (ppm): 27.15 (s, **D1**)

3.3.3 1,3-Dibromopropane

(A) An amount of 4.4 mg (0.021 mmol) of 1,3-dibromopropane was added at room temperature to 10 mg (0.021 mmol) of **A1** in 0.6 ml of C_6D_6. NMR spectra were taken at regular intervals. After 3 days at 70°C the starting complex was consumed.

(B) An amount of 8.8 mg (0.042 mmol) of 1,3-dibromopropane was added at room temperature to 10 mg (0.021 mmol) of **A1** in 0.6 ml of C_6D_6. NMR spectra were taken at regular intervals. After 3 days at 70°C the starting complex was consumed.

(C) An amount of 17.6 mg (0.084 mmol) of 1,3-dibromopropane was added at room temperature to 10 mg (0.021 mmol) of **A1** in 0.6 ml of C_6D_6. NMR spectra were taken at regular intervals. After 2 days at 70°C the starting complex was consumed.

(D) An amount of 106 mg (0.504 mmol) of 1,3-dibromopropane was added at room temperature to 10 mg (0.021 mmol) of **A1** in 0.6 ml of C_6D_6. NMR spectra were taken at regular intervals.

After 1 hour at 70°C the starting complex was consumed.

^{1}H NMR: δ (ppm): 0.16 (s, CH_4), 0.61 (d, with satellites, $^3J_{PH}$= 7.61 Hz, $^2J_{PtH}$= 70.3 Hz, CH_3-Pt_{B3}), 0.98 (s, with satellites, $^3J_{PtP}$=13.61 Hz, CH_3-N_{B3}), 1.33 (d, with satellites, $^3J_{PH}$= 3.5 Hz, $^2J_{PtH}$= 75.5 Hz, CH_3-Pt_{D2}), 2.0 (d, with satellites, $^3J_{PH}$= 6.9 Hz, $^2J_{PtH}$= 72 Hz, CH_3-Pt_{B3}), 2.54 (s, with satellites, $^3J_{PtP}$=12.15 Hz, CH_3-N_{D2}), 2.68 (s, with satellites, $^3J_{PtP}$=10.1 Hz, CH_3-N_{B3}) 7.04 (m, $C_{arom\ D2}$), 7.53 (m, $C_{arom\ D2}$).
^{31}P NMR: δ (ppm): 6.52 (s, **B3**), 27.15 (s, **D1**)

3.3.4 1,6-Dibromohexane

(A) An amount of 10.3 mg (0.084 mmol) of 1,6-dibromohexane was added at room temperature to 10 mg (0.021 mmol) of A1 in 0.6 ml of C6D6. NMR spectra were taken at regular intervals. After 3 days at 70°C the starting complex was consumed.

^{1}H NMR: δ (ppm): 0.16 (s, CH_4), 2.54 (s, with satellites, $^3J_{PtP}$=12.15 Hz, CH_3-N_{D2}), 2.68 (s, with satellites, $^3J_{PtP}$=10.1 Hz, CH_3-N_{B3}) 7.04 (m, $C_{arom\ D2}$), 7.53 (m, $C_{arom\ D2}$). The Pt-CH_3 signal was completely covered by a signal of the educt.
^{31}P NMR: δ (ppm): 28.15 (s with satellites, $^1J_{PtP}$= 4691 Hz, **D2**)

GC/MS: T_{Start} = 60°C, T_{End} = 280°C, Rate = 10°C/min
Time (min): 2.38 (m/z = 164, 162, 134, 136, 122, 120, CH_2=$CH(CH_2)_4Br$)

3.3.5 1,3-Diiodopropane

(A) An amount of 3.1 mg (0.021 mmol) of 1,3-diiodopropane was added at room temperature to 20 mg (0.042 mmol) of **A1** in 0.6 ml of C_6D_6. NMR spectra were taken at regular intervals. After 3 days at 70°C the reaction was stopped.

(B) An amount of 6.2 mg (0.042 mmol) of 1,3-diiodopropane was added at room temperature to 10 mg (0.021 mmol) of **A1** in 0.6 ml of C_6D_6. NMR spectra were taken at regular intervals. After

2 days at 70°C the starting complex was consumed.

(C) An amount of 12.4 mg (0.084 mmol) of 1,3-diiodopropane was added at room temperature to 10 mg (0.021 mmol) of **A1** in 0.6 ml of C_6D_6. NMR spectra were taken at regular intervals. After 2 days at 70°C the starting complex was consumed.

(D) An amount of 28.8 mg (0.084 mmol) of 1,3-diiodopropane was added at room temperature to 10 mg (0.021 mmol) of **A1** in 0.6 ml of C_6D_6. NMR spectra were taken at regular intervals. After 2 days at 70°C the starting complex was consumed.

^{1}H NMR: δ (ppm): 0.16 (s, CH_4), 0.78 (d, with satellites, $^3J_{PH}$= 5.73 Hz, $^2J_{PtH}$= 68.8 Hz, CH_3-Pt_{B4}), 1.52 (d, with satellites, $^3J_{PH}$= 3.5 Hz, $^2J_{PtH}$= 76.3 Hz, CH_3-Pt_{D3}), 1.78 (d, with satellites, $^3J_{PH}$= 6.76 Hz, $^2J_{PtH}$= 73.1 Hz, CH_2-Pt_{B4}), 2.17 (d, with satellites, $^3J_{PH}$= 6.9 Hz, $^2J_{PtH}$= 71.2 Hz, CH_3-Pt_{B4}) 2.61 (s, with satellites, $^3J_{PtP}$=13.18 Hz, CH_3-N_{D3}), 2.77 (s, with satellites, $^3J_{PtP}$=10.8 Hz, CH_3-N_{B4}) 7.04 (m, $C_{arom\ D3}$), 7.53 (m, $C_{arom\ D3}$)
^{31}P NMR: δ (ppm): 2.07 (s with satellites, $^1J_{PtP}$= 1189 Hz, **B4**), 28.9 (s with satellites, $^1J_{PtP}$= 4554 Hz, **D3**)

3.3.6 1,6-Diiodohexane

(A) An amount of 7.1 mg (0.021 mmol) of 1,3-diiodopropane was added at room temperature to 10 mg (0.021 mmol) of **A1** in 0.6 ml of C_6D_6. NMR spectra were taken at regular intervals. After 2 days at 70°C the starting complex was consumed.

(B) An amount of 14.2 mg (0.042 mmol) of 1,3-diiodopropane was added at room temperature to 10 mg (0.021 mmol) of **A1** in 0.6 ml of C_6D_6. NMR spectra were taken at regular intervals. After 2 days at 70°C the starting complex was consumed.

(C) An amount of 28.4 mg (0.084 mmol) of 1,3-diiodopropane was added at room temperature to 10 mg (0.021 mmol) of **A1** in 0.6 ml of C_6D_6. NMR spectra were taken at regular intervals. After 2 days at 70°C the starting complex was consumed.

^{1}H NMR: δ (ppm): 0.16 (s, CH_4), 0.78 (d, with satellites, $^3J_{PH}$= 5.73 Hz, $^2J_{PtH}$= 71 Hz, CH_3-Pt_{B5}), 1.5 (d, with satellites, $^3J_{PH}$= 4.29 Hz, $^2J_{PtH}$= 75.4 Hz, CH_3-Pt_{D3}), 1.78 (d, with satellites, $^3J_{PH}$= 7.66 Hz, $^2J_{PtH}$= 74 Hz, CH_2-Pt_{B5}), 2.16 (d, with satellites, $^3J_{PH}$= 6.9 Hz, $^2J_{PtH}$= 72.8 Hz, CH_3-Pt_{B5}) 2.61 (s, with satellites, $^3J_{PtP}$=13.18 Hz, CH_3-N_{D3}), 2.77 (s, with satellites, $^3J_{PtP}$=10.8 Hz, CH_3-N_{B5}) 7.04 (m, $C_{arom\ D3}$), 7.53 (m, $C_{arom\ D3}$). The $N(CH_3)_2$ signal was completely covered by a signal of the educt.

^{31}P NMR: δ (ppm): 2.01 (s with satellites, $^1J_{PtP}$= 1187 Hz, **B5**) 28.87 (s with satellites, $^1J_{PtP}$= 4552 Hz, **D3**)

3.4 Reactions of Complex A1 with Halogenated Hydrocarbons without CH_2- Groups in the β-Position

3.4.1 Chlorocyclohexane

(A) An amount of 9.96 mg (0.084 mmol) of chlorocyclohexane was added at room temperature to 20 mg (0.042 mmol) of **A1** in 0.6 ml of C_6D_6. NMR spectra were taken at regular intervals. After one week the reaction was stopped.

^{31}P NMR: δ (ppm): 27.16 (s, **D1**)

3.4.2 Chlorobenzene

(A) An amount of 9.46 mg (0.084 mmol) of chlorobenzene was added at room temperature to 20 mg (0.042 mmol) of **A1** in 0.6 ml of C_6D_6. NMR spectra were taken at regular intervals. After one week the reaction was stopped.

^{31}P NMR: δ (ppm): 27.18 (s, **D1**)

3.4.3 2,2-Dichloropropane

(A) An amount of 4.7 mg (0.042 mmol) of 2,2-dichloropropane was added at room temperature to 10 mg (0.021 mmol) of **A1** in 0.6 ml of C_6D_6. NMR spectra were taken at regular intervals. After one week the reaction was stopped.

^{31}P NMR: δ (ppm): 27.1 (s, **D1**)

3.4.4 Chloroacetic Acid

(A) An amount of 8 mg (0.084 mmol) of chloroacetic acid was added at room temperature to 20 mg (0.042 mmol) of **A1** in 0.6 ml of C_6D_6. Directly after start of the reaction complex **A1** was completely consumed.

^{1}H NMR: δ (ppm): 0.16 (s, CH_4), 0.97 (s, $CH_{3\,C1}$)
^{31}P NMR: δ (ppm): 20.82 (s, $^{1}J_{PtP}$= 4938 Hz, **C1**)

3.4.5 Propargyl Chloride

(A) An amount of 6.3 mg (0.084 mmol) of propargyl chloride was added at room temperature to 20 mg (0.042 mmol) of **A1** in 0.6 ml of C_6D_6. NMR spectra were taken at regular intervals. After one hour complex **A1** was completely consumed.

^{1}H NMR: δ (ppm): 0.16 (s, CH_4), 0.99 (d, with satellites, $^{3}J_{PH}$= 3.6 Hz, $^{2}J_{PtH}$= 66 Hz, CH_3-Pt_{B8}), 1.3 (d, with satellites, $^{3}J_{PH}$= 3.28 Hz, $^{2}J_{PtH}$= 74.4 Hz, CH_3-Pt_{D1}), 2.33 (d, with satellites, $^{3}J_{PH}$= 2.16 Hz, $^{2}J_{PtH}$= 65.5 Hz, CH_3-Pt_{B8}), 2.51 (s, with satellites, $^{3}J_{PtP}$=11.6 Hz, CH_3-N_{D1}), 2.71 (CH_2-Pt_{B8}), 2.74 (s, with satellites, $^{3}J_{PtP}$=9.7 Hz, CH_3-N_{B8}) 7.04 (m, $C_{arom\ D1}$), 7.53 (m, $C_{arom\ D1}$).
^{31}P NMR: δ (ppm): 12.49 (s with satellites, $^{1}J_{PtP}$= 1444 Hz, **B9**) 28.87 (s with satellites, $^{1}J_{PtP}$= 4675 Hz, **D1**)

3.4.6 2,2-Dibromopropane

(A) An amount of 4.24 mg (0.021 mmol) of 2,2-dibromopropane was added at room temperature to 10 mg (0.021 mmol) of **A1** in 0.6 ml of C_6D_6. NMR spectra were taken at regular intervals. After 3 days at 70°C the starting complex was consumed.

(B) An amount of 8.47 mg (0.042 mmol) of 2,2-dibromopropane was added at room temperature to 10 mg (0.021 mmol) of **A1** in 0.6 ml of C_6D_6. NMR spectra were taken at regular intervals. After 3 days at 70°C the starting complex was consumed.

(C) An amount of 16.94 mg (0.084 mmol) of 2,2-dibromopropane was added at room temperature to 10 mg (0.021 mmol) of **A1** in 0.6 ml of C_6D_6. NMR spectra were taken at regular intervals. After 3 days at 70°C the starting complex was consumed.

^{1}H NMR: δ (ppm): 0.16 (s, CH_4), 0.8 (s, CH_3CH_3), 1,37 (d, with satellites, $^3J_{PH}$= 3.4 Hz, $^2J_{PtH}$= 74 Hz, CH_3-Pt_{D2}), 1.56 (s, R-R), 1.62 (s, R-Me), 2.55 (s, with satellites, $^3J_{PtP}$= 11.8 Hz, CH_3-N_{D2}), 7.05 (m, $C_{arom\ D2}$), 7.52 (m, $C_{arom\ D2}$)
^{31}P NMR: δ (ppm): 28.14 (s with satellites, $^1J_{PtP}$= 4685 Hz, **D2**)

3.4.7 Bromobenzene

(A) An amount of 6.6 mg (0.042 mmol) of bromobenzene was added at room temperature to 20 mg (0.042 mmol) of **A1** in 0.6 ml of C_6D_6. NMR spectra were taken at regular intervals. After 10 days at 70°C the experiment was stopped.

(B) An amount of 13.2 mg (0.084 mmol) of bromobenzene was added at room temperature to 20 mg (0.042 mmol) of **A1** in 0.6 ml of C_6D_6. NMR spectra were taken at regular intervals. After one week at 70°C the experiment was stopped.

(C) An amount of 16.94 mg (0.084 mmol) of bromobenzene was added at room temperature to 10 mg (0.021 mmol) of **A1** in 0.6 ml of C_6D_6. NMR spectra were taken at regular intervals. After 10 days at 70°C the experiment was stopped.

^{1}H NMR: δ (ppm): 1.38 (d, with satellites, $^3J_{PH}$= 3.5 Hz, $^2J_{PtH}$= 74.2 Hz, CH_3-Pt_{D2}), 2.54 (s, with satellites, $^3J_{PtP}$=12.15 Hz, CH_3-N_{D2}), 7.04 (m, $C_{arom\ D2}$), 7.53 (m, $C_{arom\ D2}$)
^{31}P NMR: δ (ppm): 28.17 (s with satellites, $1J_{PtP}$= 4691 Hz, **D2**)

GC/MS: T_{Start} = 60°C, T_{End} = 280°C, rate = 10°C/min
Time (min): 12.90 (m/z = 156, 155, 154, C_6H_5-C_6H_5)

3.4.8 1,4-Dibromobenzene

(A) An amount of 150 mg (0.63 mmol) of 1,4-dibromobenzene was added at room temperature to 20 mg (0.042 mmol) of **A1** in 0.6 ml of C_6D_6. NMR spectra were taken at regular intervals. After 14 days at 70°C the experiment was stopped.

^{1}H NMR: δ (ppm): 1.39 (d, with satellites, $^3J_{PH}$= 3.5 Hz, $^2J_{PtH}$= 74.2 Hz, CH_3-Pt_{D2}), 2.04 (s, CH_3-PhBr), 2.54 (s, with satellites, $^3J_{PtP}$=12.15 Hz, CH_3-N_{D2}), 7.04 (m, $C_{arom\ D2}$), 7.53 (m, $C_{arom\ D2}$)
^{31}P NMR: δ (ppm): 28.17 (s with satellites, $1J_{PtP}$= 4690 Hz, **D2**)

GC/MS: T_{Start} = 60°C, T_{End} = 280°C, rate = 10°C/min
Time (min): 10.70 (m/z = 173, 172, 171, p-bromotoluene)

3.5 Fast Reactions with of Complex A1 with Halogenated Hydrocarbons without CH_2-Groups in the β-Position

3.5.1 Benzyl Chloride

(A) An amount of 2.7 mg (0.021 mmol) of benzyl chloride was added at room temperature to 10 mg (0.021 mmol) of **A1** in 0.6 ml of C_6D_6. NMR spectra were taken at regular intervals. Only about 10% of the starting complex were consumed after 10 days at 70°C.

(B) An amount of 5.4 mg (0.042 mmol) of benzyl chloride was added at room temperature to 10

mg (0.021 mmol) of **A1** in 0.6 ml of C_6D_6. NMR spectra were taken at regular intervals. After 6 days at 70°C the starting complex was consumed.

(C) An amount of 10.8 mg (0.084 mmol) of benzyl chloride was added at room temperature to 10 mg (0.021 mmol) of **A1** in 0.6 ml of C_6D_6. NMR spectra were taken at regular intervals. After 6 days at 70°C the starting complex was consumed.

(D) An amount of 40.5 mg (0.315 mmol) of benzyl chloride was added at room temperature to 10 mg (0.021 mmol) of **A1** in 0.6 ml of C_6D_6. NMR spectra were taken at regular intervals. After one day at 70°C the starting complex was consumed.

^{1}H NMR: δ (ppm): 0.16 (s, CH_4), 0.8 (s, CH_3CH_3), 1.31 (d, with satellites, $^3J_{PH}$= 3.3 Hz, $^2J_{PtH}$= 74 Hz, CH_3-Pt_{D1}), 2.11 (s, Ph-CH_3), 2.51 (s, with satellites, $^3J_{PtP}$=11.9 Hz, CH_3-N_{D1}), 2.74 (s, $PhCH_2CH_2Ph$), 5.74 (ddd, $^1J_{HH}$=2.9Hz, $^2J_{HH}$=11.9Hz, $^2J_{PH}$=Hz P-C<u>H</u>=CH_{2F1}), 6.27 (ddd, $^1J_{HH}$=2.9Hz, $^2J_{HH}$=18.5Hz, $^2J_{PH}$=22Hz P-CH=C<u>H</u>$_{2F1}$), 6.34 (ddd, $^2J_{HH}$=11.9Hz, $^2J_{HH}$=18.5Hz, $^2J_{PH}$=23.8Hz P-CH=C<u>H</u>$_{2F1}$), 7.04 (m, $C_{arom\ D1}$), 7.53 (m, $C_{arom\ D1}$),
^{31}P NMR: δ (ppm): 20.14 (s, **F1**), 27.12 (s with satellites, $^1J_{PtP}$= 4675 Hz, **D1**)

GC/MS: T_{Start} = 80°C, T_{End} = 280°C, rate = 10°C/min
Time (min): 2.13 (m/z = 106, 105, 93, 92, 91, $C_6H_5CH_2CH_3$), 12.33 (m/z = 183, 182, 92, 91, $C_6H_5CH_2CH_2C_6H_5$)

3.5.2 Benzyl Bromide

(A) An amount of 3.6 mg (0.021 mmol) of benzyl bromide was added at room temperature to 10 mg (0.021 mmol) of **A1** in 0.6 ml of C_6D_6. NMR spectra were taken at regular intervals. After 2 days at 70°C the starting complex was consumed.

(B) An amount of 7.2 mg (0.042 mmol) of benzyl bromide was added at room temperature to 10 mg (0.021 mmol) of **A1** in 0.6 ml of C_6D_6. NMR spectra were taken at regular intervals. After 2 days at 70°C the starting complex was consumed.

(C) An amount of 14.4 mg (0.084 mmol) of benzyl bromide was added at room temperature to 10 mg (0.021 mmol) of **A1** in 0.6 ml of C_6D_6. NMR spectra were taken at regular intervals. After 2 days at 70°C the starting complex was consumed.

(D) An amount of 86.4 mg (0.504 mmol) of benzyl bromide was added at room temperature to 10 mg (0.021 mmol) of **A1** in 0.6 ml of C_6D_6. NMR spectra were taken at regular intervals. After 2 hours at 70°C the starting complex was consumed.

^{1}H NMR: δ (ppm): 0.59 (d, with satellites, $^3J_{PH}$= 7.2 Hz, $^2J_{PtH}$= 70.9 Hz, CH_3-Pt_{B6a}), 0.88 (d, with satellites, $^3J_{PH}$= 7.8 Hz, $^2J_{PtH}$= 72.4 Hz, CH_3-Pt_{B6b}), 1.49 (d, with satellites, $^3J_{PH}$= 3.7 Hz, $^2J_{PtH}$= 60 Hz, CH_3-Pt_{B6b}), 1.42 (d, with satellites, $^3J_{PH}$= 5.93 Hz, CH_3-Pt_{B6b}), 1.65 (s, with satellites, $^3J_{PtP}$=12.9 Hz, CH_3-N_{B6a}), 2.57 (s, with satellites, $^3J_{PtP}$=8.94 Hz, CH_3-N_{B6b}), 3.90 (m, $^2J_{PtH}$= 443 Hz, CH_2-Pt_{B6a}), 4.51 (m, $^2J_{PtH}$= 71 Hz, $PhCH_2$-Pt_{B6b}), 5.74 (ddd, $^1J_{HH}$=2.9Hz, $^2J_{HH}$=11.9Hz, $^2J_{PH}$=Hz P-C<u>H</u>=CH_{2F1}), 6.27 (ddd, $^1J_{HH}$=2.9Hz, $^2J_{HH}$=18.5Hz, $^2J_{PH}$=22Hz P-CH=C<u>H</u>$_{2F1}$), 6.34 (ddd, $^2J_{HH}$=11.9Hz, $^2J_{HH}$=18.5Hz, $^2J_{PH}$=23.8Hz P-CH=C<u>H</u>$_{2F1}$), 7.27 (m, $C_{arom B6}$), 7.78 (m, $C_{arom B6}$)

^{31}P NMR: δ (ppm): 8.37 (s with satellites, $^1J_{PtP}$= 1237 Hz, **B6**), 20.74 (s, **F1**), 28.17 (s, **D2**)

^{13}C NMR: δ (ppm): -3.66 (Pt-CH_{3B6}), 5.96 (Pt-CH_{3B7}), 6.76 (Pt-CH_{3B6}), 13,97 ($PhCH_2$-Pt_{B7}), 17.98 ($ClCH_2$-Pt_{B7}), 34.2 ($PhCH_2$-Pt_{B6})

^{195}Pt NMR: δ (ppm): -3096 (**B6a**), -2844 (**B6b**)

GC/MS: T_{Start} = 60°C, T_{End} = 280°C, rate = 10°C/min

Time (min): 3.47 (m/z = 107, 106, 93, 92, 91, $C_6H_5CH_2CH_3$)

3.5.2 Ethyl Chloroacetate

(A) An amount of 5.1 mg (0.042 mmol) of ethylchloroacetate was added at room temperature to 10 mg (0.021 mmol) of **A1** in 0.6 ml of C_6D_6. NMR spectra were taken at regular intervals. After 3 days at 70°C the starting complex was consumed.

^{1}H NMR: δ (ppm): 0.16 (s, CH_4), 0.41 (d, with satellites, $^3J_{PH}$= 7 Hz, $^2J_{PtH}$= 50 Hz, CH_3-Pt_{B2}),

0.50 (d, with satellites, $^{3}J_{PH}$= 7.8 Hz, $^{2}J_{PtH}$= 71 Hz, CH_3-Pt_{B1}), 0.53 (d, with satellites, $^{3}J_{PH}$= 6.7 Hz, $^{2}J_{PtH}$= 69 Hz, CH_3-Pt_{B8}), 0.8(s, CH_3CH_3), 1.31 (d, with satellites, $^{3}J_{PH}$= 3.3 Hz, $^{2}J_{PtH}$= 74 Hz, CH_3-Pt_{D1}), 1.47 (d, with satellites, $^{3}J_{PH}$= 8 Hz, $^{2}J_{PtH}$= 62 Hz, CH_3-Pt_{B1}), 1.68 (d, with satellites, $^{3}J_{PH}$= 6.8 Hz, $^{2}J_{PtH}$= 73 Hz, CH_3-Pt_{B2}), 1.89 (d, with satellites, $^{3}J_{PH}$= 7.0 Hz, $^{2}J_{PtH}$= 72 Hz, CH_3-Pt_{B1}), 2.04 (d, with satellites, $^{3}J_{PH}$= 5.5 Hz, $^{2}J_{PtH}$= 71 Hz, CH_3-Pt_{B8}), 2.51 (s, with satellites, $^{3}J_{PtP}$=11.9 Hz, CH_3-N_{D1}), 2.74 (s, $PhCH_2CH_2Ph$), 2.98 (m, CH_2-Pt_{B8}), 5.74 (ddd, $^{1}J_{HH}$=2.9Hz, $^{2}J_{HH}$=11.9Hz, $^{2}J_{PH}$=Hz P-C<u>H</u>=CH_{2F1}), 6.27 (ddd, $^{1}J_{HH}$=2.9Hz, $^{2}J_{HH}$=18.5Hz, $^{2}J_{PH}$=22Hz P-CH=C<u>H</u>$_{2F1}$), 6.34 (ddd, $^{2}J_{HH}$=11.9Hz, $^{2}J_{HH}$=18.5Hz, $^{2}J_{PH}$=23.8Hz P-CH=C<u>H</u>$_{2F1}$), 7.04 (m, $C_{arom\ D1}$), 7.53 (m, $C_{arom\ D1}$)

^{31}P NMR: δ (ppm): 1.69 (s with satellites, $^{1}J_{PtP}$= 1208 Hz, **B2**), 8.78 (s with satellites, $^{1}J_{PtP}$= 1183 Hz, **B1**), 11.28 (s with satellites, $^{1}J_{PtP}$= 1587 Hz, **B8**),

^{13}C NMR: δ (ppm): -9.96 (CH_3-Pt_{B2}), -8.61 (CH_3-Pt_{B1}), -7.83 (CH_3-Pt_{B8}), 17.29 (CH_3-Pt_{B1}), 27.61 (CH_3-Pt_{C1}), 29.87 (CH_2-Pt_{B8})

^{195}Pt NMR: δ (ppm): -4173 (**C2**), -2977 (**B1**), -3030 (**B8**)

3.6 Reactions of Complex A1 with Silyl Chlorides

3.6.1 Chlorotrimethylsilane

(A) An amount of 4.5 mg (0.042 mmol) of chlorotrimethylsilane was added at room temperature to 10 mg (0.021 mmol) of **A1** in 0.6 ml of C_6D_6. NMR spectra were taken at regular intervals. The reaction was finished after 4 days at 60°C.

^{1}H NMR: δ (ppm) 0 (s, TMS), 0.12 (s, CH_3-Si-Si), 1.31 (d, with satellites, $^{3}J_{PH}$= 3.3 Hz, $^{2}J_{PtH}$= 75 Hz, CH_3-Pt_{D1}), 2.52 (s, with satellites, $^{3}J_{PtP}$=11.2 Hz, CH_3-N_{D1}), 7.05 (m, $C_{arom\ D1}$), 7.52 (m, $C_{arom\ D1}$)

^{31}P NMR: δ (ppm): 27.13 (s with satellites, $^{1}J_{PtP}$= 4676 Hz, **D1**

3.6.2 Chlorodimethylvinylsilane

(A) An amount of 2.5 mg (0.021 mmol) of chlorodimethylvinylsilane was added at room temperature to 10 mg (0.021 mmol) of **A1** in 0.6 ml of C_6D_6. NMR spectra were taken at regular intervals. The reaction was finished after 24 hours at 60°C.

(B) An amount of 5.1 mg (0.042 mmol) of chlorodimethylvinylsilane was added at room temperature to 10 mg (0.021 mmol) of **A1** in 0.6 ml of C_6D_6. NMR spectra were taken at regular intervals. The reaction was finished after 3 hours at 60°C.

(C) An amount of 10.2 mg (0.084 mmol) of chlorodimethylvinylsilane was added at room temperature to 10 mg (0.021 mmol) of **A1** in 0.6 ml of C_6D_6. NMR spectra were taken at regular intervals. The reaction was finished after 3 hours at 60°C.

^{1}H NMR: δ (ppm): 0.24 (s, CH_3-Si-Si), 1.31 (d, with satellites, $^3J_{PH}$= 3.3 Hz, $^2J_{PtH}$= 75 Hz, CH_3-Pt_{D1}), 2.52 (s, with satellites, $^3J_{PtP}$=11.2 Hz, CH_3-N_{D1}), 7.05 (m, $C_{arom\ D1}$), 7.52 (m, $C_{arom\ D1}$)
^{31}P NMR: δ (ppm): 27.12 (s with satellites, $^1J_{PtP}$= 4676 Hz, **D1**)

GC/MS: T_{Start} = 60°C, T_{End} = 250°C, rate = 20°C/min
Time (min): 1.18 (m/z = 171, 170, 144, 143, 118, 117, 103, $((CH_2{=}CH)(CH_3)_2Si)_2$)

3.6.3 Chlorotriethylsilane

(A) An amount of 3.2 mg (0.021 mmol) of chlorotriethylsilane was added at room temperature to 10 mg (0.021 mmol) of **A1** in 0.6 ml of C_6D_6. NMR spectra were taken at regular intervals. The reaction was finished after 3 days at 60°C.

(B) An amount of 6.4 mg (0.042 mmol) of chlorotriethylsilane was added at room temperature to 10 mg (0.021 mmol) of **A1** in 0.6 ml of C_6D_6. NMR spectra were taken at regular intervals. The reaction was finished after 2 days at 60°C.

(C) An amount of 12.8 mg (0.084 mmol) of chlorotriethylsilane was added at room temperature to 10 mg (0.021 mmol) of **A1** in 0.6 ml of C_6D_6. NMR spectra were taken at regular intervals. The reaction was finished after 2 days at 60°C.

^{1}H NMR: δ (ppm): 0.52 (q, $^1J_{HH}$= 23 Hz, CH_3-C$\underline{H}_2$-Si), 0.97 (t, $^1J_{HH}$= 15.4 Hz, C$\underline{H}_3$-CH_2-Si), 1.31

(d, with satellites, $^3J_{PH}$= 3.3 Hz, $^2J_{PtH}$= 75 Hz, CH_3-Pt_{D1}), 2.51 (s, with satellites, $^3J_{PtP}$=11.5 Hz, CH_3-N_{D1}), 7.04 (m, $C_{arom\ D1}$), 7.53 (m, $C_{arom\ D1}$),
31P NMR: δ (ppm): 27.12 (s with satellites, 1JPtP= 4676 Hz, **D1**)

3.6.4 Dichlorodimethylsilane

(A) An amount of 2.7 mg (0.021 mmol) of dichlorodimethylsilane was added at room temperature to 10 mg (0.021 mmol) of **A1** in 0.6 ml of C_6D_6. NMR spectra were taken at regular intervals. The reaction was finished after three days at 60°C.

(B) An amount of 5.4 mg (0.042 mmol) of dichlorodimethylsilane was added at room temperature to 10 mg (0.021 mmol) of **A1** in 0.6 ml of C_6D_6. NMR spectra were taken at regular intervals. The reaction was finished after two hours at 60°C. During this reaction complex **E1** precipitated.

(C) An amount of 10.8 mg (0.084 mmol) of dichlorodimethylsilane was added at room temperature to 10 mg (0.021 mmol) of **A1** in 0.6 ml of C_6D_6. NMR spectra were taken at regular intervals. The reaction was finished after two hours at 60°C. During this reaction complex **E1** precipitated.

^{1}H NMR (reaction solution): δ (ppm) 0.21 (s, $(CH_3)_3Cl$), 0.29 (s, CH_3-Si-Si), 1.31 (d, with satellites, $^3J_{PH}$= 3.3 Hz, $^2J_{PtH}$= 75 Hz, CH_3-Pt_{D1}), 2.52 (s, with satellites, $^3J_{PtP}$=11.2 Hz, CH_3-N_{D1}), 7.05 (m, $C_{arom\ D1}$), 7.52 (m, $C_{arom\ D1}$)
^{31}P NMR (reaction solution): δ (ppm) 27.11 (s with satellites, ^{1}JPtP= 4670 Hz, **D1**)

^{1}H NMR in $(CD_3)_2CO$: δ 0.48 (d, with satellites, $^3J_{PH}$= 3.2 Hz, $^2J_{PtH}$= 74.4 Hz, CH_3-Pt_{D1}), 2.81 (s with satellites, $^3J_{PtP}$ = 12.1 Hz, CH_3-N_{D1}) 3.13 (s with satellites, $^3J_{PtP}$ = 33.2 Hz, CH_3-N_{E1}), 7.52 (m, $H_{arom\ E1}$), (ppm) 8.01 (m, $H_{arom\ E1}$)
^{31}P NMR in $(CD_3)_2CO$: δ (ppm) 21.8 (s with satellites, ^{1}JPtP= 3963 Hz, **E1**)

GC/MS: T_{Start} = 60°C, T_{End} = 250°C, rate = 20°C/min

Time (min): 1.27 (m/z = 180, 179, 150, 149, 120, 119, $((CH_3)_2(OCH_3)Si)_2$)

3.6.5 Cyclohexylmethydichlorosilane

(A) An amount of 4.1 mg (0.021 mmol) of cyclohexylmethydichlorosilane was added at room temperature to 10 mg (0.021 mmol) of **A1** in 0.6 ml of C_6D_6. NMR spectra were taken at regular intervals. The reaction was finished after one week at room temperature

(B) An amount of 8.3 mg (0.042 mmol) of cyclohexylmethydichlorosilane was added at room temperature to 10 mg (0.021 mmol) of **A1** in 0.6 ml of C_6D_6. NMR spectra were taken at regular intervals. The reaction was finished after one week at room temperature

(C) An amount of 16.6 mg (0.084 mmol) of cyclohexylmethydichlorosilane was added at room temperature to 10 mg (0.021 mmol) of **A1** in 0.6 ml of C_6D_6. NMR spectra were taken at regular intervals. The reaction was finished after one week at room temperature

^{1}H NMR in $(CD_3)_2CO$: δ 0.48 (d, with satellites, $^3J_{PH}$= 3.2 Hz, $^2J_{PtH}$= 74.4 Hz, CH_3-Pt_{D1}), 2.81 (s with satellites, $^3J_{PtP}$ = 12.1 Hz, CH_3-N_{D1}) 3.13 (s with satellites, $^3J_{PtP}$ = 33.2 Hz, CH_3-N_{E1}), 7.52 (m, $H_{arom\ E1}$), (ppm) 8.01 (m, $H_{arom\ E1}$)
^{31}P NMR in $(CD_3)_2CO$: δ (ppm) 21.8 (s with satellites, ^{1}JPtP= 3963 Hz, **E1**)

3.6.6 Dichlorodiphenylsilane

(A) An amount of 5.5 mg (0.021 mmol) of dichlorodiphenylsilane was added at room temperature to 10 mg (0.021 mmol) of **A1** in 0.6 ml of C_6D_6. NMR spectra were taken at regular intervals. The reaction was finished after five hours at 70°C.

(B) An amount of 11 mg (0.042 mmol) of dichlorodiphenylsilane was added at room temperature to 10 mg (0.021 mmol) of **A1** in 0.6 ml of C_6D_6. NMR spectra were taken at regular intervals. The reaction was finished after five hours at 70°C.

(C) An amount of 22 mg (0.084 mmol) of dichlorodiphenylsilane was added at room temperature to 10 mg (0.021 mmol) of **A1** in 0.6 ml of C_6D_6. NMR spectra were taken at regular intervals. The reaction was finished after five hours at 70°C.

(D) An amount of 11 mg (0.084 mmol) of dichlorodiphenylsilane was added at room temperature to 10.5 mg (0.021 mmol) of **D1** in 0.6 ml of C_6D_6. NMR spectra were taken at regular intervals. The reaction was finished after one day at room temperature.

^{1}H NMR: δ (ppm): 0.69 (s, CH_3-Si-Si), 1.31 (d, with satellites, $^3J_{PH}$= 3.3 Hz, $^2J_{PtH}$= 75 Hz, CH_3-Pt_{D1}), 2.52 (s, with satellites, $^3J_{PtP}$=11.2 Hz, CH_3-N_{D1}), 7.05 (m, $C_{arom\ D1}$), 7.52 (m, $C_{arom\ D1}$)
^{31}P NMR: δ (ppm): 27.13 (s with satellites, $^1J_{PtP}$= 4676 Hz, **D1**

GC/MS: T_{Start} = 60°C, T_{End} = 250°C, rate = 20°C/min
Time (min): 7.38 (m/z = 229, 228, 213, 197, $(C_6H_5)_2(CH_3)(OCH_3)Si$)

3.6.7 Trichlorophenylsilane

(A) An amount of 2.2 mg (0.011 mmol) of trichlorophenylsilane was added at room temperature to 10 mg (0.021 mmol) of **1** in 0.6 ml of C_6D_6. NMR spectra were taken at regular intervals. Only 20% oft the starting complex were converted after 4 days at 60°C.

(B) An amount of 4.5 mg (0.021 mmol) of trichlorophenylsilane was added at room temperature to 10 mg (0.021 mmol) of **1** in 0.6 ml of C_6D_6. NMR spectra were taken at regular intervals. The reaction was finished after 30 minutes at 60°C.

(C) An amount of 8.9 mg (0.042 mmol) of trichlorophenylsilane was added at room temperature to 10 mg (0.021 mmol) of **1** in 0.6 ml of C_6D_6. NMR spectra were taken at regular intervals. The reaction was finished after 30 minutes at 60°C.

(D) An amount of 17.8 mg (0.084 mmol) of trichlorophenylsilane was added at room temperature to 10 mg (0.021 mmol) of **1** in 0.6 ml of C_6D_6. NMR spectra were taken at regular intervals. The reaction was finished after 30 minutes at 60°C.

^{1}H NMR: δ (ppm): 0.16 (s, Si-CH_3) , 0.59 (s, Si-CH_3), 1.31 (d, with satellites, $^3J_{PH}$= 3.3 Hz, $^2J_{PtH}$= 75 Hz, CH_3-Pt_{D1}), 2.52 (s, with satellites, $^3J_{PtP}$=11.2 Hz, CH_3-N_{D1}), 6.96 (m, C_{arom}), 7.05 (m, $C_{arom\ D1}$), 7.52 (m, $C_{arom\ D1}$)

^{31}P NMR: δ (ppm): 27.13 (s with satellites, ^{1}JPtP= 4676 Hz, **D1**)

GC/MS: T_{Start} = 80°C, T_{End} = 280°C, Rate = 10°C/min

Time (min): 2.99 (m/z = 167, 166, 152, 151, 135, 121, $(C_6H_5)(CH_3)_2(OCH_3)Si$), 3.99 (m/z = 183, 182, 168, 167, 151, 137, $(C_6H_5)(CH_3)(OCH_3)_2Si$), 12.53 (m/z = 304, 303, 274, 273, 244, 243, $(C_6H_5)(CH_3)(OCH_3)Si$-$Si(OCH_3)(CH_3)(C_6H_5)$), 13.86 (m/z = 319, 289, 259, $(C_6H_5)(CH_3)(OCH_3)Si$-$Si(OCH_3)_2(C_6H_5)$)

3.7 Crystal Structures

3.7.1 Crystal Data for Complex **B6a**

Empirical formula	C_{25} H_{33} Br N P Pt
Formula weight	653.49
Temperature	100(2) K
Wavelength	0.71073 Å
Crystal system, space group	Monoclinic, $P2_1/n$
Unit cell dimensions	a = 11.6635(14) Å
	b = 17.334(2) Å
	c = 12.5585(15) Å
Volume	2404.0(5) $Å^3$
Z, Calculated density	4, 1.806 Mg/m^3
Absorption coefficient	7.577 mm^{-1}
F(000)	1272

Crystal size	0.37 x 0.28 x 0.27 mm
Theta range for data collection	2.38 to 30.00 deg.
Limiting indices	-16<=h<=16, -24<=k<=22, -12<=l<=17
Reflections collected / unique	19601 / 6965 [R(int) = 0.0262]
Completeness to theta =	30.00 99.4 %
Absorption correction	Empirical
Max. and min. transmission	0.234 and 0.113
Refinement method	Full-matrix least-squares on F^2
Data / restraints / parameters	6965 / 0 / 267
Goodness-of-fit on F^2	1.076
Final R indices [I>2sigma(I)]	R1 = 0.0237, wR2 = 0.0592
R indices (all data)	R1 = 0.0262, wR2 = 0.0601
Largest diff. peak and hole	1.785 and -2.944 e.$Å^{-3}$

Atomic coordinates (x 10^4) and equivalent isotropic displacement parameters. U(eq) is defined as one third of the trace of the orthogonalized U_{ij} tensor.

	x	y	z	U(eq)
Pt(1)	7269(1)	1847(1)	7235(1)	7(1)
Br(1)	9611(1)	1736(1)	8234(1)	13(1)
P(1)	6899(1)	1929(1)	8962(1)	8(1)
N(1)	7481(2)	3155(1)	7447(2)	10(1)
C(1)	6322(2)	3570(2)	6952(3)	18(1)
C(2)	8360(3)	3486(2)	6937(2)	17(1)
C(3)	7967(2)	3309(2)	8685(2)	13(1)
C(4)	7214(2)	2947(1)	9351(2)	13(1)
C(5)	7742(2)	1351(1)	10176(2)	10(1)
C(6)	7609(2)	1493(2)	11225(2)	13(1)
C(7)	8153(2)	1008(2)	12128(2)	15(1)
C(8)	8830(2)	381(2)	11986(2)	16(1)
C(9)	8972(2)	236(2)	10952(2)	15(1)
C(10)	8431(2)	722(1)	10046(2)	12(1)

C(11)	5354(2)	1738(1)	8935(2)	9(1)
C(12)	5029(2)	975(1)	9063(2)	12(1)
C(13)	3841(2)	789(2)	8958(2)	15(1)
C(14)	2956(2)	1354(2)	8721(2)	15(1)
C(15)	3264(2)	2114(2)	8587(2)	14(1)
C(16)	4455(2)	2305(1)	8686(2)	13(1)
C(17)	5444(2)	1880(1)	6311(2)	13(1)
C(18)	7074(2)	662(1)	7142(2)	13(1)
C(19)	7592(3)	1901(2)	5670(2)	15(1)
C(20)	7490(2)	1158(2)	5042(2)	14(1)
C(21)	8464(2)	637(2)	5295(2)	16(1)
C(22)	8352(3)	-74(2)	4764(2)	18(1)
C(23)	7274(3)	-285(2)	3962(2)	20(1)
C(24)	6301(3)	224(2)	3689(3)	22(1)
C(25)	6418(3)	943(2)	4219(2)	18(1)

3.7.2 Crystal Data for Complex **B6b**

Empirical formula	C_{25} H_{33} Br N P Pt
Formula weight	653.49
Temperature	100(2) K
Wavelength	0.71073 Å
Crystal system, space group	Monoclinic, $P2_1/n$
Unit cell dimensions	a = 11.6635(14) Å
	b = 17.334(2) Å
	c = 12.5585(15) Å
Volume	2404.0(5) $Å^3$
Z, Calculated density	4, 1.806 Mg/m^3

Absorption coefficient	7.577 mm^{-1}
F(000)	1272
Crystal size	0.37 x 0.28 x 0.27 mm
Theta range for data collection	2.38 to 30.00 deg.
Limiting indices	-16<=h<=16, -24<=k<=22, -12<=l<=17
Reflections collected / unique	19601 / 6965 [R(int) = 0.0262]
Completeness to theta =	30.00 99.4 %
Absorption correction	Empirical
Max. and min. transmission	0.234 and 0.113
Refinement method	Full-matrix least-squares on F^2
Data / restraints / parameters	6965 / 11 / 287
Goodness-of-fit on F^2	1.076
Final R indices [I>2sigma(I)]	R1 = 0.0234, wR2 = 0.0584
R indices (all data)	R1 = 0.0260, wR2 = 0.0594
Largest diff. peak and hole	1.775 and -2.942 e.$Å^{-3}$

Atomic coordinates (x 10^4) and equivalent isotropic displacement parameters. U(eq) is defined as one third of the trace of the orthogonalized U_{ij} tensor.

	x	y	z	U(eq)
Pt(1)	7269(1)	1847(1)	7235(1)	7(1)
Br(1)	9611(1)	1736(1)	8234(1)	13(1)
P(1)	6899(1)	1929(1)	8962(1)	8(1)
N(1)	7481(2)	3155(1)	7447(2)	10(1)
C(1)	6322(2)	3570(2)	6952(2)	18(1)
C(2)	8361(3)	3486(2)	6937(2)	17(1)
C(3)	7967(2)	3309(1)	8684(2)	13(1)
C(4)	7213(2)	2947(1)	9351(2)	13(1)
C(5)	7742(2)	1352(1)	10175(2)	10(1)
C(6)	7609(2)	1493(2)	11225(2)	13(1)
C(7)	8153(2)	1008(2)	12128(2)	15(1)
C(8)	8830(2)	380(2)	11986(2)	16(1)

C(9)	8973(2)	236(2)	10952(2)	15(1)
C(10)	8431(2)	721(1)	10045(2)	12(1)
C(11)	5354(2)	1738(1)	8935(2)	10(1)
C(12)	5028(2)	975(1)	9062(2)	12(1)
C(13)	3841(2)	788(2)	8958(2)	15(1)
C(14)	2956(2)	1354(2)	8721(2)	15(1)
C(15)	3264(2)	2114(2)	8587(2)	14(1)
C(16)	4455(2)	2306(1)	8686(2)	13(1)
C(17)	5444(2)	1880(1)	6311(2)	13(1)
C(18)	7079(6)	663(2)	7149(3)	12(1)
C(19)	7582(5)	1900(3)	5664(4)	14(1)
C(20)	7490(2)	1158(2)	5042(2)	12(1)
C(21)	8464(2)	638(2)	5295(2)	14(1)
C(22)	8351(3)	-73(2)	4758(3)	18(1)
C(23)	7269(4)	-288(3)	3963(3)	20(1)
C(24)	6302(3)	228(2)	3687(3)	20(1)
C(25)	6419(2)	943(2)	4219(2)	16(1)
C(18A)	7830(80)	1920(70)	5830(50)	0(20)
C(19A)	6960(150)	650(20)	6970(60)	8(8)
C(20A)	7010(30)	352(14)	5880(20)	7(6)
C(21A)	8180(20)	190(20)	5880(30)	9(7)
C(22A)	8360(30)	-110(40)	4910(40)	9(7)
C(23A)	7370(40)	-240(40)	3950(30)	9(7)
C(24A)	6210(30)	-80(30)	3960(20)	8(7)
C(25A)	6030(20)	219(18)	4920(30)	8(6)

3.7.3 X-ray Data for Complex **D2**

Empirical formula	$C_{17}H_{23}BrNPPt$
Formula weight	547.33

Temperature	298(2) K
Wavelength	0.71073 Å
Crystal system, space group	Orthorhombic, $Pna2_1$
Unit cell dimensions	a = 13.772(8) Å
	b = 9.743(6) Å
	c = 13.772(8) Å
Volume	1848.0(18) $Å^3$
Z, Calculated density	4, 1.967 Mg/m^3
Absorption coefficient	9.836 mm^{-1}
F(000)	1040
Crystal size	0.20 x 0.15 x 0.10 mm
Theta range for data collection	2.56 to 28.31 deg.
Limiting indices	-17<=h<=18, -12<=k<=13, -13<=l<=18
Reflections collected / unique	12137 / 3926 [R(int) = 0.1069]
Completeness to theta =	28.31 99.8 %
Absorption correction	Empirical
Max. and min. transmission	0.440 and 0.187
Refinement method	Full-matrix least-squares on F^2
Data / restraints / parameters	3926 / 13 / 191
Goodness-of-fit on F^2	0.970
Final R indices [I>2sigma(I)]	R1 = 0.0559, wR2 = 0.1093
R indices (all data)	R1 = 0.0963, wR2 = 0.1255
Absolute structure parameter	0.01(2)
Largest diff. peak and hole	2.642 and -1.066 $e.Å^{-3}$

Atomic coordinates (x 10^4) and equivalent isotropic displacement parameters. U(eq) is defined as one third of the trace of the orthogonalized U_{ij} tensor.

	x	y	z	U(eq)
Pt(1)	7937(1)	6697(1)	2496(1)	41(1)
Br(1)	8626(1)	8874(2)	3148(1)	64(1)

P(1)	7345(2)	4821(4)	1870(3)	42(1)
N(1)	7085(11)	7779(14)	1369(11)	72(4)
C(1)	7640(20)	8910(20)	889(19)	126(10)
C(2)	6210(16)	8430(19)	1850(19)	101(7)
C(3)	6827(15)	6768(18)	623(14)	74(5)
C(4)	6422(12)	5445(18)	1012(13)	69(5)
C(5)	6722(10)	3637(14)	2650(16)	51(4)
C(6)	7078(11)	2319(15)	2859(10)	50(4)
C(7)	6587(16)	1467(16)	3465(14)	70(5)
C(8)	5733(16)	1910(20)	3875(15)	85(6)
C(9)	5383(16)	3180(20)	3715(18)	93(7)
C(10)	5836(12)	4047(19)	3103(15)	80(5)
C(11)	8196(11)	3795(15)	1179(10)	47(3)
C(12)	9159(12)	3884(19)	1378(13)	73(5)
C(13)	9847(14)	3110(20)	823(18)	93(7)
C(14)	9497(14)	2298(19)	94(12)	72(5)
C(15)	8564(14)	2250(20)	-134(13)	75(5)
C(16)	7882(12)	2994(19)	409(15)	70(5)
C(17)	8634(11)	5655(16)	3553(11)	56(4)

3.7.4 X-ray Data for Complex **D3**

Empirical formula	C_{17} H_{23} I N P Pt
Formula weight	594.32
Temperature	100(2) K
Wavelength	0.71073 Å
Crystal system, space group	Orthorhombic, $P2_12_12_1$
Unit cell dimensions	a = 11.5701(11) Å
	b = 12.1859(11) Å

c = 13.0098(12) Å

Volume	1834.3(3) $Å^3$
Z, Calculated density	4, 2.152 Mg/m^3
Absorption coefficient	9.414 mm^{-1}
F(000)	1112
Crystal size	0.20 x 0.05 x 0.05 mm
Theta range for data collection	2.29 to 28.28 deg.
Limiting indices	-13<=h<=15, -15<=k<=16, -12<=l<=17
Reflections collected / unique	12606 / 4537 [R(int) = 0.0342]
Completeness to theta =	28.28 99.8 %
Absorption correction	Empirical
Max. and min. transmission	0.6504 and 0.2547
Refinement method	Full-matrix least-squares on F^2
Data / restraints / parameters	4537 / 0 / 190
Goodness-of-fit on F^2	1.037
Final R indices [I>2sigma(I)]	R1 = 0.0253, wR2 = 0.0615
R indices (all data)	R1 = 0.0263, wR2 = 0.0619
Absolute structure parameter	-0.005(5)
Largest diff. peak and hole	2.608 and -1.700 $e.Å^{-3}$

Atomic coordinates (x 10^4) and equivalent isotropic displacement parameters. U(eq) is defined as one third of the trace of the orthogonalized U_{ij} tensor.

	x	y	z	U(eq)
Pt(1)	1999(1)	1140(1)	9111(1)	12(1)
I(1)	1369(1)	-856(1)	9744(1)	21(1)
N(1)	524(3)	1305(3)	8034(3)	14(1)
C(1)	727(5)	540(5)	7158(4)	22(1)
C(2)	-620(5)	1042(5)	8505(5)	24(1)
C(3)	461(4)	2457(4)	7645(4)	16(1)
C(4)	1642(4)	2907(4)	7371(4)	14(1)

P(1)	2539(1)	2734(1)	8525(1)	12(1)
C(5)	2196(4)	3924(4)	9310(4)	14(1)
C(6)	1680(4)	3777(4)	10270(4)	19(1)
C(7)	1330(5)	4677(4)	10847(5)	23(1)
C(8)	1494(5)	5717(5)	10479(4)	22(1)
C(9)	2021(5)	5880(4)	9523(4)	22(1)
C(10)	2358(4)	4985(4)	8947(4)	18(1)
C(11)	4020(4)	2884(4)	8083(4)	13(1)
C(12)	4772(4)	3715(4)	8407(4)	17(1)
C(13)	5872(4)	3796(4)	7970(4)	19(1)
C(14)	6216(5)	3055(5)	7239(4)	20(1)
C(15)	5500(5)	2198(4)	6936(4)	20(1)
C(16)	4402(3)	2118(3)	7355(3)	17(1)
C(17)	3414(3)	1079(3)	10076(3)	21(1)

3.7.5 X-ray Data for Complex **E1**

Empirical formula	C_{16} H_{20} Cl2 N P Pt
Formula weight	523.29
Temperature	100(2) K
Wavelength	0.71073 Å
Crystal system, space group	Orthorhombic, $Pna2_1$
Unit cell dimensions	a = 12.0796(15) Å
	b = 12.3945(15) Å
	c = 11.4614(14) Å
Volume	1716.0(4) $Å^3$
Z, Calculated density	4, 2.026 Mg/m^3
Absorption coefficient	8.574 mm^{-1}

F(000)	1000
Crystal size	0.15 x 0.07 x 0.07 mm
Theta range for data collection	2.35 to 28.30 deg.
Limiting indices	-16<=h<=11, -16<=k<=10, -15<=l<=14
Reflections collected / unique	8450 / 4119 [R(int) = 0.0337]
Completeness to theta =	28.30 99.8 %
Absorption correction	Empirical
Max. and min. transmission	0.550 and 0.366
Refinement method	Full-matrix least-squares on F^2
Data / restraints / parameters	4119 / 228 / 218
Goodness-of-fit on F^2	0.956
Final R indices [I>2sigma(I)]	R1 = 0.0272, wR2 = 0.0563
R indices (all data)	R1 = 0.0331, wR2 = 0.0576
Absolute structure parameter	0.017(8)
Largest diff. peak and hole	2.036 and -0.783 e.$Å^{-3}$

Atomic coordinates (x 10^4) and equivalent isotropic displacement parameters. U(eq) is defined as one third of the trace of the orthogonalized Uij tensor.

	x	y	z	U(eq)
Pt(1)	7149(1)	3499(1)	2499(1)	17(1)
Cl(1)	6664(2)	5206(1)	2958(2)	38(1)
Cl(2)	6147(1)	3697(2)	737(1)	34(1)
P(1)	8096(1)	3259(1)	4111(1)	16(1)
N(1)	7627(5)	1902(5)	2055(4)	30(1)
C(1)	6801(10)	1094(11)	2247(11)	33(4)
C(2)	8059(12)	1844(17)	821(11)	28(3)
C(3)	8741(9)	1621(9)	2756(9)	30(2)
C(1A)	6560(11)	1314(12)	1675(15)	26(3)
C(2A)	8384(15)	1890(20)	1093(15)	27(4)
C(3A)	7926(11)	1318(11)	3185(11)	27(3)
C(4)	8652(6)	1882(7)	3932(7)	33(2)

C(5)	9278(4)	4130(4)	4364(5)	17(1)
C(6)	10060(5)	3909(5)	5236(5)	24(1)
C(7)	10949(5)	4592(5)	5396(5)	24(1)
C(8)	11095(5)	5486(5)	4707(5)	26(1)
C(9)	10322(5)	5723(5)	3849(6)	31(1)
C(10)	9434(5)	5056(5)	3665(5)	25(1)
C(11)	7310(5)	3253(4)	5464(5)	17(1)
C(12)	6324(5)	3819(5)	5537(5)	22(1)
C(13)	5727(5)	3861(5)	6551(5)	23(1)
C(14)	6102(4)	3336(4)	7529(9)	28(1)
C(15)	7081(4)	2752(4)	7465(10)	29(1)
C(16)	7680(5)	2701(5)	6458(5)	27(1)

4. Summary

Oxidative addition reactions are a very important step in synthetic chemistry and are used in various industrial catalysis pathways, such as the *Monsanto* process. Therefore, apart from pure scientific interest in the properties of these reactions the understanding of the conditions that influence oxidative additions is of tremendous interest for the development of new synthetic pathways.

In this context, complexes with hemilabile ligands play an important role: The weaker donor atom can decoordinate and thus open a vacant coordination site for addition of a new ligand or for rearrangements in the coordination sphere that could support formation and elimination of new compounds. These ligands can be tailored to support different reactions of importance in synthetic chemistry.

In the current work the reactivity of the Pt(II) complex [(κ^2-*P*,*N*)-$Ph_2PCH_2CH_2NMe_2$]$PtMe_2$ (**A1**) towards halogenated hydrocarbons and silyl chlorides was investigated.

4.1 Halogenated Hydrocarbons

The first aim of this thesis was to investigate the reactivity of the complex **A1** with different halogenated hydrocarbons. The only information about these reactions previous to this work consisted of reactions with chlorinated methyl derivatives (Fig. 104).

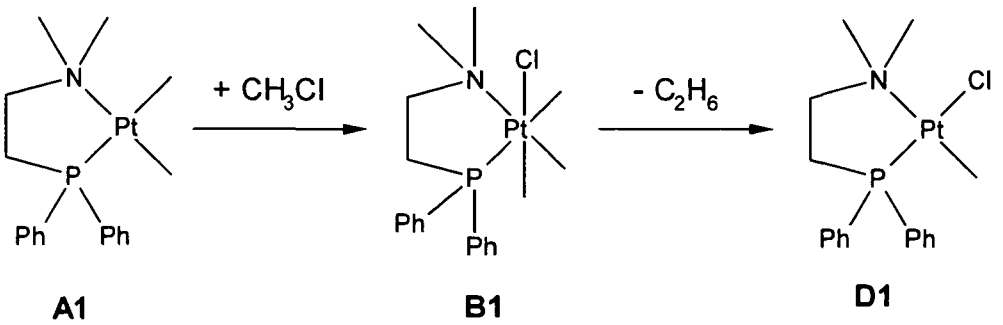

Fig. 104: Reaction of complex **A1** with methyl chloride

What was known so far, was that complex **B1** can be transformed into **D1** by elimination of ethane. Therefore it was important to find out, whether also other compounds can be eliminated, consisting of one methyl ligand and the organic moiety group originating from the organic halide. During the experimental work it turned out, that the compounds can be divided into three groups, according to the different reaction pathways monitored:

- Halogenated hydrocarbons with β-CH_2 groups
- Halogenated hydrocarbons without β-CH_2 groups and low reactivity towards **A1**
- Halogenated hydrocarbons without β-CH_2 groups and high reactivity towards **A1**

- In the first group chlorides, bromides and iodides were investigated. No indications for methylation of the dehalogenated organic groups or for their coupling were found. The main reaction pathway of these compounds was β-elimination of an unsaturated compound from the octahedral complex formed by oxidative addition (Fig. 105).

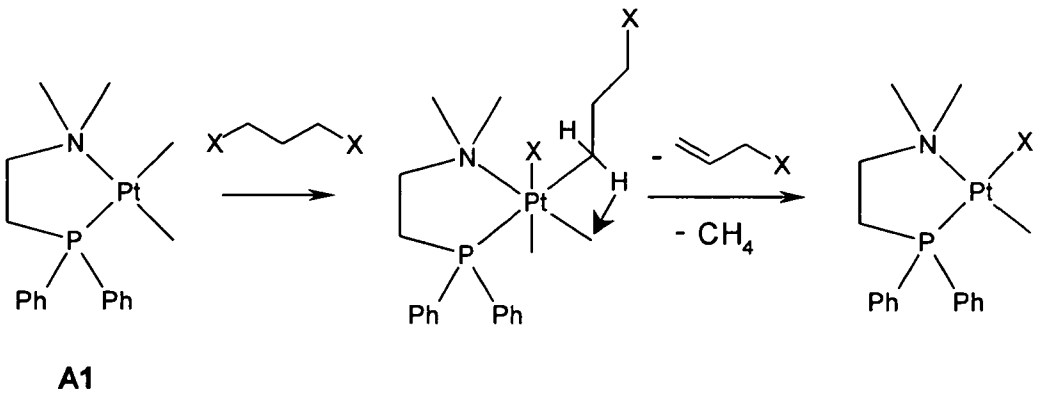

A1

Fig. 105: β-elimination of an unsaturated compound

The different rate of oxidative addition due to the C-X bond dissociation energies was clearly observed. While with bromides and iodides the octahedral type **B** intermediate was formed within hours, so that they mostly were observed in the NMR spectra for a long period throughout the reaction, no octahedral intermediate formed by activation of a C-Cl bond was observed.

In the reactions with bromides and iodides the bromo-methyl complex **D2** and the iodo-methyl complex **D3** were formed (Fig. 106); their crystal structures were determined by X-ray diffraction.

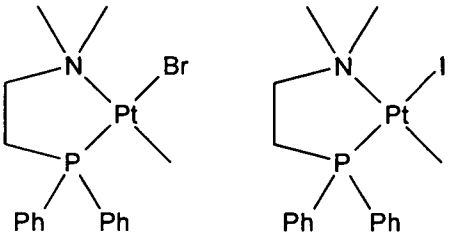

D2 **D3**

Fig. 106: Complexes D2 and D3

- In the second group of reactants, chlorides and bromides were investigated. Here the low activation rate of the C-Cl group was also obvious. While at least some reaction was observed with 1,3-dichloropropane, compounds with the chlorine bound to secondary carbons did not react with complex **A1** at all. This is typical for oxidative addition reactions that proceed through a nucleophilic substitution mechanism. With 2,2-dibromopropane, formation of the corresponding coupling product 2,3-dibromo-2,3-dimethylbutane could be monitored. Also brominated aromatic compounds were investigated. In contrast to chlorobenzene, activation took place, but also at a very slow rate. In this case dehalogenative coupling and methylation were observed.

- The third group turned out to be the most interesting. At the first look, benzyl chloride and bromide reacted with **A1** by dehalogenative coupling or methylation. But at second look it became clear, that another reaction mechanism must be involved: First, the amount of products formed by dehalogenative coupling and methylation does not match that of complex **D1** produced, and in the case of ethyl chloroacetate no coupling or methylation product was found at all. Second, methane and ethyl acetate or toluene were found in the reactions. They are products of reaction of different intermediate complexes with hydrogen halides. This raises the question, where these halides originate from. Third, NMR signals of vinylic products were found, which appeared to be the same in all the reactions of that group of compounds. Also the reaction rate of these compounds is much higher than with all other halogenated hydrocarbons.

During further investigation it turned out that activation of C-C bonds may take place here, yielding complexes with CH_2X ligands. The vinylic signals turned out to belong to a vinyl group bonded to a P atom that also carries phenyl groups. Analysis by mass spectroscopy revealed, that a methylene group was inserted into the Pt-P bond, forming an ylide ligand (Fig. 107).

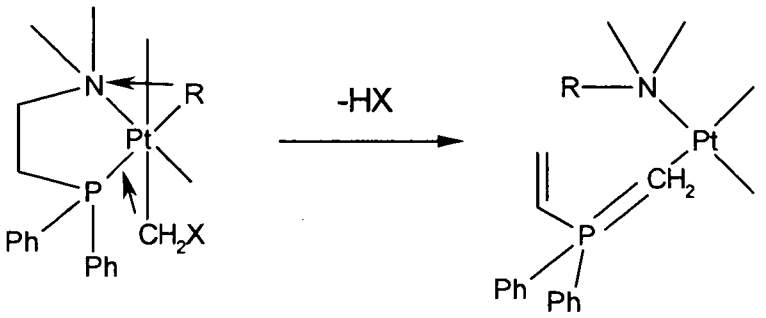

Fig. 107: Formation of an ylide ligand by methylene insertion

During this reaction, the *P,N* ligand was split by abstraction of a proton from the aliphatic spacer between the two donor groups, yielding the double bond as well as the hydrohalogenic acid, that is responsible for the formation of methane, toluene and ethyl acetate through coordination to **A1** or **C** type complexes (Fig. 108), that carry a methyl group and another organic ligand.

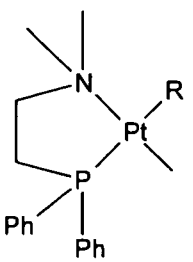

R = any organic moiety

Fig. 108: A **C**-type complex

Experiments from the other two groups of compounds were reviewed. Evidence for ylide formation was found in the reactions with propargyl chloride, chloroacetic acid and bromides

and iodides with β-CH_2 groups to a minor amount. A general trend behind appears to be, that ylide formation is favoured by organic halides that carry C-C bonds activated by π-bonds in β-position or a terminal CH_2 group that carries a bromine or an iodine. This is in accordance to literature data of C-C activation, another hint that oxidative addition of carbon-carbon bonds takes place here.

4.2 Silyl Chlorides

The second aim of this work was the further investigation of the reactivity of silyl chlorides with complex **A1**. Two experiments were performed previous to this work with silyl halides, showing methylation and coupling of the dehalogenated silyl groups. The silyl chlorides used in the current work can be divided into two groups:

- Silyl monochlorides
- Silyl di- and trichlorides

Remarkable for both groups was the high reactivity of the silyl halides with complex **A1**. In some cases the reaction was finished at room temperature within a few hours. The silyl monochlorides reacted with the starting complex by dehalogenative methylation or coupling, with some compounds both reaction pathways were monitored.

The silyl di- and trichlorides also exhibited dehalogenative coupling and methylation but here also another reaction pathway was discovered. Investigation of precipitates formed in these reactions showed the precipitate to be the dichloro complex **E1**. To find out whether **E1** is formed from **A1** or **D1**, a sample of **D1** was treated with dichlorodiphenylsilane. The formation of the dichloro complex was observed in this reaction (Fig. 109). The structure of this complex was determined by X-ray diffraction.

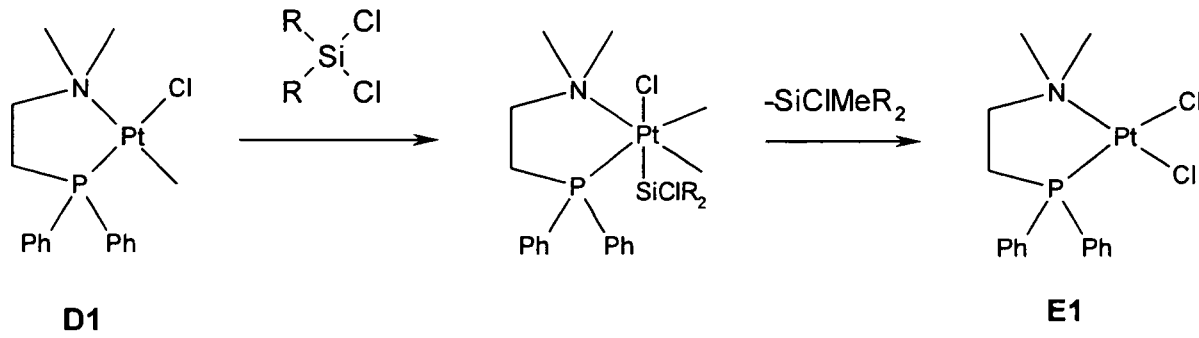

Fig. 109: Formation of complex **E1**

4.3. List of Reaction Products

Compound	Reaction time [h]	Reaction products and their amount at molar ratio 1:2*
1,3-Dichloropropane	504	-Complex **D1** (30% **A1**) -Allyl chloride (traces) -Amorphous precipitate (maybe polymerized allyl chloride)
(3-Chloropropyl)trimethyl-silane	120	-Complex **D1** (traces)
1,3-Dibromopropane	48	-Complex **B3** (25% **A1**) -Complex **D2** (75% **A1**) -Allyl bromide (traces) -Amorphous precipitate (maybe polymerized allyl bromide) -F-type complex (traces)
1,6-Dibromohexane	96	-Complex **D2** (100% **A1**) -F-type complex (traces)
1,3-Diiodopropane	1	-Complex **B4** (40% **A1**) -Complex **D3** (60% **A1**) -Amorphous precipitate (maybe polymerized allyl bromide) -F-type complex (traces)
1,6-Diiodohexane	24	-Complex **B5** (20% **A1**) -Complex **D3** (80% **A1**) -Amorphous precipitate -F-type complex (traces)
Chlorocyclohexane	168	-Complex **D1** (traces)

Chlorobenzene	168	-Complex **D1** (traces)
2,2-Dichloropropane	168	-Complex **D1** (traces)
Chloroacetic Acid	24	-Complex **C1** (99% **A1**) -**F**-type complex (traces)
Propargyl Chloride	20	-Unknown precipitate (90% **A1**) -Complex **D1** (2% **A1**) -**F**-type complex (traces)
2,2-Dibromopropane	72	-Complex **D2** (100% **A1**) -2,3-dibromo-2,3-dimethylbutane (76% org.)
Bromobenzene	240	-Complex **D2** (50% **A1**) -Biphenyl (%org. not definable)
1,4-Dibromobenzene	366	-Complex **D2** (65% **A1**) -4-bromotoluene (60% org.)
Benzyl Chloride	96	-Complex **D1** (90% **A1**) -Complex **F1** (10% **A1**) -Bisphenyl (25% org.) -Toluene (30% org.)
Benzyl Bromide	6	-Complex **B6** (50% **A1**) -Complex **D2** (50% **A1**) -Ethyl benzene (50% org.) -**F**-type complex (traces)
Ethyl Chloroacetate	48	-Complex **D1** (90% **A1**) -Complex **F2** (10% **A1**) -Ethyl acetate (40% org.)
Chlorotrimethylsilane	48	-Complex **D1** (60% **A1**) -Tetramethylsilane (25% org.) -Hexamethyldislane (25% org.)
Chlorodimethylvinylsilane	50	-Complex **D1** (50% **A1**) -Tertramethyldivinyldisilane (50% org.)
Chlorotriethylsilane	48	-Complex **D1** (90% **A1**) -Hexaethyldisilane (80% org.)
Dichlorodiphenylsilane	5	-Complex **D1** (100% **A1**) -Complex **E1** (% **A1** not definable) -Chloro-methyldiphenylsilane (30% org.)
Dichlordimethylsilane	48	-Complex **D1** (100% **A1**) -Tetramethyl-dichlorodisilane (50% org.)
Cyclohexylmethydichlorosilane	120	-Complex **D1** (35% **A1**) -Complex **E1** (65% **A1**)
Trichlorophenylsilane	0.5	-Complex **D1** (100% **A1**) -Disilanes, methylsilanes

* % org. = Percentage of the organic starting compound equimolar to **A1** turned into the specified compound

* % **A1**. = Percentage of complex **A1** turned into the specified compound

5. Appendix

5.2 Abbrevations

δ	chemical shift [ppm]
°C	degrees Celsius
aliph.	aliphatic
d	doublet in NMR spectra
DEE	diethyl ether
Et	ethyl
h	hours
Hz	Hertz
HMBC	Heteronuclear multiple bond correlation
HSQC	Heteronuclear single bond correlation
iPr	isopropyl
M	Metal
m	multiplet in NMR spectra
Me	methyl
NMR	nuclear magnetic resonance
nbd	norbornadiene
Ph	phenyl
R	alkyl or aryl
s	singlet in NMR spectra
t	triplet in NMR spectra
tBu	tert-butyl
X	an unspecified halogen
XRD	X-ray diffraction

5.2 Key to Complex Nomenclature

A-group (Square planar Pt(II) complexes with a *P,N*-ligand and two methyl ligands):

- **A1**: [(κ^2-*P*,*N*)-$Ph_2PCH_2CH_2NMe_2$]$PtMe_2$ (the starting complex)
- **A2**: [(κ^2-*P*,*N*)-$Ph_2PCH_2CH_2CH_2NMe_2$]$PtMe_2$
- **A3**: [(κ^2-*P*,*N*)-2-diphenylphosphine-phenyl dimethylamine]$PtMe_2$
- **A4**: [(κ^2-*P*,*N*)-2-diphenylphosphine-benzyl dimethylamine]$PtMe_2$
- **A5**: [(κ^2-*P*,*N*)-$Ph_2PCH_2CH_2NMe_2$]$Pt(CD_3)_2$

B-group (Octahedral Pt(IV) complexes with a *P*,*N*-ligand, two methyl ligands and two ligands attached by oxidative addition):

- **B1**: [(κ^2-*P*,*N*)-$Ph_2PCH_2CH_2NMe_2$]$PtMe_3Cl$
- **B2**: [(κ^2-*P*,*N*)-$Ph_2PCH_2CH_2NMe_2$]$PtMe_2Cl_2$
- **B3**: [(κ^2-*P*,*N*)-$Ph_2PCH_2CH_2NMe_2$]$Pt((CH_2)_3Br)Me_2Br$
- **B4**: [(κ^2-*P*,*N*)-$Ph_2PCH_2CH_2NMe_2$]$Pt((CH_2)_3I)IMe_2$
- **B5**: [(κ^2-*P*,*N*)-$Ph_2PCH_2CH_2NMe_2$]$Pt((CH_2)_6I)IMe_2$
- **B6**: [(κ^2-*P*,*N*)-$Ph_2PCH_2CH_2NMe_2$]$PtMe_2BzBr$
- **B7**: [(κ^2-*P*,*N*)-$Ph_2PCH_2CH_2NMe_2$]$PtMe_2Cl(CH_2COOEt)$
- **B8**: [(κ^2-*P*,*N*)-$Ph_2PCH_2CH_2NMe_2$]$PtMe_2(CH_2Cl)(COOEt)$
- **B9**: [(κ^2-*P*,*N*)-$Ph_2PCH_2CH_2NMe_2$]$PtMe_2(CH_2Cl)(C{\equiv}CH)$
- **B10**: [(κ^2-*P*,*N*)-$Ph_2PCH_2CH_2NMe_2$]$PtMe_2((CH_3)_3Si)Cl$

C-group (Square planar Pt(II) complexes with a *P*,*N*-ligand and two different ligands except the combination methyl and halogen):

- **C1**: [(κ^2*P*,*N*)$Ph_2PCH_2CH_2NMe_2$]$Pt(OOCCH_2Cl)Me$
- **C2**: [(κ^2*P*,*N*)$Ph_2PCH_2CH_2NMe_2$]$Pt(CH_2COOCH_2CH_3)Me$
- **C3**: [(κ^2*P*,*N*)$Ph_2PCH_2CH_2NMe_2$]Pt((MeCl)SiPh)Me

D-group (Square planar Pt(II) complexes with a *P*,*N*-ligand, a methyl ligand and a halogen ligand):

- **D1**: [(κ^2-*P*,*N*)-$Ph_2PCH_2CH_2NMe_2$]PtMeCl
- **D2**: [(κ^2-*P*,*N*)-$Ph_2PCH_2CH_2NMe_2$]PtMeBr
- **D3**: [(κ^2-*P*,*N*)-$Ph_2PCH_2CH_2NMe_2$]PtMeI

- **D4**: [(κ^2-*P*,*N*)-$Ph_2PCH_2CH_2NMe_2$]Pt(CD_3)Cl

E-group (Square planar Pt(II) complexes with a *P*,*N*-ligand and two halogen ligands):

- **E1**: [(κ^2-*P*,*N*)-$Ph_2PCH_2CH_2NMe_2$]$PtCl_2$

F-group (Square planar Pt(II) complexes with an amino ligand, an ylide ligand and two methyl ligands):

- **F1**: Pt($CH_2PPh_2(C_2H_3)$)(NMe_2Ph)Me_2
- **F2**: Pt($CH_2PPh_2(C_2H_3)$)(NMe_2COOEt)Me_2

[1] A. Hollemann, N. Wiberg, *Lehrbuch der Anorganischen Chemie, Walter de Gruyter* **2007**, 2145
[2] Scaliger, J. C., *Exotericarum exercitationum liber quintus decimus de subtilitate, ad Hieronymum Cardanum*, Lutetia: Michael Vascosani, **1557**
[3] W. Watson, *Philosophical Transactions of the Royal Society of London*, **1750**, *46*, 584
[4] A. Hollemann, N. Wiberg, *Lehrbuch der Anorganischen Chemie, Walter de Gruyter* **2007**, 1722
[5] source: german wikipedia
[6] D. Astruc, *Organometallic Chemistry and Catalysis*, **2007**, 109
[7] E. O. Fischer, *Advanced Organometallic Chemistry*, **1976**, *1*, 14
[8] C.P. Casey, W.M. Miles, *Journal of Organometallic Chemistry*, **1983**, *254*, 333
[9] A. Hollemann, N. Wiberg, *Lehrbuch der Anorganischen Chemie, Walter de Gruyter* **2007**, 1382
[10] F. Basolo, R.G. Pearson, *Progress in Inorganic Chemistry*, **1962**, *4*, 381
[11] B. J.Coe, S. J.Glenwright, *Coordination Chemistry Reviews*, **2000**, *203*, 5
[12] D. Astruc, *Organometallic Chemistry and Catalysis*, **2007**, 81
[13] D. Astruc, *Organometallic Chemistry and Catalysis*, **2007**, 137
[14] K. Noack, F. Calderazzo, *Journal of Organometallic Chemistry*, **1967**, *10*, 101
[15] S.M. Sbovata, A. Tassan, G. Facchin, *Inorganica Chimica Acta*, **2008**, *361*, 3177
[16] C. Engelter, J. R. Moss, L. R. Nassimbeni, M. L. Niven, G. Reid, J. C. Spiers, *Journal of Organometallic Chemistry*, **1986**, *315*, 255
[17] J. F.Hoover, J. M. Stryker, *Organometallics*, **1988**, *7*, 2082
[18] R. Zolk, H. J.Werner, *Journal of Organometallic Chemistry*, **1986**, *303*, 233.
[19] M. L. H. Green, P. J. Knowles, *Chemical Communications*, **1970**, *24*, 1677
[20] L. M. Rendina, R.J.Puddephatt, *Chemical Reviews*, **1997**, *97*, 1735
[21] D. Rabinovich, G. Parkin (Ed.), *Comprehensive Organometallic Chemistry III, Vol. 1*, **2007**, 101
[22] J. Halpern, *Inorganica Chimica Acta*, **1985**, *100*, 41
[23] R. Toreki, *Organometallic HyperTextBook*, http://www.ilpi.com/organomet
[24] A. Gillie, J. K. Stille, *Journal of the American Chemical Society*, **1980**, *102*, 4933
[25] W. Lau, J. C. Huffman, J. K. Kochi, *Organometallics*, **1982**, *1*, 155
[26] S. Komiya, T. A. Albright, A. Hoffmann, J. K. Kochi, *Journal of the American Chemical Society*, **1976**, *98*, 7255
[27] H. Wu, M. B. Hall, *Dalton Transactions*, **2009**, 5933
[28] S. J. Blanksby, G. B. Ellison, *Accounts of Chemical Research*, **2003**, *36*, 255
[29] T. R. Cundari, S. Vaddadi, *Inorganica Chimica Acta*, **2004**, *357*, 2863.
[30] V. De Felice, B. Giovannitti, A. De Renzi, D. Tesauro, A Panunzi, *Journal of Organometallic Chemistry*, **2000**, *593*, 445
[31] G. Van Koten, *Pure Applied Chemistry*, **1989**, *61*, 1681.
[32] B. Rybtchinski, S. Oevers, M. Montag, A. Vigalok, H. Rozenberg, J. M. L. Martin, D.Milstein, *Journal of the American Chemical Society*, **2001**, *123*, 9064
[33] J. J. Low, W. A. Goddard III, *Journal of the American Chemical Society*, **1984**, *106*, 8321
[34] B. Rybtchinski, D. Milstein, *Angewandte Chemie, International Edition*, **1999**, *38*, 870
[35] J. A. Martinho Simoes, J. L. Beauchamp, *Chemical Reviews*, **1990**, *90*, 629
[36] D. M.Adams, J. Chatt, R. G. Guy, N. Sheppard, *Journal of the American Chemical Society*, **1961**, 738
[37] L. Cassar, J.Halpern, *Journal of the Chemical Society, Chemical Communications*, **1970**, 1082
[38] L. Cassar, P. E. Eaton, J.Halpern, *Journal of the American Chemical Society*, **1970**, *92*, 3515
[39] J. J. Eisch, A. M. Piotrowski, K. I. Han, C. Krüger, Y. H. Tsay, *Organometallics*, **1985**, *4*, 22
[40] J. W. Suggs, C. H. Jun, *Journal of the Chemical Society, Chemical Communications*, **1985**, 92
[41] J. F. Hartwig, R. A. Andersen, R. G. Bergmann, *Journal of the American Chemical Society*, **1989**, *111*, 2717
[42] A. W. Kaplan, R. G. Bergmann, *Organometallics*, **1997**, *16*, 1106
[43] P. Eilbracht, P. Dahler, *Journal of Organometallic Chemistry*, **1977**, *135*, C23
[44] F. W. S. Benfield, M. L. H. Green, *Journal of the Chemical Society, Dalton Transactions*, **1974**, 1324
[45] F. Urbanos, M. A. Halcrow, J. Fernandez-Baeza, F. Dahan, D. Labroue, B. Chaudret, *Journal of the American Chemical Society*, **1993**, *115*, 3484
[46] S. Y. Liou, M. Gozin, D. Milstein, *Journal of the American Chemical Society*, **1995**, *117*, 9774
[47] M. E. van der Boom, H.-B. Kraatz, Y. Ben-David, D. Milstein, *Chemical Communications*, **1996**, 2167.
[48] J. A. Martinho Simoes, J.L.Beauchamp, *Chemical Reviews*, **1990**, *90*, 629
[49] S. J. Blanksby, G. B. Ellison, *Accounts of Chemical Research*, **2003**, *36*, 255
[50] M. Gandelman, A. Vigalok, L. J. W. Shimon, D. Milstein, *Organometallics*, **1997**, *16*, 3981.
[51] R. Walsh, *Accounts of Chemical Research*, **1981**, *14*, 246

[52] C. J. Levy, R. J. Puddephatt, *Organometallics*, **1995**,*14*, 5019
[53] D. V. Meek, T. J. Mazanec, *Accounts of Chemical Research*, **1981**, *14*, 266
[54] C. Anderson, M. Crespo, M. Font-Bardia, A. Klein, X. Solans, *Journal of Organometallic Chemistry*, **2000**, *601*, 22
[55] M. A. Fedotov, *Russian Chemical Bulletin, International Edition*, **2003**, *52*, 781
[56] T. G.Appleton, M. A. Bennett, *Inorganic Chemistry*, **1978**, *17*, 738
[57] J. R. L. Priqueler, I. S. Butler, F. D.Rochon, *Applied Spectroscopy Reviews*, **2006**, *41*, 185
[58] J. Pfeiffer, G. Kickelbick, U.Schubert, *Organometallics*, **2000**, *19*, 62
[59] K. J. Bonnington, M. C.Jennings, R. J.Puddephatt, *Organometallics*, **2008**, *27*, 6521
[60] F. Stöhr, D. Sturmayr, G. Kickelbick, U. Schubert, *European Journal of Inorganic Chemistry*, **2002**, 2305
[61] C. Elschenbroich, *Organometallchemie*, *Teubner* **2008**, 264
[62] G. O. Evans, C. U. Pittman, R. McMillan, R.T. Beach, *Journal of Organometallic Chemistry*, **1974**, *67*, 295
[63] A. Behr, *Angewandte homogene Katalyse, Wiley VCH* **2007**, 65
[64] B. Rosenberg, *Interdisciplinary Science Reviews*, **1978**, *3*, 134
[65] M. Peyrone, *Ann. Chemie. Pharm.*, **1845**, *51*, 129.
[66] M. Galanski, V.B. Arion, M.A. Jakupec, B.K. Keppler, *Current Pharmaceutical Design*, **2003**, *9*, 2078
[67] C. S. Slone, D. A. Weinberger, C. A. Mirkin, *Progress in Inorganic Chemistry*, **1999**, *48*, 233.
[68] J. Pfeiffer, U. Schubert, *Organometallics*, **1999**, *18*, 3245
[69] S.M. Thompson, F. Stöhr, D. Sturmayr, G. Kickelbick, U.Schubert, *Journal of Organometallic Chemistry*, **2003**, *686*, 183
[70] F. Stöhr, D. Sturmayr, U. Schubert, *Chemical Communications*, **2002**, 2222
[71] R. L.Rominger, R. F. See, C. H. Lake, M. R. Churchill, J. D. Atwood, *Journal of Coordination Chemistry*, **1998**, *46*, 165
[72] J. L. Butikofer, J. M. Hoerter, R. G.Peters, D. M. Roddik, *Organometallics*, **2004**, *23*, 400
[73] T. G. Appleton, J.R. Hall, M. A. Williams, *Journal of Organometallic Chemistry*, **1986**, *303*, 139

CURRICULUM VITAE

Personal Data

Name:	Mag. Christian Martschitsch
Date of birth:	April 12th 1978
Place of birth:	Vienna
Citizenship:	Austria
Adress:	Anton-Baumgartner-Straße 44 1230 Wien
Family status:	Married

Educational Background

03/2005 – present	PhD thesis in Technical Chemistry at the Technical University of Vienna
02/2004:	Graduation from General Chemistry at the University of Vienna
10/1996 – 02/2004:	Study of General Chemistry at the University of Vienna
09/1988 – 06/1996:	High School in Vienna (Joseph Haydn Realgymnasium, Wien-Margareten)

Professional Background

07/2009 – present:	Scientist in product developement at Gabriel-Chemie in Gumpoldskirchen / Lower Austria
01/2005 – 01/2009:	University Assistant at the Technical University of Vienna
05/2004 – 12/2004:	Project Assistant at the Technical University of Vienna